

Mechanisms Regulating Cytokinetic
Contractile Ring Formation and
Anchoring in *Schizosaccharomyces*
pombe

By

Alaina Hollister Willet

Dissertation

Submitted to the Faculty of the
Graduate School of Vanderbilt University
in partial fulfillment of the requirements
for the degree of

DOCTOR OF PHILOSOPHY

in

Cell and Developmental Biology

August 11, 2017

Nashville, Tennessee

Approved:

Kathleen L. Gould, Ph.D.

Irina Kaverina, Ph.D.

Matthew J. Tyska, Ph.D.

Alissa M. Weaver, Ph.D.

Professor Ryoma Ohi

To my parents and fiancé,
for their endless love and support

TABLE OF CONTENTS

	Page
DEDICATION.....	ii
LIST OF FIGURES.....	v
LIST OF ABBREVIATIONS	vii
Chapter	
1 Introduction	1
1.1 Overview of the eukaryotic cell cycle.....	1
1.2 <i>Schizosaccharomyces pombe</i> as a model system to study cell division.....	3
1.3 Formation of the contractile ring in <i>S. pombe</i>	5
Contractile ring precursors	5
An ordered assembly of components?	6
1.4 Introduction to formins.....	8
Formin domains and mechanisms of action	8
Cytokinetic formin function in cytokinesis.....	10
Regulation of formins during <i>S. pombe</i> contractile ring assembly	12
1.5 Formation of a division septum.....	16
Function of glucans in the division septa	16
Septum formation forces	18
1.6 A primer on a role for plasma membrane lipid composition in cytokinesis	20
1.7 Summary	20
2 The F-BAR Cdc15 promotes contractile ring formation through direct recruitment of the formin Cdc12	22
2.1 Introduction	22
2.2 Results and Discussion.....	25
Cdc12 binds the Cdc15 F-BAR through a conserved N-terminal motif.....	25
Cells lacking the Cdc12-Cdc15 interaction are prone to cytokinesis failure	28
Cdc12-Cdc15 interaction is important for normal Cdc12 recruitment.....	28
Efficient Cdc12 recruitment is important for F-actin accumulation in the CR.....	32
The Cdc12-Cdc15 interaction is important during CR formation.....	35

3 Cdk1-dependent phospho-inhibition of a formin F-BAR interaction inhibits cytokinesis	39
3.1 Introduction	39
3.2 Results and Discussion	43
Cdc12 is a Cdk1 substrate	43
Cdk1 phosphorylation of Cdc12 inhibits the Cdc12-Cdc15 interaction	45
Cell with constitutive inhibition of the Cdc12-Cdc15 interaction are prone to cytokinesis failure	48
Cdk1-dependent regulation of the Cdc12-Cdc15 interaction is important for Cdc12 recruitment	49
Cdk1-dependent regulation of the Cdc12-Cdc15 interaction is important for the initial formation of F-actin in the forming CR	51
Cdk1-dependent phosphorylation of Cdc12 is important during CR formation	55
4 Phosphoinositide-mediated ring anchoring resists perpendicular forces to promote medial cytokinesis	57
4.1 Introduction	57
4.2 Results and Discussion	60
The Stt4 complex is important for medial cell division in <i>S. pombe</i>	60
<i>efr3Δ</i> have off-center septa due to CR sliding	63
Efr3-dependent and Cdc15-dependent CR sliding are independent mechanisms..	65
<i>efr3Δ</i> combined with mutants that have misplaced CRs have exacerbated off-center septa defects.....	68
Efr3-dependent CR sliding requires myosin V Myo51	71
5 Conclusions and future directions	76

APPENDIX

A. Materials and Methods	82
Yeast methods	82
Protein methods	84
In vitro binding	85
Microscopy	86
Mean squared displacement analysis	87
Mass spectrometry	89
B. Cdc12 mutants used in Chapters II and III	90
BIBLIOGRAPHY	91

LIST OF FIGURES

Figure	Page
1-1 Schematic of the canonical cell cycle	2
1-2 Cytokinesis in yeast and animal cells.....	4
1-3 Mid1 sets up two redundant modules of protein recruitment for CR formation.....	6
1-4 Two <i>S. pombe</i> formins, Cdc12 and For3, are important for contractile ring formation	8
1-5 Formins nucleate and elongate F-actin	9
1-6 Roles of septation in <i>S. pombe</i> cytokinesis	15
2-1 An N-terminal Cdc12 motif directly interacts with the Cdc15 F-BAR	24
2-2 The conserved Cdc12 motif promotes Cdc12 localization to the cell middle	25
2-3 Genetic interactions of mutant <i>cdc12</i> -P31A	26
2-4 Genetic interactions of the mutant <i>cdc12</i> - Δ 24-36 and <i>cdc12</i> -P31A	27
2-5 Cells lacking Cdc12-Cdc15 interaction accumulate less Cdc12 in the CR	29
2-6 Cdc12 lacking the Cdc12-Cdc15 interaction localizes independently of F-actin to the CR.....	31
2-7 Cells lacking the Cdc12-Cdc15 accumulate less F-actin in the CR.....	33
2-8 Cdc12 lacking the Cdc12-Cdc15 interaction exhibit slower CR formation.....	35
3-1 Formin Cdc12 is a Cdk1 substrate	42
3-2 Identification of Cdk1-phosphorylated sites on Cdc12.....	44
3-3 Cdc12 Cdk1 phosphorylation inhibits Cdc12-Cdc15 binding	45
3-4 Cdc15 expression <i>in vitro</i> and <i>in vivo</i>	46
3-5 Genetic interactions of mutants <i>cdc12</i> -6A and <i>cdc12</i> -6D.....	47

3-6	Cdc12 with constitutive Cdk1 phosphorylation accumulates less Cdc12 in the CR	48
3-7	Cdc12 with constitutive Cdk1 phosphorylation cannot be recruited by Cdc15 in abnormal cell cycle conditions.....	50
3-8	Cells with constitutive Cdc12 Cdk1 phosphorylation accumulates less F-actin in the CR.....	52
3-9	Cells with constitutive Cdc12 Cdk1 phosphorylation accumulate less Ain1 in the CR.....	53
3-10	Cells with constitutive Cdc12 Cdk1 phosphorylation exhibit slower CR formation	54
4-1	<i>efr3Δ</i> display off-center septa	59
4-2	<i>stt4</i> and <i>ypp1</i> are essential in <i>S. pombe</i>	60
4-3	<i>efr3Δ</i> display abnormal PIP composition.....	61
4-4	CRs slide from the cell middle in <i>efr3Δ</i>	62
4-5	Cytokinesis timing is unperturbed in <i>efr3Δ</i>	64
4-6	Localization of membrane-binding proteins in <i>efr3Δ</i>	66
4-7	The Stt4 complex and CR positioning machinery cooperate in septum positioning	67
4-8	<i>efr3Δ</i> CR sliding events depend on Myo51	69
4-9	<i>efr3Δ</i> CR sliding does not depend on Myo2	70
4-10	N- and C- termini of Myo51 are necessary for <i>efr3Δ</i> CR sliding	73
4-11	Model for CR anchoring during cytokinesis	75

LIST OF ABBREVIATIONS

ARM	armadillo repeats
CB	coomassie blue
Cdk1	Cyclin dependent kinase 1
CR	cytokinetic ring
DAD	diaphanous autoregulatory domain
DID	diaphanous inhibitory domain
F-ACTIN	filamentous-actin
F-BAR	FER/Cip4 homology Bin–Amphiphysin–Rvs
FH	formin homology
GFP	green fluorescent protein
KA	kinase active
KD	kinase dead
Lat-A	Latrunculin-A
MBP	maltose binding protein
mNG	mNeonGreen
PCH	pombe Cdc15 homology
PI(4)P	phosphoinositides-4-phosphate
PI(4,5)P ₂	phosphatidylinositol-4,5-bisphosphate
PIP	phosphoinositides
PM	plasma membrane
SEM	standard error of the mean
SIN	septation initiation network

SPB	spindle pole body
TRITC	tetramethylrhodamine
wt	wild-type
YE	yeast extract

CHAPTER 1

INTRODUCTION

1.1 Overview of the eukaryotic cell cycle

Cells are the fundamental units of life that must divide in order to propagate life. Cells undergo both periods of growth and division that are organized into distinct phases that compose the cell cycle. Interphase is a cell cycle segment that consists of three phases; G1, S and G2 (Fig. 1-1). G1 and G2 are phases of cell growth and in between these two growth phases is S phase. S phase is when chromosomal DNA is duplicated so that the cell contains two copies of the entire genome. After completion of interphase, cells can undergo the next phase, mitosis (Fig. 1-1). Mitosis is the process of nuclear division wherein the genome is segregated to the opposite poles of the cell. After the genome is segregated, the two halves of the cytoplasm must also be physically separated from one another in order to form two new daughter cells. This process is termed cytokinesis (Fig. 1-1).

Mitosis and cytokinesis are spatially and temporally coordinated to ensure accurate segregation of the genome. Failure to do so can lead to chromosome segregation errors that can be detrimental to cell survival (Fujiwara et al., 2005; Vinciguerra et al., 2010). In addition, complete failure of cytokinesis can lead to tetraploid intermediates that can lead to cell death or cancer (Gordon et al., 2012).

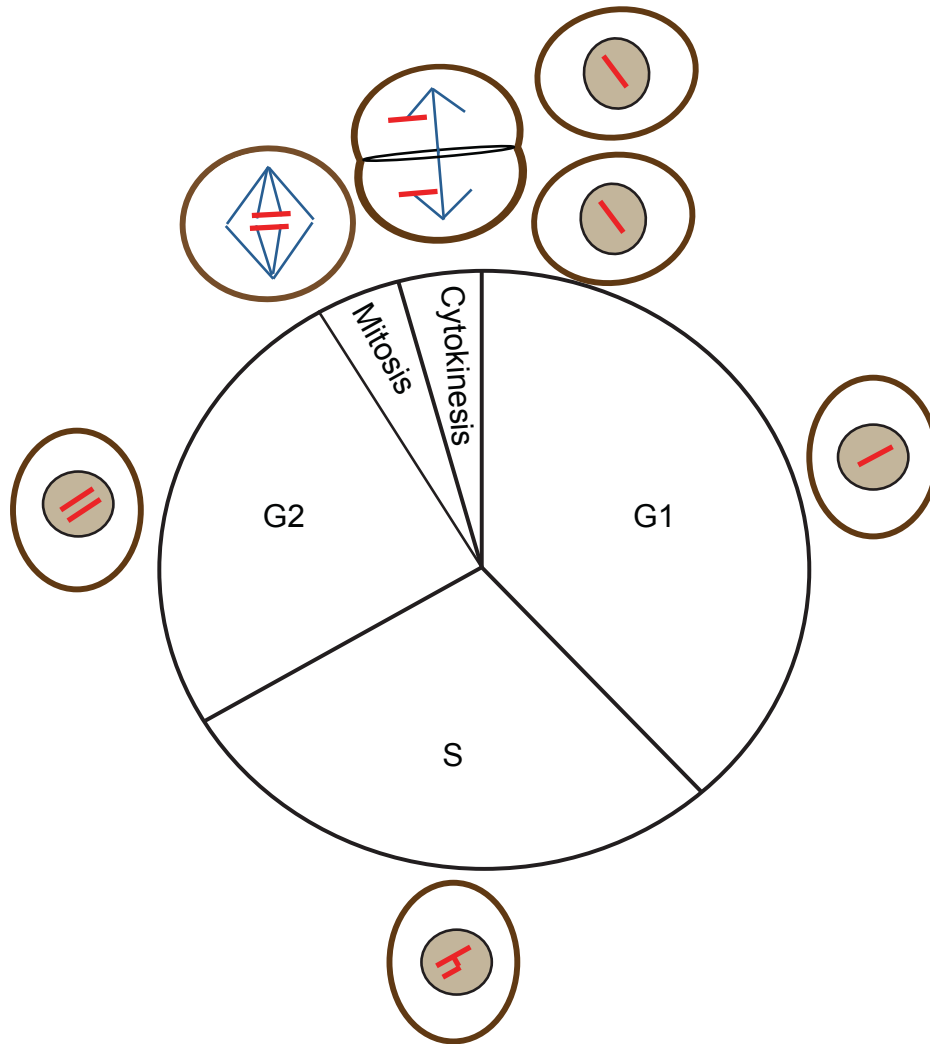


Figure 1-1

Schematic of a canonical eukaryotic cell cycle.

Interphase consists of G1, S, and G2 phases. Cell growth occurs in G1 and G2 phases, and the genome (red) is replicated during S phase. During mitosis, the replicated genome segregates via the mitotic spindle (blue) to the two poles of the dividing cell. Then the two daughter cells are physically separated in cytokinesis using a cytokinetic ring (black). In animal cells (pictured), the nuclear envelope (black) is disassembled during mitosis but re-made after cytokinesis.

To complete cytokinesis many organisms build an F-actin (filamentous actin)- and myosin-based contractile apparatus termed the cytokinetic ring (CR) (Pollard and Wu, 2010) (Fig. 1-2). Constriction of the CR at the division site during cytokinesis leads to the physical separation of the daughter cells. In metazoans, CR ingression manifests as a cleavage furrow in the plasma membrane (PM). The cleavage furrow eventually

constricts into a dense midbody structure that can later be resolved during cellular abscission (Fig. 1-2). In fungi, such as yeasts, cell wall material is deposited behind the ingressing CR and PM at the division plane (Balasubramanian et al., 2012) (Fig. 1-2). Overall, cytokinesis is a conserved process that relies on a myosin- and actin-based contractile apparatus to drive cellular division.

1.2 *Schizosaccharomyces pombe* as a model system to study cell division

Many molecular mechanisms dictating cellular division in higher eukaryotes were initially revealed through studies using simpler model organisms. One such model organism is *Schizosaccharomyces pombe*, which is considered a “fission yeast”. This unicellular organism is rod-shaped due to growth occurring almost solely at the cell tips (Mitchison and Nurse, 1985). The cell length strongly correlates with cell-cycle stage, making *S. pombe* particularly suitable for cell cycle studies. In addition, through multiple genetic screens and years of molecular study, there is nearly a complete list of proteins known to be involved in *S. pombe* cytokinesis, most of which are conserved in higher eukaryotes. Thus, genetic and biochemical analyses using this organism can reveal conserved regulatory mechanisms directing cytokinesis.

While mechanisms regulating cell division are conserved throughout eukaryotes, there are notable differences between the human and fission yeast cell division process. One such difference is that *S. pombe* undergo a closed mitosis wherein the nuclear envelope does not break down during mitosis, whereas human cells disassemble the

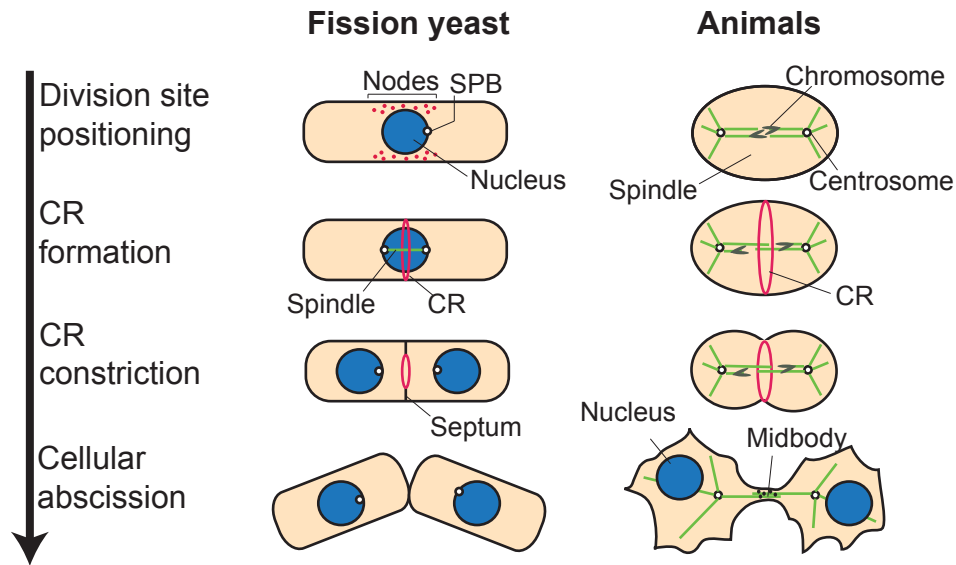


Figure 1-2

Stages of eukaryotic cytokinesis.

Schematics of cytokinesis in fission yeast *Schizosaccharomyces pombe* and animal cells. The individual stages of cytokinesis are shown with the progression through the cell cycle oriented downward. In fission yeast the CR assembles after spindle pole body (SPB) separation from node-like structures containing formin and myosin II, F-BAR Cdc15, IQGAP Rng2 and anillin-like Mid1. Following constriction of the CR in fission yeast, new cell wall is deposited at the division site to form a septum, which is remodeled to allow cell separation. In animal cells the midbody is a dense microtubule-based structure that is a remnant of the anaphase spindle midzone. Abscission occurs via cleavage of the plasma membrane on one side of the midbody.

nuclear envelope in early mitosis and re-form it at the end of cell division. Furthermore, while both build an actomyosin-based CR to complete cytokinesis, they do so during different cell cycle stages (*S. pombe* in early mitosis and human cells in anaphase) and, as noted previously, fission yeast have a cell wall that helps drive cellular division. Despite some differences, *S. pombe* provides an excellent model system to understand molecular mechanisms that are important for cells to divide.

1.2 Formation of the contractile ring in *S. pombe*

Contractile ring precursors

In *S. pombe* the CR forms from cortical precursor nodes that assemble in the cell middle (Wu et al., 2003) (Fig. 1-2). Detailed study of these precursors revealed two distinct populations of cortical nodes, termed type 1 and type 2. Type 1 nodes (containing mitosis-promoting kinases Cdr1 and Cdr2) assemble during interphase and merge with type 2 nodes (containing Blt1, kinesin Klp8p, RhoGEF Gef2 and binding partner Nod1) during G2 (Akamatsu et al., 2014). Late in G2, the anillin-like protein Mid1 is exported from the nucleus and associates with the merged nodes nearby, thereby linking the position of the nucleus to the site of cell division (Paoletti and Chang, 2000; Sohrmann et al., 1996). Upon mitotic entry, core CR components are recruited by Mid1 to the cell division site, including myosin II heavy and light chains (Myo2, Rlc1 and Cdc4), IQGAP Rng2, the F-BAR protein Cdc15, and the formin Cdc12 (reviewed in (Pollard and Wu, 2010)). However, *mid1* is not essential; in its absence, precursor nodes are still formed, but are not tightly restricted to the center of the cell (Saha and Pollard, 2012). In the absence of Mid1, CR formation is reliant on the Septation Initiation Network (SIN, reviewed in (Simanis, 2015)), and occurs later during anaphase (Hachet and Simanis, 2008; Huang et al., 2008). Both mechanisms can lead to CR formation; however, in the absence of *mid1* CRs are often obliquely oriented or off-center (Huang et al., 2008; Saha and Pollard, 2012). In *S. pombe*, Mid1 also recruits the essential polo-like kinase Plo1 and phosphatase Clp1/Cdc14, which may help promote CR assembly before anaphase (Bahler et al., 1998). In a related fission yeast, *Schizosaccharomyces japonicus*, Mid1 also forms cortical nodes that anchor CR components, but it is not required for

positioning the CR in the cell middle (Gu and Oliferenko, 2015). Outside of fission yeasts, CR precursor nodes have not been conclusively observed. Despite this, the molecules and mechanisms used in *S. pombe* CR formation appear to be widely conserved throughout eukaryotes (Pollard and Wu, 2010).

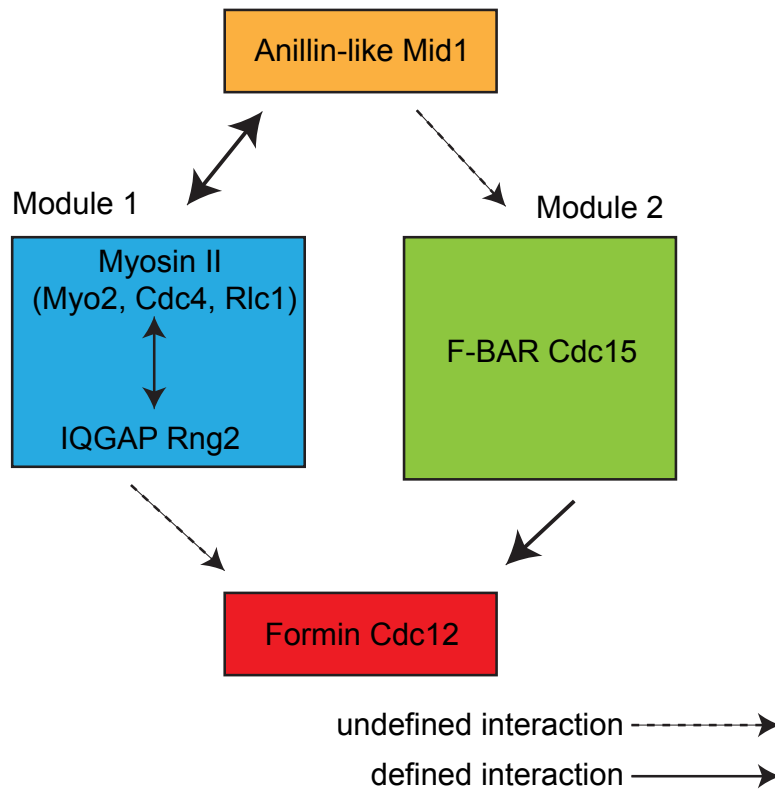


Figure 1-3

Mid1 sets up two redundant module of protein recruitment for CR formation.

The anillin-like Mid1 (orange) organizes two parallel modules of protein recruitment at the cell division site. The first module consists of functional myosin II and the IQGAP protein Rng2 (Blue). The second module consists of the F-BAR scaffold Cdc15 (green). Both modules converge to recruit formin Cdc12 to the cell division site (red). Cdc12 then makes the F-actin for the CR.

An ordered assembly of components?

During CR formation, proteins are recruited to the cell division site in precise order, suggesting a hierarchical mechanism of ring assembly (Laporte et al., 2011; Wu et

al., 2003). Mid1 localizes to the cell middle in G2, Rng2 and Myo2 localize to nodes ~10 minutes prior to spindle pole body (SPB) separation, and formin Cdc12 and F-BAR Cdc15 accumulate in nodes as SPBs separate. In addition, it is proposed that Mid1 organizes two distinct modules of protein recruitment to build the CR (Laporte et al., 2011) (Fig. 1-3). The first module consists of IQGAP Rng2 and functional Myosin II (Myo2, Rlc1 and Cdc4). The second module consists of the F-BAR scaffold Cdc15. Both of these modules then converge to promote the recruitment of the formin Cdc12 to the cell division site where it makes the F-actin in the CR (Fig. 1-3). After all the components arrive to the cell division site the precursor nodes condense into a ring ~10 minutes after SPB separation in mitosis (Laporte et al., 2011; Padmanabhan et al., 2011; Sohrmann et al., 1996; Wu et al., 2003) (Fig. 1-2). The importance of ordered assembly was tested by ectopically localizing CR proteins to medial precursor nodes in the absence of Mid1 (Tao et al., 2014). Interestingly, Rng2, Myo2 and Cdc12, but not Cdc15, were each able to initiate CR formation when they were the first to arrive at the medial cortex. Therefore, an invariant order of recruitment is not strictly required; instead, these core proteins appear to collaborate to build the CR. Future mechanistic studies are needed to clarify why some core proteins (Cdc12, Myo2 and Rng2) are competent for promoting ectopic CR formation while others (Cdc15) are not.

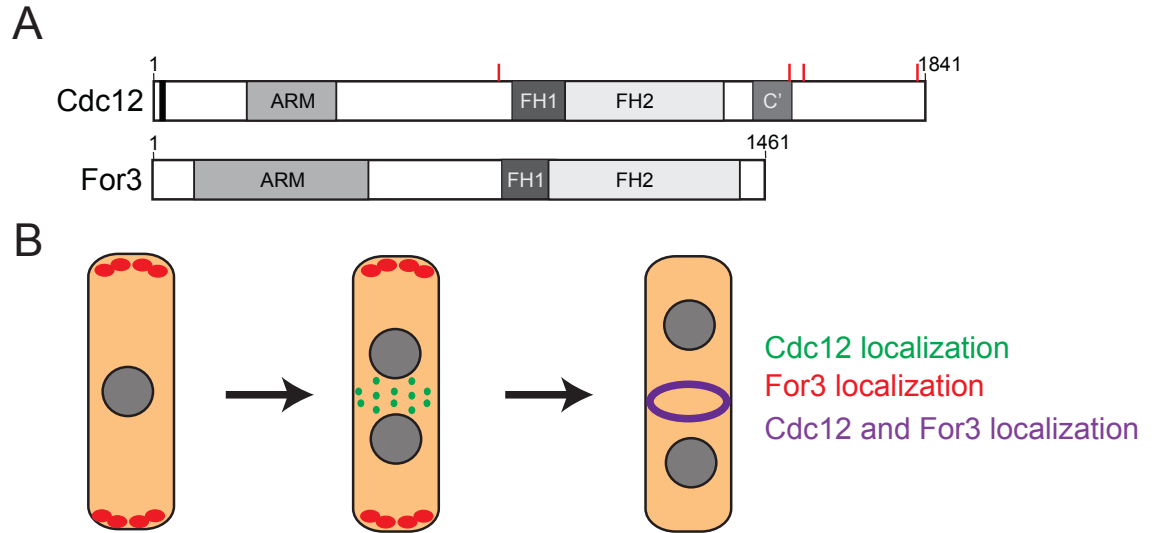


Figure 1-4

Two *S. pombe* formins, Cdc12 and For3, are important for contractile ring formation.

(A) A schematic of the domain layout of Cdc12 and For3 drawn to scale. The red lines on Cdc12 represent the residues that are phosphorylated by Sid2. (B) A schematic of the localization of Cdc12 and For3 throughout the cell cycle. During interphase For3 localizes to the cell tips in a punctate pattern (Red). In early mitosis Cdc12 localizes to medial cortical nodes as the CR forms (Green). Once the CR is fully formed both Cdc12 and For3 co-localize in the CR (Purple).

1.4 Introduction to Formins

Formin domains and mechanisms of action

The formin family of F-actin assembly factors are defined by FH (formin homology) domains. The FH1 and FH2 domains comprise a characteristic core responsible for multiple formin activities (Figs. 1-4A, 1-5). Dimeric FH2 domains (Xu et al., 2004) are sufficient to nucleate F-actin assembly *in vitro* (Pruyne et al., 2002; Sagot et al., 2002) (Fig. 1-5), but *in vivo* may also interact with cofactors such as budding yeast Bud6, which enhances nucleation efficiency (Graziano et al., 2011). Whereas FH2 domains remain processively associated to F-actin barbed ends with high affinity (Kovar et al., 2006; Kovar and Pollard, 2004; Pruyne et al., 2002), rapid F-actin elongation also requires FH1 domain binding to the actin monomer-binding protein profilin via poly-

proline tracts (Fig. 1-5)(Kovar et al., 2003; Romero et al., 2004; Sagot et al., 2002) The FH1 domain increases local G-actin (globular actin) concentrations near the FH2 domain and is hypothesized to orient monomers on to the FH2-associated barbed end (Kovar et al., 2003; Otomo et al., 2005; Vavylonis et al., 2006). How are the actin assembly properties of the formin FH1–FH2 core regulated? One mode of formin regulation

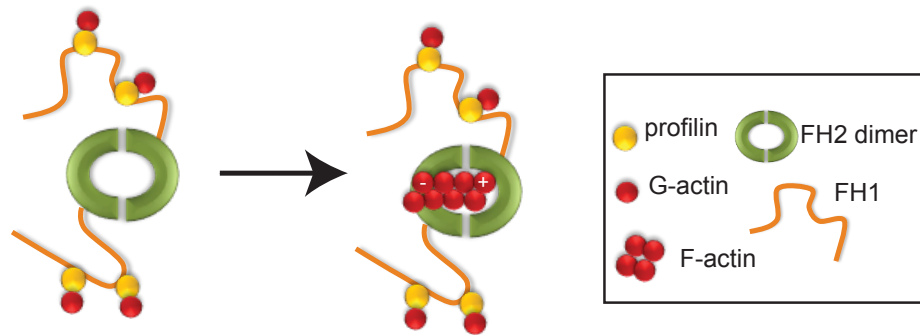


Figure 1-5

Formins nucleate and elongate F-actin.

All Formins contain Formin Homology 1 and 2 domains (FH1, FH2). The FH1 domain is predicted to be a rope-like domain that bind profilin-G-actin complex via poly-proline tracts. The dimeric FH2 domain is sufficient for nucleation of F-actin but requires additional G-actin monomers via delivery from the FH1 domain in order to elongate F-actin. The FH2 domain remains associated with the barbed (plus) end of F-actin filaments and therefore competes with capping factors.

involves two additional formin domains, the N-terminal DID (diaphanous inhibitory domain) and the C-terminal DAD (diaphanous autoregulatory domain) (Fig. 1-4A). DID–DAD *cis* interactions can establish an autoinhibitory conformation that precludes F-actin assembly by the FH1–FH2 core (Chesarone et al., 2010). Formins autoregulated by DID–DAD interactions must be freed from autoinhibition for full activity. Interaction with Rho proteins, via Rho-binding domains near the DID domain on formins, commonly relieves DID–DAD autoinhibitory interactions partially (Chesarone et al., 2010), although some formins, including *Saccharomyces cerevisiae* Bni1 and mammalian FHOD1, are freed from autoinhibition by phosphorylation on the C-terminus near the DAD motif (Takeya et

al., 2008; Wang et al., 2009). It should be noted that not all formins are regulated in this manner; some formins do not contain DID and/or DAD domains (ex. metazoan INF1, Delphilin, FHOD1 and FMN1) (Higgs, 2005) while other formins contain these domains but they do not seem to control formin activities (ex. fission yeast Cdc12) (Yonetani et al., 2008). Further mechanistic studies are needed to gain insight into DID/DAD-independent modes of formin regulation.

Beyond nucleation and elongation, formins modify the actin cytoskeleton through additional activities, such as F-actin bundling and severing. Intriguingly, some formins, including mammalian formins FRL1 and mDia2 and plant formin FH8, perform these activities via their FH1–FH2 domains, whereas others, including mammalian formins INF2 and FRL2 and yeast Cdc12 possess distal domains responsible for these functions (Bohnert et al., 2013; Takeya et al., 2008; Wang et al., 2009). In the future, it will be important to clarify the conservation of these additional activities among eukaryotic formins and the extent to which they influence formin-mediated actin assembly.

Cytokinetic formin function in cytokinesis

Formins participate in cytokinesis in a variety of eukaryotes, ranging from single-celled yeast to multicellular organisms. In *S. cerevisiae*, two formins, Bni1 and Bnr1, localize to the bud neck and together are required for assembly of an actin-based CR (Imamura et al., 1997; Tolliday et al., 2002). A strain lacking both formins exhibits a high degree of multinucleation, whereas those lacking either individually undergo relatively efficient cytokinesis (Imamura et al., 1997) suggesting they perform redundant functions

in cytokinesis. Although F-actin is required for budding yeast cytokinesis (Bi et al., 1998), myosin-independent cytokinesis can occur in certain strain backgrounds by a mechanism relying on septins and abnormal cell wall deposition (Tolliday et al., 2003). Formins affect myosin-independent cytokinesis in *S. cerevisiae* because Bni1-mediated actin assembly influences septin ring formation, and Bnr1 and Bni1 interact with the chitin synthase activator Hof1 (Kamei et al., 1998), an F-BAR protein whose homologue Cdc15 in fission yeast *S. pombe* likewise participates in a formin interaction during cytokinesis (Carnahan and Gould, 2003) (Fig. 1-3). Rho binding and phosphorylation affect cytokinetic formin targeting and activation in *S. cerevisiae*. Specifically, Bnr1- and Bni1-dependent actin assembly is influenced by Rho1, Rho3 and Rho4 GTPases (Dong et al., 2003; Tolliday et al., 2002), and phosphorylation of Bni1 by Prk1 facilitates Bni1 activation to relieve DID-DAD autoinhibition (Wang et al., 2009).

In metazoans, formins are central players in cytokinesis, although the range of their activities towards actin and their mechanisms of regulation are less characterized. Both *Caenorhabditis elegans* and *Drosophila melanogaster* require formins CYK-1 and Diaphanous respectively for early embryonic divisions, owing to their essential roles in building the cytokinetic machinery (Castrillon and Wasserman, 1994; Severson et al., 2002). In human cells, formin mDia2 localizes to the division site and nucleates F-actin for CR formation (Watanabe et al., 2008). Furthermore, mDia2, similar to budding yeast Bnr1 (Moseley and Goode, 2005), bundles F-actin *in vitro* (Harris et al., 2006) hinting that cytokinetic formins may generally cross-link F-actin to aid in CR formation. At the conclusion of cytokinesis, mDia2 is primed for degradation by ubiquitination (DeWard

and Alberts, 2009), providing a turnover mechanism that may be pertinent to CR disassembly.

Despite the studies described above, our understanding of how cytokinetic formins function and are regulated is incomplete. To provide a more comprehensive view, our laboratory is interested in defining mechanisms controlling the sole fission yeast cytokinetic formin, Cdc12. Although it is the least abundant protein that has been measured at the fission yeast CR (Wu and Pollard, 2005), Cdc12 is essential for *S. pombe* cell division. In its absence, cells undergo mitosis, but never form a CR, and *cdc12*-null cells die as multinucleates (Chang et al., 1997). As the timing and relative order of events has been well described for *S. pombe* cytokinesis and a catalogue of molecular participants has been established (Pollard and Wu, 2010), *S. pombe* provides a useful genetically tractable system in which to investigate formin contributions to cell division. As discussed below, many elements of Cdc12 function and regulation remain to be clarified.

Regulation of formins during *S. pombe* contractile ring assembly

After amassing core CR machinery at the cell middle, precursor nodes condense into a contiguous ring prior to anaphase, a process which can be modeled by a search-capture-pull-release mechanism (Vavylonis et al., 2008). A primary driver of this process is actin nucleation and elongation by the formin Cdc12. Thus, how the formin Cdc12 is targeted to and regulated at the site of division has been the subject of several recent studies.

One study shed light on how Cdc12 finds the cell middle. Specifically, a binding interaction between a short motif in Cdc12's N terminus and the F-BAR domain of the scaffolding protein Cdc15 was shown to contribute to Cdc12 recruitment (Carnahan and Gould, 2003; Willet et al., 2015a) (Fig. 1-4A). In the absence of this interaction, F-actin and F-actin binding proteins accumulate less and CR formation was delayed (Willet et al., 2015a). This and previous studies point to the existence of additional targeting cues within the Cdc12 protein, the nature of which are currently being investigated (Yonetani et al., 2008).

Two other recent studies provided insight into Cdc12 regulation. One study reported that formin function is limited simply through competition with other F-actin nucleators for G-actin monomers, based on the observation that inhibition of the branched actin nucleator Arp2/3 increased the abundance of formin-nucleated actin structures and vice versa (Burke et al., 2014). Although profilin binds all G-actin in the cell, it also directly binds the FH1 domain, favoring formin-mediated F-actin nucleation over Arp2/3-mediated F-actin nucleation, even though the Arp2/3 complex is more abundant (Suarez et al., 2015). Thus, modulation of profilin levels or its interaction with Cdc12 could be means of regulating Cdc12 nucleation and elongation activities at the division site.

In another study tackling the question of Cdc12 regulation, a multimerization domain was identified in Cdc12's C-terminus (Fig. 1-4, C'), which during interphase mediates oligomerization to form puncta of different sizes on the cortex. In mitosis, when the SIN becomes active, Cdc12 is phosphorylated on 4 residues by the SIN kinase Sid2 (Fig. 1-4A), inhibiting multimerization and consequent F-actin bundling (Bohnert et al.,

2013). Without Sid2-mediated inhibition of Cdc12 multimerization, the CR cannot be formed in the absence of Mid1 or maintained in a cytokinetic arrest, establishing multimerization as one layer of Cdc12 regulation that is essential for proper CR assembly and maintenance. Thus far, purified formins have been found to be strictly dimeric so it remains to be determined if other formins multimerize in a regulated manner in cells. Also, whether multimerization and F-actin bundling impact the F-actin nucleation and elongation activities of Cdc12's catalytic core awaits further study.

Interestingly, once the CR has formed, Cdc12 function appears to become dispensable for the completion of cytokinesis. Although F-actin turns over quickly in the CR, Cdc12 is not required for CR constriction *in vitro* (Mishra et al., 2013). In light of this finding, it will be interesting to learn whether Cdc12 activity is purposefully terminated to ensure efficient CR constriction and the associated reduction in F-actin.

While Cdc12's function is restricted to CR formation (Chang et al., 1997; Yonetani et al., 2008), formin For3 forms longitudinal actin cables important for polarized cell growth (Feierbach and Chang, 2001) (Fig. 1-4B). *Johnson et al.* ectopically localized each formin to cell tips or the cell middle in the absence of the other formin (Johnson et al., 2014). Intriguingly, each formin formed F-actin with specific properties: Cdc12 formed F-actin with a high growth rate bound by acetylated tropomyosin, while For3 nucleated F-actin with a slow growth rate bound by unacetylated tropomyosin. Tropomyosin is important for stabilizing F-actin structures, especially the CR, and acetylated tropomyosin is a more stable conformer (Skau et al., 2009; Skoumpla et al., 2007; Stark et al., 2010). Despite forming F-actin without acetylated tropomyosin, For3 was able to form a CR, but these rings often collapsed, demonstrating that Cdc12's

unique properties are important for CR stability. It will be interesting to determine if other actin binding proteins exhibit a preference for F-actin nucleated by certain formins and the mechanism of this specificity. In addition, that Cdc12 could form actin structures

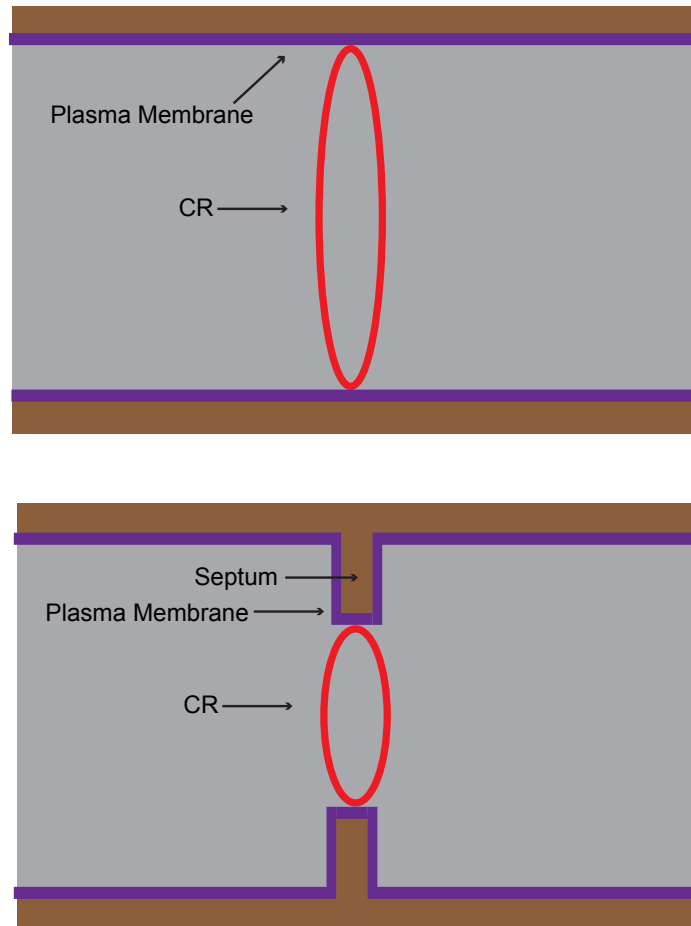


Figure 1-6

Roles of septation in *S. pombe* cytokinesis.

Top) Once the CR (red) is formed it remains tightly associated with the plasma membrane (purple). Bottom) Primary and secondary septa (brown) are formed simultaneously as the contractile ring constricts. Formation of the septum “locks” the ring into place and prevents sliding from the cell middle.

when forced to localize to the cell tip suggests that it may not have regulated activity, but rather cell cycle regulated localization to controls its function.

Although For3 and Cdc12 have distinct properties and Cdc12 is the only formin required for cytokinesis, For3-nucleated F-actin cables are also pulled into the CR in *S. pombe* (Arai and Mabuchi, 2002; Huang et al., 2012). Cells lacking *for3* have synthetic lethal genetic interactions with many essential players in CR formation, further supporting a role for this actin network during the initial stages of cytokinesis (Coffman et al., 2013). *cdc12* alleles lacking an N-terminus ($\Delta 503cdc12$) are also synthetically lethal in combination with *for3* Δ , suggesting that when Cdc12 function is compromised, For3's function becomes essential for cell division. Animal cells also assemble the cleavage furrow with a combination of pre-existing cortical actin cables and de novo formin-based F-actin assembly (Green et al., 2012). Thus, while both of these formins play a role in CR formation, their roles are distinct. Cdc12 is essential for de-novo F-actin formation at the cell division site whereas For3 makes actin cables that also incorporate into the CR.

1.5 Formation of a division septum

Function of glucans in the division septa

Once the CR is formed, it constricts in a myosin-dependent manner (Mishra et al., 2013; Stachowiak et al., 2014). However, as cell-walled organisms, cytokinesis in *S. pombe* also requires the synthesis of a new cell wall between daughter cells. A tri-layer division septum, composed of an inner primary septum flanked by secondary septa, is deposited behind the constricting actomyosin ring to maintain a contiguous cell wall (Fig. 1-5). After septum formation, glucanases are secreted to break down the inner primary

septum, which splits the daughter cells. Degradation of the primary septum in combination with outward turgor pressure facilitates gentle separation and rounding of each daughter cell's new end (Cortes et al., 2012).

The *S. pombe* primary septum is predominantly composed of linear $\beta(1,3)$ glucans, while the SS contains $\alpha(1,3)$ glucans, branched $\beta(1,3)$ glucans, linear $\beta(1,3)$ glucans, and galactomannans (Humbel et al., 2001). *S. pombe* septa do not contain chitin, unlike the prominent chitin ring present at *S. cerevisiae* septa (Roncero and Sanchez, 2010). At least three essential glucan synthases form the primary and secondary septa; catalytic subunits of these complexes are Bgs1, Bgs4, and Ags1. Bgs1 forms linear $\beta(1,3)$ glucans and is essential for primary septum formation. Bgs4 forms branched $\beta(1,3)$ glucans, while Ags1 forms $\alpha(1,3)$ glucans.

Recent work has defined the functions of Bgs4-derived branched β -glucans and α -glucans produced by Ags1. When Ags1 function was compromised, the primary septum was improperly anchored to the cell wall and grew in an uncoordinated manner toward the cell middle (Cortes et al., 2012). In the absence of efficient anchoring, the primary septum often tore and cells lysed during separation. Thus, α -glucans are required to anchor the primary septum to the cell wall. Branched β -glucans, on the other hand, are an essential component of the secondary septa. Cells lacking branched β -glucans never formed a secondary septum, and only formed a twisted and unsupported primary septum (Munoz et al., 2013). If cells attempted to separate without a secondary septum, over-degradation of cell wall material occurred, resulting in lysis. Therefore, linear β -glucans, branched β -glucans, and α -glucans formed by Bgs1, Bgs4, and Ags1, are all essential, cooperating to build the division septum.

Septum formation forces

Septum formation has been recognized for years as necessary for CR constriction and completion of cytokinesis. Certain mutations compromising Bgs1 (*cps1-191*) lead to cell cycle arrest and the maintenance of CRs without constriction (Liu et al., 2000; Liu et al., 1999). In the absence of microtubules (presumably impacting the cell polarity machinery) CRs in *cps1-191* cells slid toward cell tips, suggesting they were dynamic and not locked into their medial position (Pardo and Nurse, 2003).

More information has emerged recently to explain how septum formation contributes to CR stabilization and constriction. First, with more advanced microscopy techniques, it has been confirmed that compromising glucan synthase activity permits CRs to slide and unravel (Arasada and Pollard, 2014; Munoz et al., 2013). This has also been evident in spheroplast studies; when cell walls were removed by digestion and prevented from re-forming, CRs slid from the cell middle (Stachowiak et al., 2014). However, when digesting enzymes were removed from spheroplasts, CRs formed and pinched the cell (Mishra et al., 2013). Formation of the septum, therefore, is capable of “locking” the CR in place (Fig. 1-5).

In addition to preventing CR sliding, recent measurements of the forces necessary for cell division indicate septum formation contributes the predominant constriction force, in accord with its requirement for cell division. The CR and septum must overcome turgor pressure, which in *S. pombe* cells is ~1 MPa (Proctor et al., 2012). Calculations of the maximum force myosin motors in the CR can exert (~15 nN, 10 kPa) indicate myosins within the CR are not sufficient (Proctor et al., 2012). Synthesis of extracellular

glucans may be able to exert a “ratchet” force as glucan synthases add subunits to glucan chains, which push against the PM, similar to models proposed for actin at the leading edge of animal cells (Mogilner and Oster, 2003; Proctor et al., 2012). Further mechanistic study of glucan synthases and glucan chains will clarify how this force is generated. The dependence on septum synthesis for CR constriction is similar in *S. cerevisiae* and possibly other cell walled organisms (Roncero and Sanchez, 2010; Schmidt et al., 2002). Animal cells, on the other hand, do not need to overcome large turgor pressures and can constrict with the force of myosin alone; however, there are contexts where extracellular elements contribute to cytokinesis in animal cells as well (Mizuguchi et al., 2003; Xu and Vogel, 2011).

These conclusions have led to speculation about the purpose of the CR in fungi, if not to provide force for ingression. In *S. cerevisiae*, cytokinesis can complete in the absence of myosin-II through the over-synthesis of chitin to physically separate the daughter from mother bud (Tolliday et al., 2003). In *S. pombe*, cells are able to complete cell division even when the F-actin in their CRs is depolymerized after constriction has begun (Proctor et al., 2012; Zhou et al., 2015). However, F-actin depolymerization does not remove all components of the CR. Presumably the remaining proteins keep the glucan synthases active to complete division, similar to the *S. cerevisiae* chitin synthesis mechanism. CR contractility (through Myo2) has also been shown (historically and recently (Mishra et al., 2013)) to be essential for CR constriction. The CR, therefore, remains essential for each step in cytokinesis: positioning the division plane, recruiting cytokinetic proteins, and activating constriction and septum synthesis. Furthermore,

clearance of CR remnants is required to reinitiate polarized growth at new daughter cell ends (Bohnert and Gould, 2012).

1.6 A primer on plasma membrane lipid composition and cytokinesis

Tight association of the CR and PM throughout the CR constriction process ensures that the PM closes inward to form a physical barrier between the two new daughter cells. Therefore, precise PM lipid composition is thought to be important in cytokinesis due to the tight association of the CR and PM (Fig. 1-5) and many proteins important for cytokinesis directly bind lipids (Cauvin and Echard, 2015). PI4P, PI(4,5)P₂ and PI-kinases have been shown to be important for cytokinesis in various organisms. In human cells, PI(4,5)P₂ and PI-5 kinases are enriched at the cleavage furrow during cytokinesis (Emoto et al., 2005; Field et al., 2005) and depletion of PI(4,5)P₂ causes detachment of the cortical actin from the PM (Emoto et al., 2005; Field et al., 2005). In *Drosophila* when the PI-4-kinase, PI4KIII α , is depleted from cells, they fail cytokinesis and become tetraploid (Brill et al., 2000b; Eggert et al., 2004b). A fission yeast PI-4-5-kinase, Its3, was also found to be important for proper cell division and septation, and our lab recently found that deletion of a *S. pombe* PI-4-kinase scaffold (*efr3 Δ*) leads to abnormal off-center divisions (Chen et al., 2014). It is hypothesized that cells with altered lipid composition have mis-localized PIP-binding proteins that are important for adhering the CR to the PM. However the exact complement of proteins that rely on these lipid species for proper localization during cytokinesis has not been reported.

1.7 Summary

In this work, I will describe mechanisms of protein regulation that contribute to CR formation and anchoring important for cytokinesis. In chapter 2, I will define the direct interaction between formin Cdc12 and the F-BAR of Cdc15 and describe how this interaction is important for Cdc12 recruitment to the division site and timely formation of the CR. In chapter 3 I will build upon my findings in chapter 2 by investigating the role of Cdc12 phospho-regulation by Cdk1. Lastly, in chapter 4 I will describe how a lipid kinase scaffold is important to anchor the newly formed CR in its medial position by resisting perpendicular forces in a myosin V-dependent manner. All together these studies have advanced our understanding of the mechanisms of protein recruitment and post-translation modification that are needed to orchestrate the formation and anchoring of the contractile apparatus for faithful cytokinesis.

CHAPTER 2

THE F-BAR CDC15 PROMOTES CONTRACTILE RING FORMATION THROUGH DIRECT RECRUITMENT OF THE FORMIN CDC12

Willet AH, McDonald NA, Bohnert KA, Baird MA, Allen JR, Davidson MW, Gould KL
(2015)

The Journal of Cell Biology 16;208(4):391-9

2.1 Introduction

Cytokinesis is the terminal stage in cell division that results in the physical separation of two daughter cells. In many eukaryotic cells, an actomyosin-based cytokinetic ring (CR) forms between the two segregated genomes and eventually constricts, dividing the mother cell into two daughter cells. In *Schizosaccharomyces pombe*, a powerful model organism for cytokinesis studies, assembly of the CR relies on a single formin, Cdc12, which is essential for nucleation and elongation of F-actin during CR formation (Chang et al., 1997; Kovar et al., 2003; Kovar and Pollard, 2004; Nurse et al., 1976), and also contributes to CR maintenance by bundling F-actin (Bohnert et al., 2013). Cdc12 recruitment to the medial cortex during CR formation relies on two redundant genetic modules (Laporte et al., 2011; Wachtler et al., 2006). Specifically, mutation of either IQGAP Rng2 or Myosin II in combination with the FER/Cip4 homology Bin–Amphiphysin–Rvs (F-BAR) scaffold Cdc15 eliminates Cdc12 recruitment to the division site and CR formation (Laporte et al., 2011). However, the mechanistic contributions of these genetic pathways are unknown.

Cdc15 is the founding member of the Pombe Cdc15 Homology (PCH) family of proteins, which generally dimerize and bind membranes through their conserved N-terminal F-BAR domains (Tsujita et al., 2006) and interact with proteins through C-terminal protein-binding domains (Roberts-Galbraith and Gould, 2010). Although Cdc15 is essential for cytokinesis, it is unclear whether Cdc15's role in Cdc12 recruitment is important for CR assembly. Some studies reported that *cdc15* temperature sensitive mutants lack CRs, or produce them in only a fraction of cells (Carnahan and Gould, 2003; Chang et al., 1996; Fankhauser et al., 1995). Others found that cells lacking *cdc15* formed rings of F-actin at the cell middle during early stages of mitosis but these rings were not maintained during anaphase, leading to the conclusion that CR formation per se is independent of Cdc15 (Arai and Mabuchi, 2002; Arasada and Pollard, 2014; Balasubramanian et al., 1998; Hachet and Simanis, 2008; Laporte et al., 2011; Wachtler et al., 2006). Given that Cdc15 defines one of two genetic pathways of formin recruitment (Laporte et al., 2011), it is important to clarify its role in CR assembly. To do so, we defined the Cdc15-binding motif within the Cdc12 N-terminus and constructed Cdc12 mutants that cannot interact with Cdc15. Cells lacking the Cdc12-Cdc15 interaction assembled CRs but had reduced Cdc12 in the CR, a delay in the medial accumulation of F-actin and actin-binding proteins, delayed CR formation, and were unable to survive other perturbations to CR assembly. Thus, the Cdc12-Cdc15 interaction is an important contributor to Cdc12 localization and CR formation.

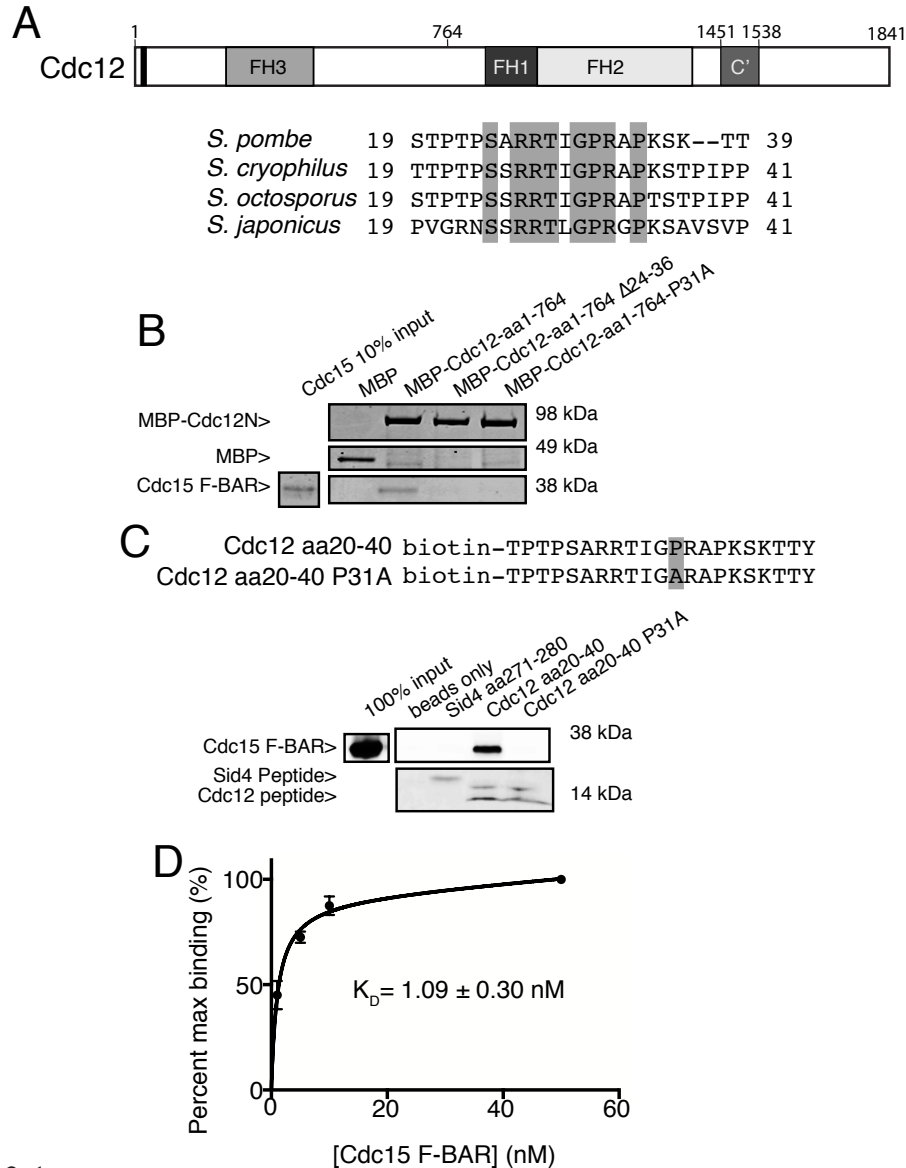


Figure 2-1

An N-terminal Cdc12 motif directly interacts with the Cdc15 F-BAR.

(A) A drawn to scale schematic of Cdc12 with the relative position of amino acids 24-36 indicated by a black bar, and other relevant amino acids and domains indicated. Below is a ClustalW alignment of Cdc12 amino acids 19-39, with sequences from *Schizosaccharomyces cryophilus* (SPOG_01981), *Schizosaccharomyces octosporus* (SOCG_00524) and *Schizosaccharomyces japonicus* (SJAG_11279) Cdc12-related proteins. Shading indicates identical amino acids. (B) In vitro binding of bead-bound recombinant MBP, MBP-Cdc12aa1-764, MBP-Cdc12aa1-764-Δ24-36 or MBP-Cdc12aa1-764-P31A with recombinant Cdc15 F-BAR(19-312). Samples were washed, resolved by SDS-PAGE and stained with Coomassie blue. (C) Above sequence of Cdc12 peptides with variation in sequence shaded. Below, peptides conjugated to streptavidin beads were incubated with recombinant Cdc15 F-BAR(19-312). Samples were washed, resolved with SDS-PAGE and bead-bound proteins were detected by immunoblotting. An unrelated peptide (Sid4-aa271-280) was used as a negative control. (D) Titration of Cdc12(20-40) with Cdc15 F-BAR(19-312). Binding assays were performed with increasing concentrations of Cdc15 F-BAR(19-312) and the amount of bound protein was measured. The dissociation constant was determined with least-squares fitting (Graphpad Prism 6.)

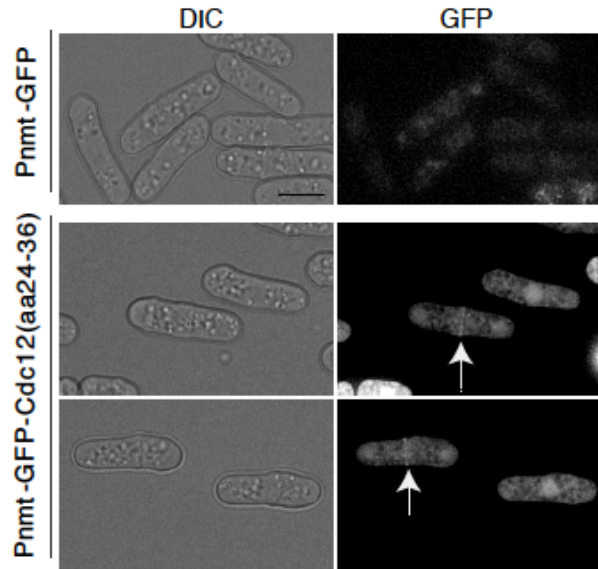


Figure 2-2

The conserved Cdc12 motif promotes Cdc12 localization to the cell middle.

Cells expressed either GFP alone or GFP-Cdc12aa24-36 off a plasmid under control of the *nmt81* promoter for 24 hours at 32°C. Arrows indicate localization of GFP-Cdc12-aa24-36 in a ring at the cell middle. Bar, 5 µm.

2.2 Results and discussion

Cdc12 binds the Cdc15 F-BAR through a conserved N-terminal motif

We previously detected an interaction between Cdc15 and the Cdc12 N-terminus that depended upon the phosphorylation state of Cdc15 (Carnahan and Gould, 2003; Roberts-Galbraith et al., 2010). The Cdc12-Cdc15 interaction was unprecedented because it involved the F-BAR domain of Cdc15 rather than its SH3 domain (Carnahan and Gould, 2003). Because the first 151 residues of Cdc12 localized GFP to the division site (Yonetani et al., 2008), we examined these amino acids for a candidate Cdc15-interaction motif. Sequence comparison of Cdc12 1-151 with its orthologs in other *Schizosaccharomyces* species revealed one conserved motif (aa24-36) (Fig. 2-1A). Deletion of this motif (Δ 24-36) or mutation of a conserved proline within it (P31A) resulted in loss of interaction with the Cdc15 F-BAR domain *in vitro* (Fig. 2-1B). A

synthetic peptide containing the motif (aa20-40) bound the Cdc15 F-BAR, while mutation of P31 to alanine within the peptide abolished the interaction (Fig. 2-1C). Titration binding assays between the Cdc12 peptide and the Cdc15 F-BAR revealed a

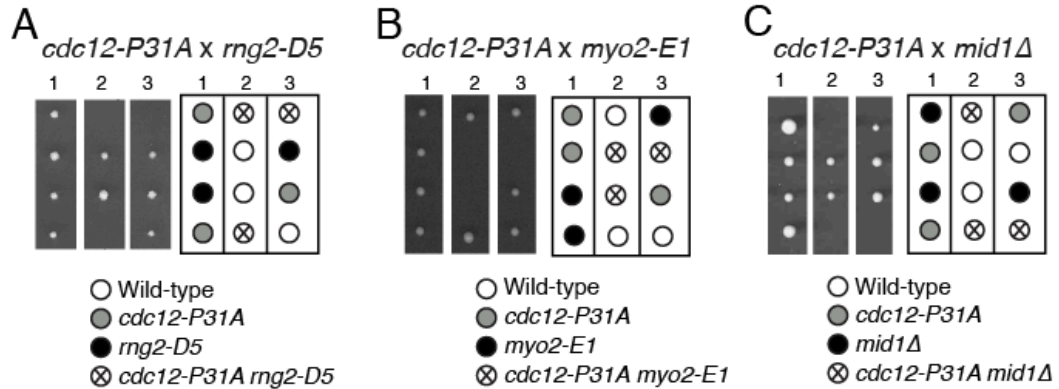


Figure 2-3

Genetic interactions of mutant *cdc12-P31A*.

Tetrads from *cdc12-P31A* crossed to (A) *rng2-D5*, (B) *myo2-E1* and (C) *mid1Δ* are shown with a schematic of relevant genotypes.

dissociation constant of 1.1 nM, indicating a strong affinity (Fig. 2-1D). Because Cdc12 is a low abundance protein (Wu and Pollard, 2005), a strong interaction may be necessary to recruit or maintain it at the cell middle. In fact, other protein-protein interactions that promote the localization of other formins are also in the nM affinity range (Brandt et al., 2007; Watanabe et al., 2010). As might be expected from this tight association, Cdc12 (aa24-36) fused to GFP localized to the division site (Fig. 2-2), supporting the possibility that this motif participates in directing Cdc12 to the cell middle.

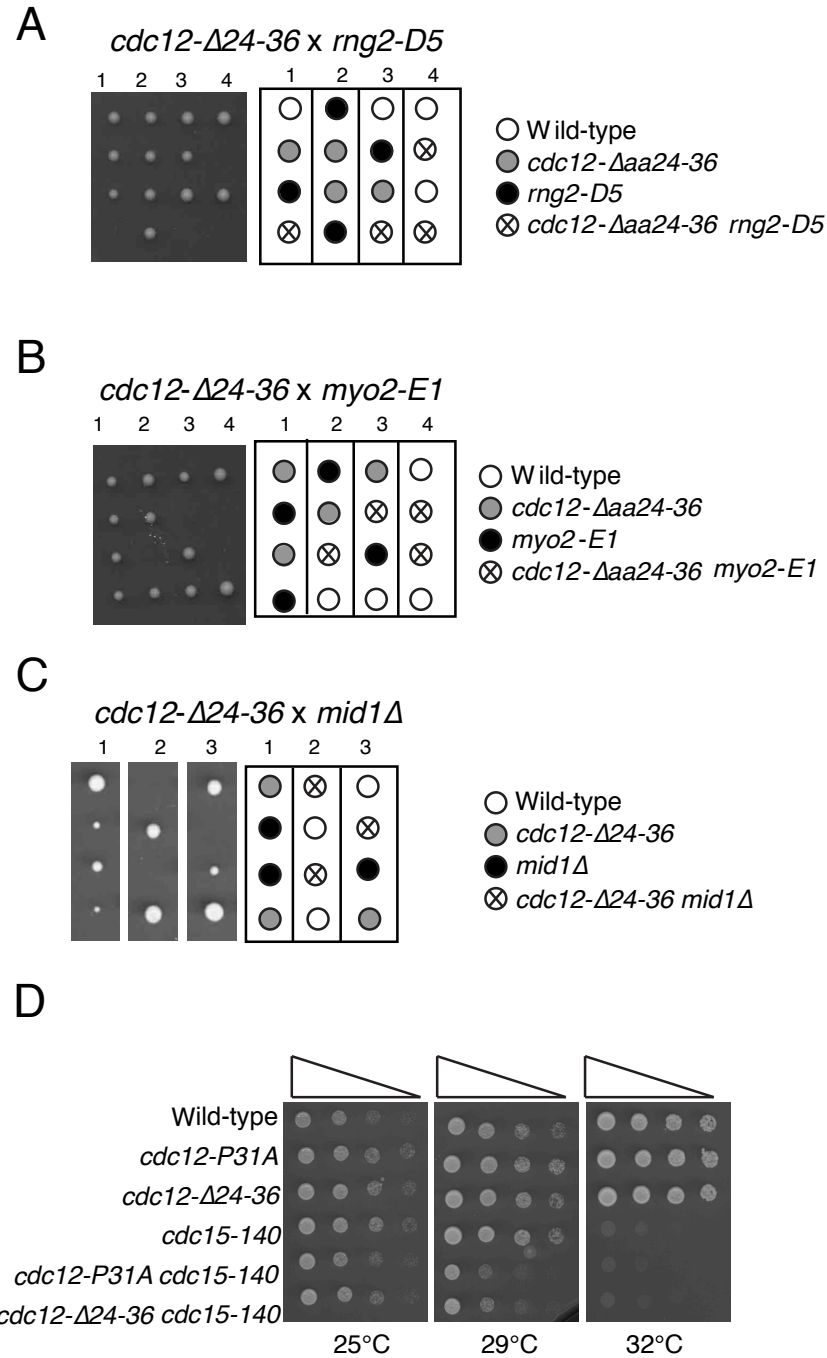


Figure 2-4

Genetic interactions of the mutant *cdc12-Δ24-36* and *cdc12-P31A*.

Tetrads from *cdc12-Δ24-36* crossed to (A) *rng2-D5*, (B) *myo2-E1* and (C) *mid1Δ* are shown with a schematic of the relevant genotypes. (D) Serial 10-fold dilutions of the indicated strains at the indicated temperatures.

Cells lacking the Cdc12-Cdc15 interaction are prone to cytokinesis failure

To determine the functional consequence of disrupting the Cdc12-Cdc15 interaction, we constructed *cdc12* alleles at the endogenous locus in which the binding motif was mutated or deleted. While *cdc12*-P31A and *cdc12*- Δ 24-36 cells are viable, they displayed synthetic lethal genetic interactions with *rng2*-D5, *myo2*-E1 and *mid1* Δ (Fig. 2-3A-C, Fig. 2-4A-C). Myo2, Rng2 and Mid1 contribute to Cdc12 recruitment through a common genetic pathway distinct from Cdc15 (Laporte et al., 2011) and therefore synthetic lethality likely results from the combined disruption of both Cdc12 recruitment pathways. *cdc12*-P31A and *cdc12*- Δ 24-36 did not show a strong genetic interaction with *cdc15*-140 (Fig. 2-4D), as would be expected if these alleles disrupt a major Cdc15 pathway during cytokinesis.

Cdc12-Cdc15 interaction is important for normal Cdc12 recruitment

In order to test if Cdc12 binding to Cdc15 influences Cdc12 localization to the CR, we tagged wild-type and mutant alleles with a single copy of mNeonGreen (mNG), a brighter and more photostable variant of GFP (Shaner et al., 2013). We compared mutant and wild-type cells in the same field of view using TRITC-conjugated lectin cell wall staining to differentiate between strains (Fig. 2-5A). In addition, we used the spindle pole body (SBP) marker Sid4-GFP to define the stages of mitosis based on the distance between spindle poles. At mitotic onset, SPBs separate to opposite sides of the nucleus as the spindle forms and they maintain a constant distance from one another throughout metaphase and anaphase A of \sim 2.5 μ m (Hagan, 1998; Nabeshima et al., 1998). We refer

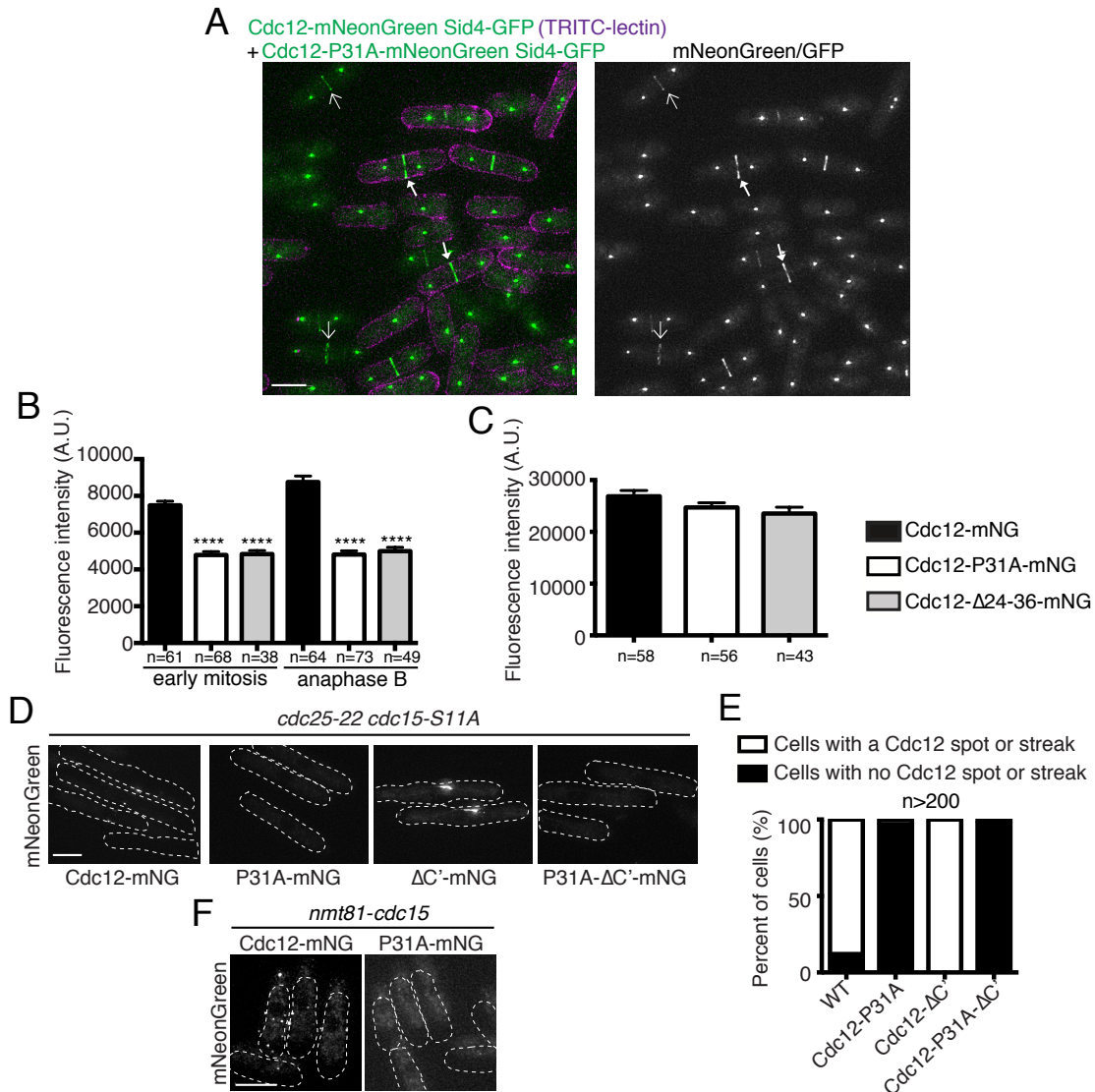


Figure 2-5

Cells lacking Cdc12-Cdc15 interaction accumulate less Cdc12 in the CR.

(A) Live-cell imaging of endogenously-tagged Cdc12-mNeonGreen (mNG) or Cdc12-P31A-mNG with Sid4-GFP. The cell wall of wild-type cells was labeled with TRITC-lectin and then mixed with mutant cells prior to imaging. Closed arrowheads indicate Cdc12-mNG in the CR and open arrowheads indicate Cdc12-P31A-mNG in the CR. (B) Quantification of fluorescence intensity of the CR from mNG images of cells of the indicated genotypes and cell cycle stage. (C) Quantification of whole cell fluorescence intensity from Cdc12-mNG images of cells with CRs of the indicated genotypes. These measurements were made with stains that do not contain Sid4-GFP (wild-type vs. Cdc12-P31A $p = 0.14$ and wild-type vs. Cdc12-Δ24-36 $p = 0.052$). Measurements in the graphs from (B) and (C) represent three biological replicates. **** $p \leq 0.0001$. Error bars represent SEM. (D) Cdc12-mNG localization in *cdc15-S11A cdc25-22* cells shifted to 36°C for 3.5 hours. (E) Quantification from (D). (F) Localization of Cdc12-mNG in cells overexpressing Cdc15 from the *nmt81* promoter for 20 h at 32°C. Bars, 5 μm.

to these stages combined as “early mitotic” as only ~1/9 of cells with constant spindle length are in anaphase A (Nabeshima et al., 1998). SPBs move apart again at the onset of anaphase B. CRs in early mitotic cells had 35-36% less Cdc12-P31A-mNG or Cdc12-

$\Delta 24-36$ -mNG than wild-type Cdc12-mNG and the amount of mutant Cdc12 did not increase during anaphase B like wild-type Cdc12 (Fig. 2-5A and B). However, there was no difference in total Cdc12 protein levels in mitotic cells amongst strains (Fig. 2-5C). Thus, Cdc15 helps recruit/maintain Cdc12 at the medial cortex during mitosis. These results also indicate that significantly less CR-associated Cdc12 is sufficient for CR formation, a finding that is in accord with the survival of diploids with a single functional copy of *cdc12*⁺ (Chang et al., 1997).

Cdc15 also influences Cdc12 localization in abnormal cell cycle situations (Carnahan and Gould, 2003; Roberts-Galbraith et al., 2010). For example, a *cdc15* phospho-mutant (*cdc15-S11A*) precociously localizes to the medial cortex when cells are arrested in G2; concomitantly, Cdc12 forms one or two medial cortical spots (Roberts-Galbraith et al., 2010). To test if this precocious Cdc12 recruitment depends on Cdc15 binding, we visualized *cdc25-22 cdc15-S11A* cells with Cdc12-mNG or Cdc12-P31A-mNG. In contrast to Cdc12-mNG that localized as bright central dots, Cdc12-P31A-mNG was diffuse in the cytoplasm (Fig. 2-5D and E). A Cdc12 mutant lacking the C-terminal oligomerization domain (C') (Cdc12- Δ C'-mNG) (Bohnert et al., 2013) formed a central streak rather than focused spots under these conditions, in accord with its lack of self-association (Fig. 2-5D and E). However, the double mutant (Cdc12-P31A- Δ C'-mNG) showed diffuse cytoplasmic localization (Fig. 2-5D and E), revealing the importance of the Cdc15 association for precocious Cdc12 medial recruitment. Over-expression of *cdc15* also results in the formation of large puncta of Cdc12 (Carnahan and Gould, 2003); this pattern was abolished by the P31A mutation in *cdc12* (Fig. 2-5F). Thus, in both

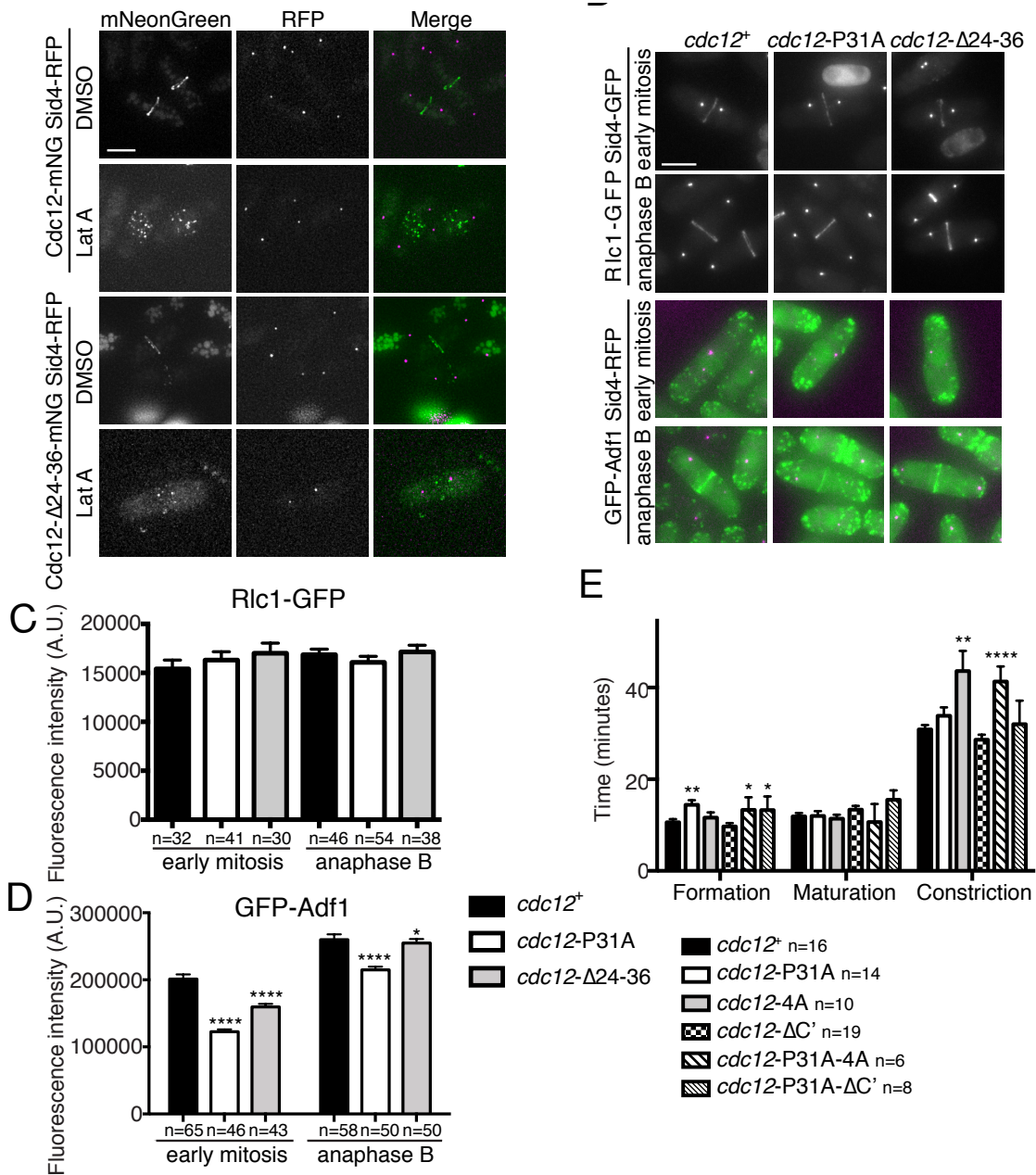


Figure 2-6

Cdc12 lacking the Cdc12-Cdc15 interaction localizes independently of F-actin to the CR.

(A) Live cell imaging of asynchronous cells expressing Sid4-RFP along with endogenously-tagged Cdc12-mNG or Cdc12-P31A-mNG. Cells were treated with 100 μ M Lat-A or DMSO for 10 minutes at 25°C. (B) Live cell imaging of *cdc12⁺*, *cdc12-P31A* and *cdc12-Δ24-36* cells expressing endogenously-tagged Rlc1-GFP and GFP-Adf1 with fluorescently-tagged Sid4. (C-D) Quantification of fluorescence intensity of the CR in cells of the indicated genotypes and cell cycle stage from (B). For early mitosis Rlc1-GFP wild-type vs. P31A $p = 0.464$ and wild-type vs. $\Delta 24-36$ $p = 0.244$. (E) Quantification of cytokinesis event timing from live-cell imaging of *cdc12⁺*, *cdc12-P31A*, *cdc12-4A*, *cdc12-ΔC'*, *cdc12-P31A-4A* and *cdc12-P31A-ΔC'* expressing Rlc1-GFP Sid4-GFP during cell division (A). Measurements in the graphs from (C-E) represent three biological replicates. For *cdc12⁺* and *cdc12-P31A*, these data were also shown in Fig. 2-8. Bars, 5 μ m. * $p \leq 0.05$, ** $p \leq 0.01$, **** $p \leq 0.0001$. Error bars represent SEM.

normal and abnormal conditions, Cdc15 directs Cdc12's localization via a single binding site comprising residues 24-36.

Wild-type Cdc12 and Cdc15 localize to the medial cortex independently of F-actin (Wu et al., 2003; Wu et al., 2006). In contrast, N-terminal truncations of Cdc12 ($\Delta 503$ -*cdc12* and $\Delta 841$ -*cdc12*) require F-actin for medial recruitment (Coffman et al., 2013). To determine whether abrogation of Cdc15 binding led to F-actin dependence, we treated wild-type and the *cdc12* mutant cells with a high dose of Latrunculin-A (Lat-A) to deplete F-actin. Both Cdc12-mNG and Cdc12- $\Delta 24$ -36-mNG localized in medial cortical dots in Lat-A-treated cells, but just as in CRs (Fig. 2-5A and B), Cdc12- $\Delta 24$ -36-mNG was less abundant (Fig. 2-6A). Thus, lack of Cdc15 binding does not render Cdc12 localization dependent on F-actin.

Efficient Cdc12 recruitment is important for F-actin accumulation in the CR

Our results indicate that cell lacking the Cdc12-Cdc15 interaction have 33% less Cdc12 at the division site (Fig. 2-2). Assuming that both wild-type and mutant Cdc12 nucleate and elongate F-actin at the same rate, cells lacking the Cdc12-Cdc15 interaction could then take 33% longer to form the F-actin in the CR. Thus, if Cdc12 activity is not otherwise regulated, mutant cells lacking the Cdc12-Cdc15 interaction may still have time to produce sufficient amounts of F-actin for the CR. On the other hand, because F-actin in the CR is rapidly and constantly turned over (Pelham and Chang, 2002), less CR-associated Cdc12 might lead to less F-actin. Therefore, we compared the amount of F-actin in the CR between early mitotic and anaphase B wild-type and mutant cells. There was ca. 26% less F-actin, visualized with LifeAct-mCherry, in the CR of *cdc12*-P31A cells compared to wild-type cells during early mitosis (Fig. 2-7A and B). However there

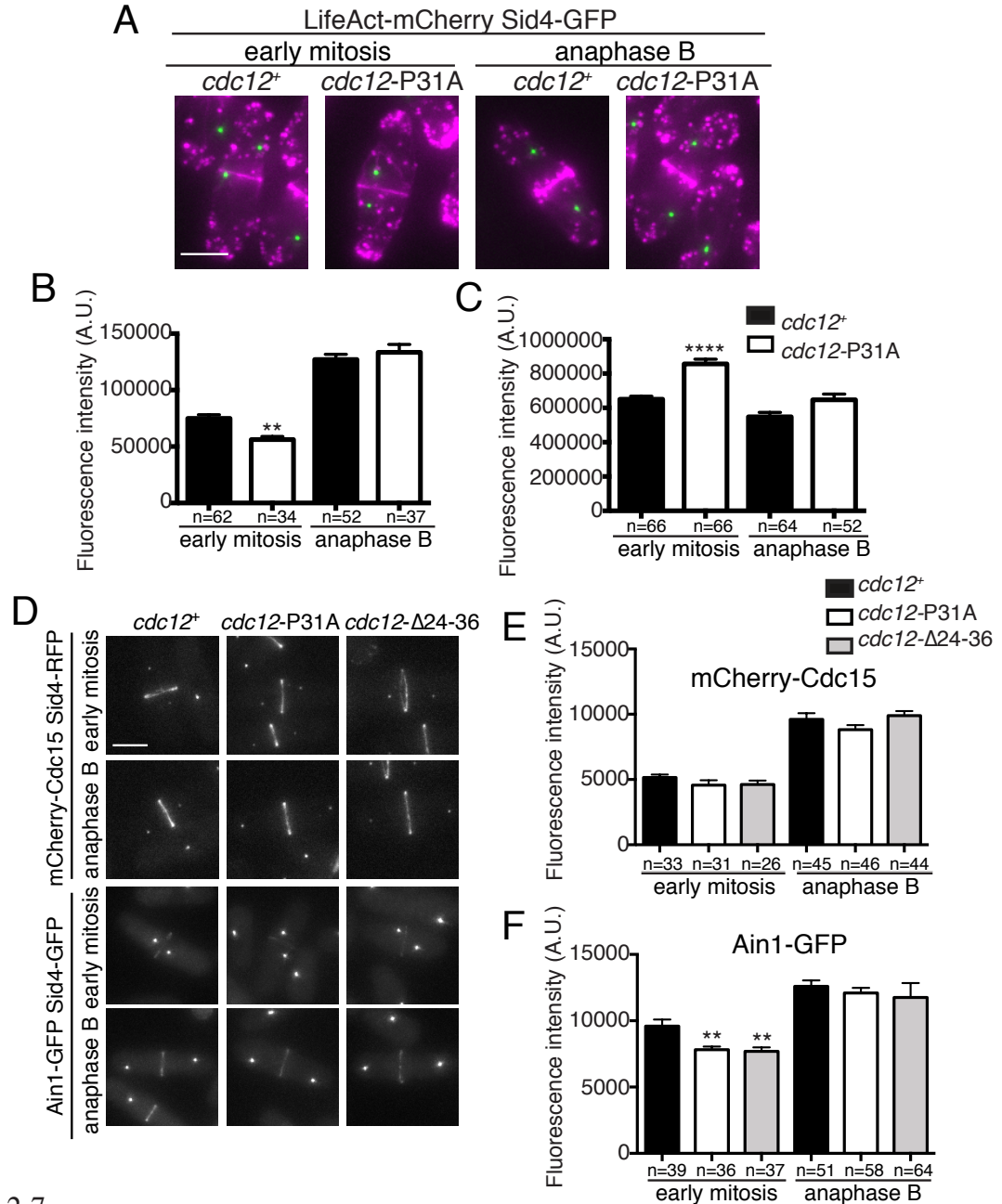


Figure 2-7

Cells lacking Cdc12-Cdc15 interaction accumulate less F-actin in the CR.

(A) Live-cell imaging of *cdc12⁺* or *cdc12-P31A* cells expressing LifeAct-mCherry Sid4-GFP. (B) Quantification of fluorescence intensity of the CR in cells of the indicated genotypes and cell cycle stage from (A). Wild-type anaphase B vs. *cdc12-P31A* anaphase B $p = 0.42$. (C) Quantification the fluorescence intensity at the cell tips of the indicated genotypes at the indicated cell cycle stage. Wild-type anaphase B vs. *cdc12-P31A* anaphase B $p = 0.12$. (D) Live cell imaging of *cdc12⁺*, *cdc12-P31A* and *cdc12-Δ24-36* cells expressing endogenously-tagged mCherry-Cdc15 or Ain1-GFP with fluorescently-tagged Sid4. (E-F) Quantification of fluorescence intensity in cells of the indicated genotypes and cell cycle stage from (D). For early mitosis mCherry-Cdc15 wild-type vs. P31A $p = 0.174$ and wild-type vs. $\Delta24-36$ $p = 0.152$. Measurements in the graphs from (B-C) and (E-F) represent three biological replicates. Bars, 5 μm . ** $p \leq 0.01$ **** $p \leq 0.0001$. Error bars represent SEM.

was no difference in the amount of F-actin in the CR between the two strains during

anaphase B (Fig. 2-7A and B). Thus, the mutant Cdc12 produces the same amount of F-actin in the CR as wild-type given time. We did not observe a difference in longitudinal F-actin cable number (data not shown), in accord with Cdc12 specifically producing F-actin for the CR (Chang et al., 1997). Formins compete with the Arp2/3 complex for G-actin and mutations disrupting formin function have increased F-actin patch density (Burke et al., 2014). As expected, we found ca. 24% increase in fluorescence intensity of actin patches at the cell tips in early mitosis but not anaphase B in the mutants compared to wild-type (Fig. 2-7A and C) as expected given that less F-actin was incorporated into the CR in the mutant cells.

Although there was less F-actin in the CRs of *cdc12* mutants lacking the Cdc12-Cdc15 interaction in early mitosis, we expected that proteins targeted there independently of F-actin, such as Cdc15 (Wu et al., 2006) and myosin II (Naqvi et al., 1999) would not be affected in the mutant cells. Indeed, mCherry-Cdc15 and the myosin light chain Rlc1-GFP did not have altered protein levels in CRs of mutant cells compared to wild-type in any mitotic stage (Fig. 2-7D and E and Fig. 2-6B and C). In contrast, we anticipated that proteins localizing to the CR in an F-actin-dependent manner would exhibit decreased abundance in the CR of *cdc12* mutants. Indeed, there was ca. 18-19% decrease in Ain1-GFP (an alpha-actinin protein) (Wu et al., 2001) and ca. 39% decrease in GFP-Adf1 (a cofilin protein) (Nakano et al., 2001) abundance in the CR in the *cdc12* mutants compared to wild-type during early mitosis (Fig. 2-7D and F, Fig. 2-6B and D). Like F-actin, Ain1-GFP recovered to wild-type levels during anaphase B although GFP-Adf1 did not. We do not have an explanation for this difference.

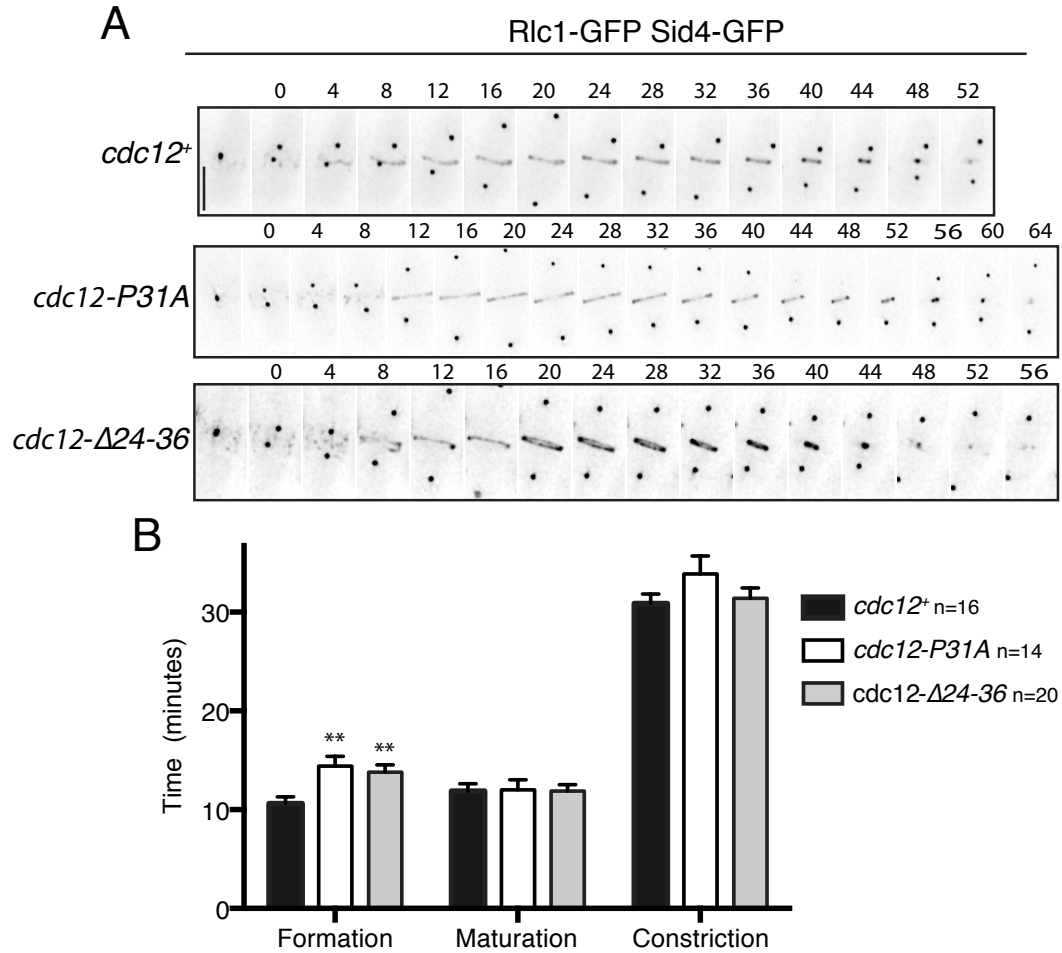


Figure 2-8

Cells lacking the Cdc12-Cdc15 interaction exhibit slower CR formation.

(A) Live-cell imaging of *cdc12⁺*, *cdc12-P31A* or *cdc12-Δ24-36* expressing Rlc1-GFP Sid4-GFP during cell division. Images were acquired every 2 minutes and representative timepoints are shown. Bar, 5 μ m. (B) Quantification of cytokinesis event timing for each mutant from (A). ** $p \leq 0.01$. Error bars represent SEM.

The Cdc12-Cdc15 interaction is important during CR formation

Because the above results indicated that loss of the Cdc15-Cdc12 interaction adversely affects CR assembly (Fig. 2-3B and C), we used time-lapse microscopy to examine cytokinetic progression. Using Rlc1-GFP and Sid4-GFP as markers for the CR and mitotic progression, respectively, we found that CR formation in *cdc12-P31A* and

cdc12-Δ24-36 mutants was 26% and 23% slower, respectively, from the time of initial SPB separation compared to wild-type (Fig. 2-8A and B), in remarkable agreement with the reduction in F-actin. In contrast to some other mutations affecting CR formation (Coffman et al., 2009; Roberts-Galbraith et al., 2010; Tebbs and Pollard, 2013; Wang et al., 2014), we did not observe a compensatory decrease in the amount of time for CR maturation.

We wondered whether binding to Cdc15 cooperated with previously described regulatory inputs into Cdc12 localization and function. We therefore carefully assessed CR dynamics in *cdc12* mutant cells lacking its oligomerization domain (*cdc12-ΔC'*) and a phosphomutant whose multimerization cannot be regulated by the septation initiation network (SIN) (*cdc12-4A*) (Bohnert et al., 2013). The latter mutant renders CR assembly completely dependent on Mid1 (Bohnert et al., 2013). While no changes in CR dynamics were observed in *cdc12-ΔC'* cells compared to wild-type, CR assembly and constriction took significantly longer in *cdc12-4A* cells (Fig. 2-6E). Next, we assayed CR dynamics in double mutants with *cdc12-P31A*. The phenotypes reflected the defects of the individual single mutants and therefore the mutations are not additive (Fig. 2-6E). Thus, Cdc15 and the SIN affect different aspects of Cdc12 function; Cdc15 binding to Cdc12 promotes its medial recruitment while SIN-dependent phosphorylation of Cdc12 controls its oligomerization state that is important later in cytokinesis.

While little Cdc12 is required for CR formation, its medial recruitment depends on multiple inputs. Here, we have established that Cdc15 is one of these inputs, contributing to Cdc12 recruitment during mitosis via direct binding. Our findings provide a rationale for why Cdc15 localizes early in the process of CR assembly (Fankhauser et

al., 1995) despite its other described roles later in cell division (Arasada and Pollard, 2014; Roberts-Galbraith et al., 2009; Roberts-Galbraith et al., 2010; Vjestica et al., 2008; Wachtler et al., 2006). The existence of multiple inputs for formin recruitment occurs in other biological contexts although the details differ (Chesarone et al., 2010). Of the formins with described recruitment pathways, many rely on a combination of intrinsic properties (membrane binding and/or dimerization/multimerization) (Bohnert et al., 2013; Rouso et al., 2013) and extrinsic pathways (protein binding partners) (Chesarone et al., 2010; Copeland et al., 2007; Liu et al., 2012; Seth et al., 2006). *H. sapiens* mDia2, for example, requires interactions with both RhoA and Anillin to direct its localization and control its function during cytokinesis (Watanabe et al., 2010). *S. cerevisiae* Bni1 localization to the bud neck requires dimerization of its N-terminus in combination with two protein-binding domains, one for Rho1 and another for Spa2 (Fujiwara et al., 1998; Liu et al., 2012). Thus, it is likely that still more formins will be found to utilize a combination of sequence motifs to direct their intracellular localization and some may be similar to the Cdc12 mechanism.

In the absence of Cdc15 binding, Cdc12 is still recruited for CR formation, likely through other N-terminal interactions with Rng2 and/or Myo2 based on genetic evidence (Laporte et al., 2011) and recent synthetic targeting experiments (Johnson et al., 2014; Tao et al., 2014). To elaborate, precocious targeting of Myo2 or Rng2 to the medial cortex is sufficient for Cdc12 recruitment and vice-versa (Tao et al., 2014). Future studies will be aimed at determining the relative importance of various regulatory inputs into Cdc12 recruitment and function. We note that although Cdc15 can promote Cdc12 localization to medial cortical spots during interphase, this is insufficient for Cdc12

activation and the formation of CR F-actin (Roberts-Galbraith et al., 2010) (Fig. 2-5D). Thus, other interactions and/or protein modifications must promote Cdc12 F-actin nucleation and elongation functions.

Formin Cdc12 recruitment to the cell middle via direct binding to the Cdc15 F-BAR domain provides one of the first examples of a bifunctional F-BAR domain that interacts with a protein partner as well as the membrane. Since our original observation (Carnahan and Gould, 2003), only one other example has emerged (Kostan et al., 2014). Pacsin2, in addition to binding membranes can interact with F-actin via its F-BAR domain (Kessels et al., 2006; Kostan et al., 2014; Qualmann et al., 1999). However, these two partners of the Pacsin2 F-BAR compete to bind the same surface of the domain (Kostan et al., 2014). Although we do not yet know whether Cdc12 competes with membrane for binding to the Cdc15 F-BAR, it is likely that the F-BAR domain binds both simultaneously because both Cdc15-Cdc12 and Cdc15-membrane interactions are restricted to the same narrow time window when Cdc15 is dephosphorylated during mitosis (Roberts-Galbraith et al., 2010; Wachtler et al., 2006). Simultaneous binding would position the N-terminus of the formin very close to the PM to establish a tight bridge between the membrane and CR during cell division. Further study of other F-BAR domains may reveal additional examples of bifunctional binding properties.

CHAPTER 3

CDK1-DEPENDENT PHOSPHO-INHIBITION OF A FORMIN-F-BAR INTERACTION INHIBITS CYTOKINESIS

3.1 Introduction

Cytokinesis is the final stage in cell division that results in the physical separation of two daughter cells. Many eukaryotic cells utilize an actin- and myosin-based cytokinetic ring (CR) that forms between the two segregated genomes and eventually constricts, dividing the mother cell into two daughter cells. In *S. pombe*, CR assembly depends on a single formin, Cdc12, which is essential for nucleation and elongation of F-actin during CR formation (Bohnert et al., 2013; Chang et al., 1997; Kovar et al., 2003; Kovar and Pollard, 2004; Nurse et al., 1976). Cdc12 also bundles F-actin, which is important for CR maintenance (Bohnert et al., 2013). Recruitment of Cdc12 to the cell division site at mitotic onset depends on two redundant genetic modules (Laporte et al., 2011; Wachtler et al., 2006). The first module consists of IQGAP Rng2 and functional myosin II (Myo2, Cdc4 and Rlc1) while the second module consists of the F-BAR scaffold Cdc15 (Laporte et al., 2011). Whereas the molecular mechanism by which the first module recruits Cdc12 is completely unknown, our lab found that Cdc15's F-BAR domain directly interacts with and recruits Cdc12 to the cell division site. More specifically, we identified the Cdc15-binding motif within the Cdc12's N terminus (residues 24-36) and made Cdc12 mutants that cannot interact with Cdc15 (*cdc12-P31A* and *cdc12-Δ24-36*). Cells lacking the Cdc12–Cdc15 interaction had reduced Cdc12 cell

division site localization, delayed medial accumulation of F-actin and actin-binding proteins, delayed CR formation, and were unable to survive other perturbations to CR assembly (Willet et al., 2015a). Thus, the Cdc12–Cdc15 interaction is an important contributor to Cdc12 localization and CR formation.

Cdc15 is the founding member of the Pombe Cdc15 Homology (PCH) family of proteins, which form dimers that can oligomerize and bind membranes through their conserved N-terminal F-BAR domains (McDonald et al., 2016; Tsujita et al., 2006) and interact with proteins through C-terminal protein-binding domains (Bohnert and Gould, 2012; Ren et al., 2015; Roberts-Galbraith et al., 2009). Cdc15 activity is under strong cell cycle–dependent phospho-regulation: it is hyper-phosphorylated during interphase and hypo-phosphorylated during mitosis (Roberts-Galbraith et al., 2009). It is hypothesized that Cdc15 is in a closed conformation when hyper-phosphorylated and therefore inhibited from binding membranes, oligomerizing and binding protein partners. De-phosphorylation of Cdc15 induces an open conformation allowing it to bind membrane, oligomerize and scaffold protein partners (McDonald et al., 2016; Roberts-Galbraith et al., 2010). It was previously found that Cdc12 and Cdc15 associate in mitosis when Cdc15 is in a hypo-phosphorylated state and *cdc15* alleles with phospho-abolishing mutations precociously recruit Cdc12 and other interacting proteins to the cell middle (Roberts-Galbraith et al., 2009). We previously reported that precocious recruitment of Cdc12 via Cdc15 phospho-mutants or Cdc15 over-expression is dependent on Cdc12's Cdc15 binding motif (Willet et al., 2015a). Therefore it is established that Cdc15 is regulated to control its interaction with Cdc12 and other binding partners, yet whether or not Cdc12 is also regulated to control its interaction with Cdc15 was unknown.

Like Cdc15, Cdc12 is phosphorylated in a cell cycle-dependent manner; however its peak of phosphorylation occurs in M phase (Bohnert et al., 2013). Cdc12 is phosphorylated by Sid2, the terminal kinase in the Septation Initiation Network (SIN) on four residues to control a C-terminal oligomerization domain (C'). However Cdc12 with all 4 Sid2 phospho-sites mutated to phospho-abolishing residues (*cdc12-4A*) is still phosphorylated (Bohnert et al., 2013), evidence that other kinases phosphorylate Cdc12.

Cdk1 is a mitotic kinase of particular interest. It is generally regarded as a cytokinetic inhibitor and low Cdk1 activity is a hallmark of mitotic exit (reviewed in (Bohnert and Gould, 2012; Wolf et al., 2007)). It is also required for mitotic commitment however cytokinesis is not initiated until later in mitosis when Cdk1 activity is low (Chang et al., 2001; Dischinger et al., 2008; Guertin et al., 2000; He et al., 1997; Wolf et al., 2007).

Here we show that Cdc12 is a Cdk1 substrate and Cdk1 phosphorylation of Cdc12 inhibits binding to Cdc15 *in vitro*. Cells with an allele of *cdc12* with phospho-mimicking mutations (*cdc12-6D*) display phenotypes similar to an allele of *cdc12* lacking Cdc15 binding (*cdc12-P31A*); they both have reduced Cdc12 accumulation at the cell division site and delayed CR formation. These results underscore the importance of fine-tuning formin regulation in order to ensure proper cytokinetic timing and are consistent with a role in Cdk1 inhibiting cytokinesis until chromosome segregation complete.

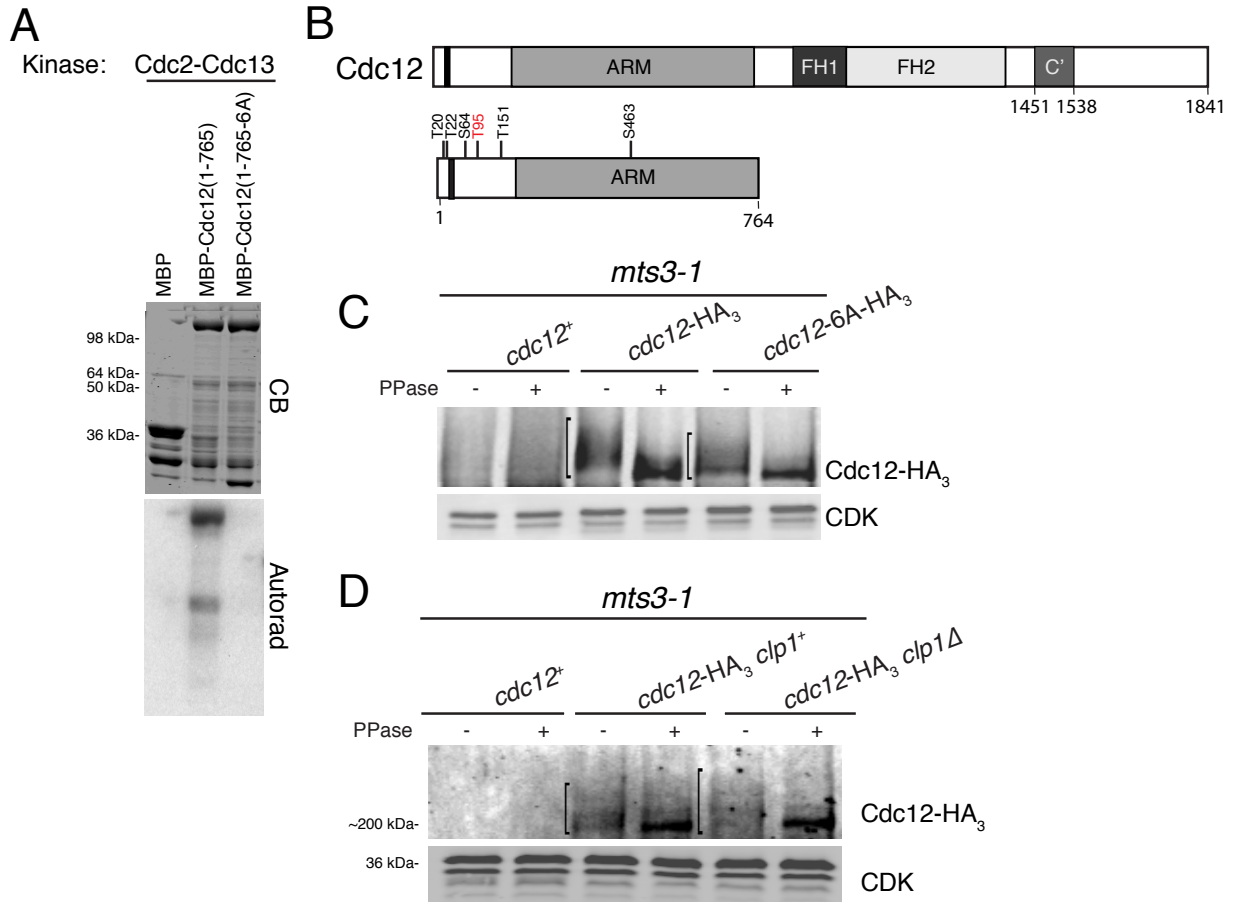


Figure 3-1

Formin Cdc12 is a Cdk1 substrate.

(A) In vitro kinase assays using kinase-active Cdk1 complex (Cdc2-Cdc13) purified from insect cells with bacterial-produced recombinant MBP, MBP-Cdc12, and MBP-Cdc12-6A fragments. The protein gel was stained with Coomassie blue (CB), and proteins labeled by γ -P32 were detected by autoradiography. (B) A schematic, drawn to scale, of Cdc12 with Cdk1 targeted residues labeled. The Cdc15 binding motif (residues 24-36) is indicated by the black bar. T95 is highlighted in red. (C) Denatured cell lysates were prepared from asynchronous *cdc12*⁺, *cdc12*-HA₃, or *cdc12*-HA₃ *clp1*Δ cells. Anti-HA immunoprecipitates of the samples were subjected to either phosphatase treatment or a buffer control before being resolved by SDS-PAGE and immunoblotted. (D) Denatured cell lysates were prepared from mitotically-arrested *mts3-1 cdc12*-HA₃ or *mts3-1 cdc12*-6A-HA₃ cells. Anti-HA immunoprecipitates of the samples were subjected to either phosphatase treatment or a buffer control before being resolved by SDS-PAGE and immunoblotted. PhosTag (5 μ M) was included in the protein gel to enhance separation. (C and D) Brackets span phosphorylated smears. CDK was used as a loading control.

3.2 Results and Discussion

Cdc12 is a Cdk1 substrate

The absence of Sid2 activity only partially eliminated Cdc12 phosphorylation, indicating that other kinases also phosphorylate Cdc12 (Bohnert et al., 2013). The peak hyper-phosphorylated species of Cdc12 correlates temporally with high Cdk1 activity, and threonine 95 on Cdc12 was identified as a Cdk1 target in a large-scale phosphoproteomic screen designed to identify Cdk1 substrates (Swaffer et al., 2016). Therefore we investigated whether Cdk1 regulates Cdc12 function. The Cdc12 N-terminus was an excellent Cdk1 target *in vitro* (Fig. 3-1A). In accord with the known specificity of Cdk1, serines and threonines within S/T-P motifs were targeted in Cdc12's N-terminus (Fig. 3-2A). Individual alanine mutation of each Cdk1 consensus site identified residues T20, T22, S64, T151 and S463 in addition to T95 as major Cdk1 targeted residues (Fig. 3-2B). When all six sites were mutated to alanine (MBP-Cdc12(1-765-6A)), Cdk1-mediated Cdc12 phosphorylation is abolished (Fig. 3-1A). In addition, we constructed an endogenously expressed *cdc12* allele where all six phosphorylated residues were mutated to alanines (*cdc12-6A*). When immunoprecipitated from cells, we detected a reduced mobility shift for Cdc12-6A-HA₃ compared to wild-type Cdc12-HA₃ in mitotically arrested cells (Fig. 3-1C). Both bands were collapsed upon lambda-phosphatase treatment, indicating that the reduced mobility of Cdc12-6A-HA₃ relative to Cdc12-HA₃ is due to a loss in phosphorylation. The remaining phosphorylation observed is at least partially due to Sid2 kinase activity, which also contributes to Cdc12 phosphorylation (Bohnert et al., 2013), and possibly additional kinases. Clp1 is a S/T-P directed phosphatase that is capable of dephosphorylating Cdk1 phosphorylated sites

(Chen et al., 2013b; Clifford et al., 2008; Mocciaro and Schiebel, 2010; Stegmeier and Amon, 2004). Therefore we examined Cdc12 phosphostate in *clp1⁺* and *clp1Δ*. In

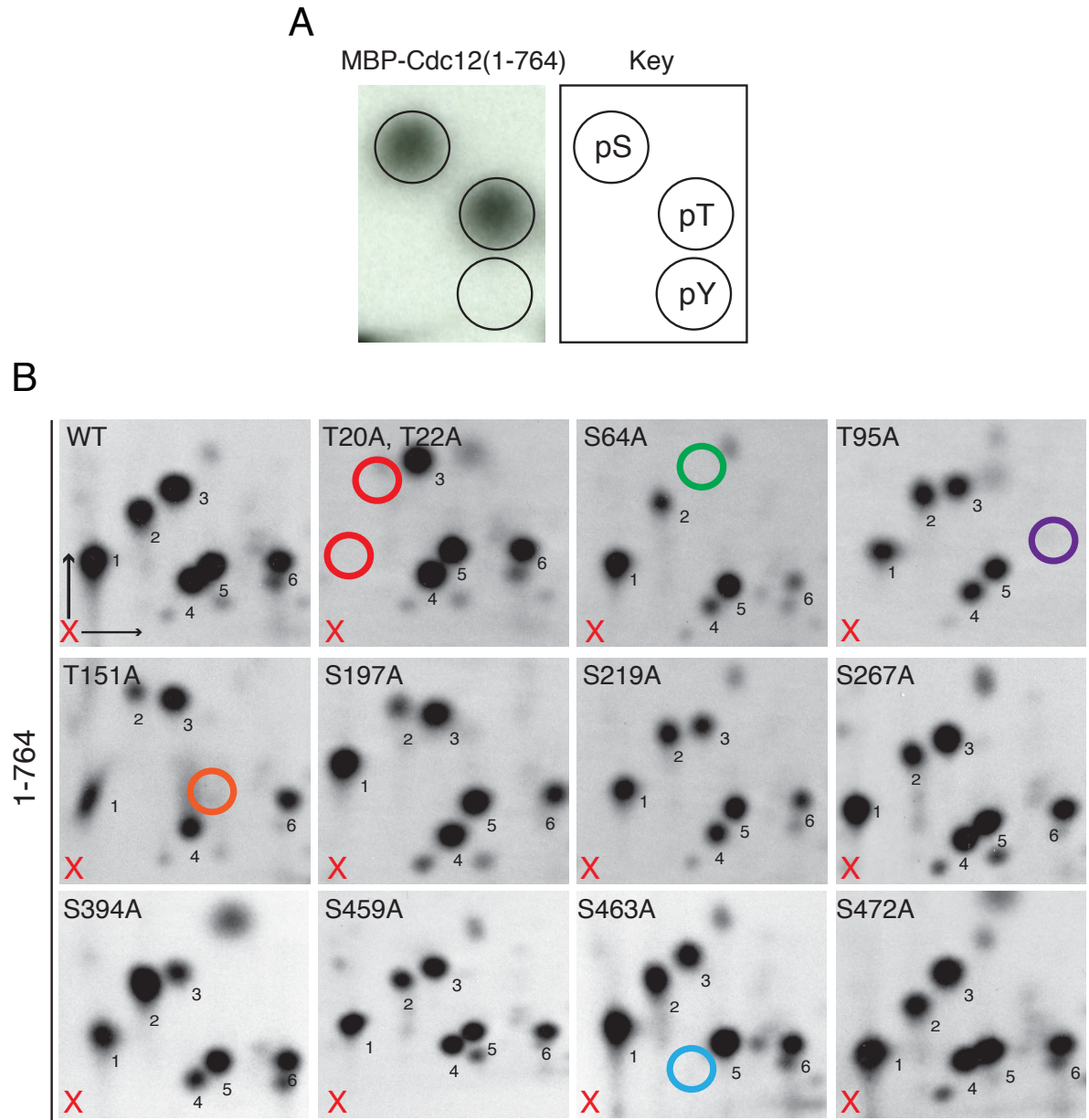


Figure 3-2

Identification of Cdk1-phosphorylated sites on Cdc12.

(A) Phosphoamino acid analysis of MBP-Cdc12(1-764) fragment phosphorylated by Cdk1 complex. The positions of phospho-serine, phospho-threonine and phospho-tyrosine standards are indicated in the key. (B) Phospho-tryptic peptide analysis of MBP-Cdc12(1-764) wildtype and mutant fragments phosphorylated by Cdk1 kinase. The positions of the origin are indicated by the red “X”, and major spots are numbered. The anode is on the left. Loss of phosphorylated species for the T20A T22A, S64A, T95A, T151A and S463A mutants are indicated by red, green, dark blue, orange and light blue circles, respectively.

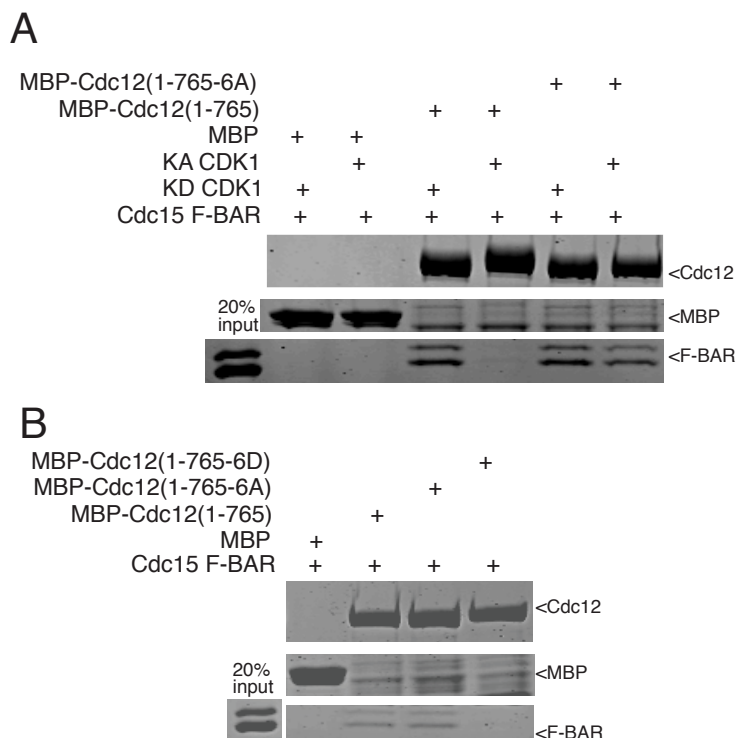


Figure 3-3

Cdc12 Cdk1 phosphorylation inhibits Cdc12-Cdc15 binding.

(A) In vitro binding assay of bead-bound recombinant MBP, MBP-Cdc12(1-764) or MBP-Cdc12(1-764-6A) with recombinant Cdc15 F-BAR(19-312) incubated with either kinase active (KA) or kinase dead (KD) Cdk1 complex. Samples were washed, resolved by SDS-PAGE and stained with CB. (B) In vitro binding assay of bead-bound recombinant MBP, MBP-Cdc12(1-764), MBP-Cdc12(1-764-6A) or MBP-Cdc12(1-764-6D) with recombinant Cdc15 F-BAR(19-312). Samples were washed, resolved by SDS-PAGE and stained with CB. Cdc15 F-BAR appears as a double band due to incomplete his6-tag cleavage (Fig. 3-4A).

accordance with Cdc12 being phosphorylated by Cdk1 *in vitro*, we detected an increased mobility shift of Cdc12-HA₃ when *clp1* is deleted compared to *clp1*⁺ (Fig. 3-1D). We conclude the Cdk1 phosphorylates formin Cdc12 during cytokinesis.

Cdk1 phosphorylation of Cdc12 inhibits the Cdc12-Cdc15 interaction

Because Cdk1 phosphorylation sites on Cdc12 are near the Cdc15 F-BAR binding motif (Willet et al., 2015a) (Fig. 3-1B), we investigated whether Cdc12 phosphorylation

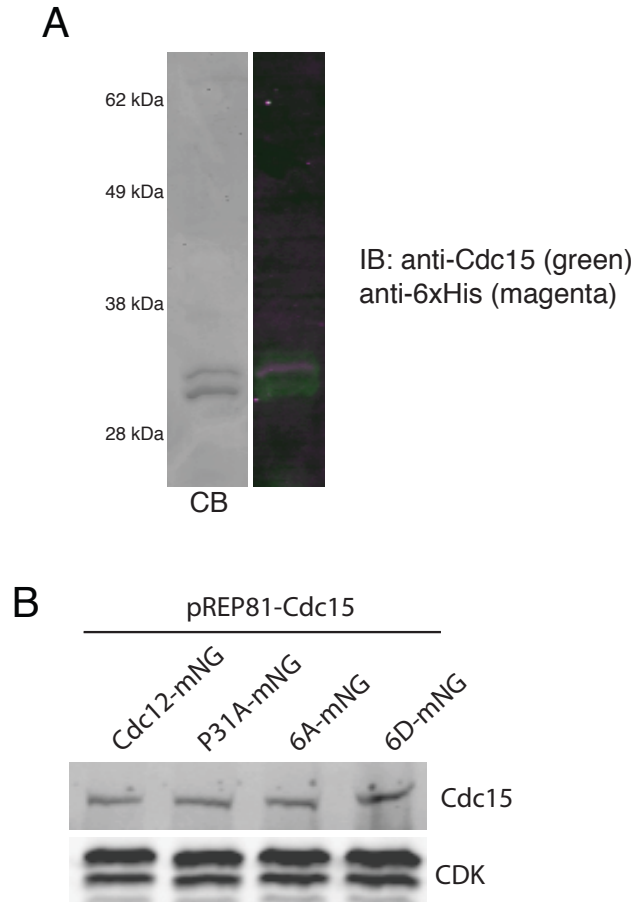


Figure 3-4

Cdc15 expression in vitro and in vivo.

(A) Cdc15(19-312) resolved by SDS-PAGE and either CB stained (left panel) or antibody labeled with an anti-His₆ (magenta) and anti-Cdc15 (green) antibodies (right panel). (B) Expression of *cdc15* from the indicated genotypes from Fig. 3-7B. CDK was used as a loading control.

influences its binding to Cdc15. Whereas *in vitro*, MBP-Cdc12(1-765) binds Cdc15 F-BAR (Fig. 3-3A) (Carnahan and Gould, 2003; Willet et al., 2015a) that runs as a double band due to an incomplete His₆-tag cleavage (Fig. 3-4A), incubation of MBP-Cdc12(1-765) with Cdk1 prior to the binding reaction abolished Cdc15 F-BAR binding (Fig. 3-3A). When all six Cdk1 sites were mutated to alanine (MBP-Cdc12(1-765-6A)), this fragment bound Cdc15 F-BAR, but incubation with Cdk1 no longer abolished Cdc15 F-BAR binding (Fig. 3-3A). Additionally, a Cdc12 fragment with all six Cdk1 sites

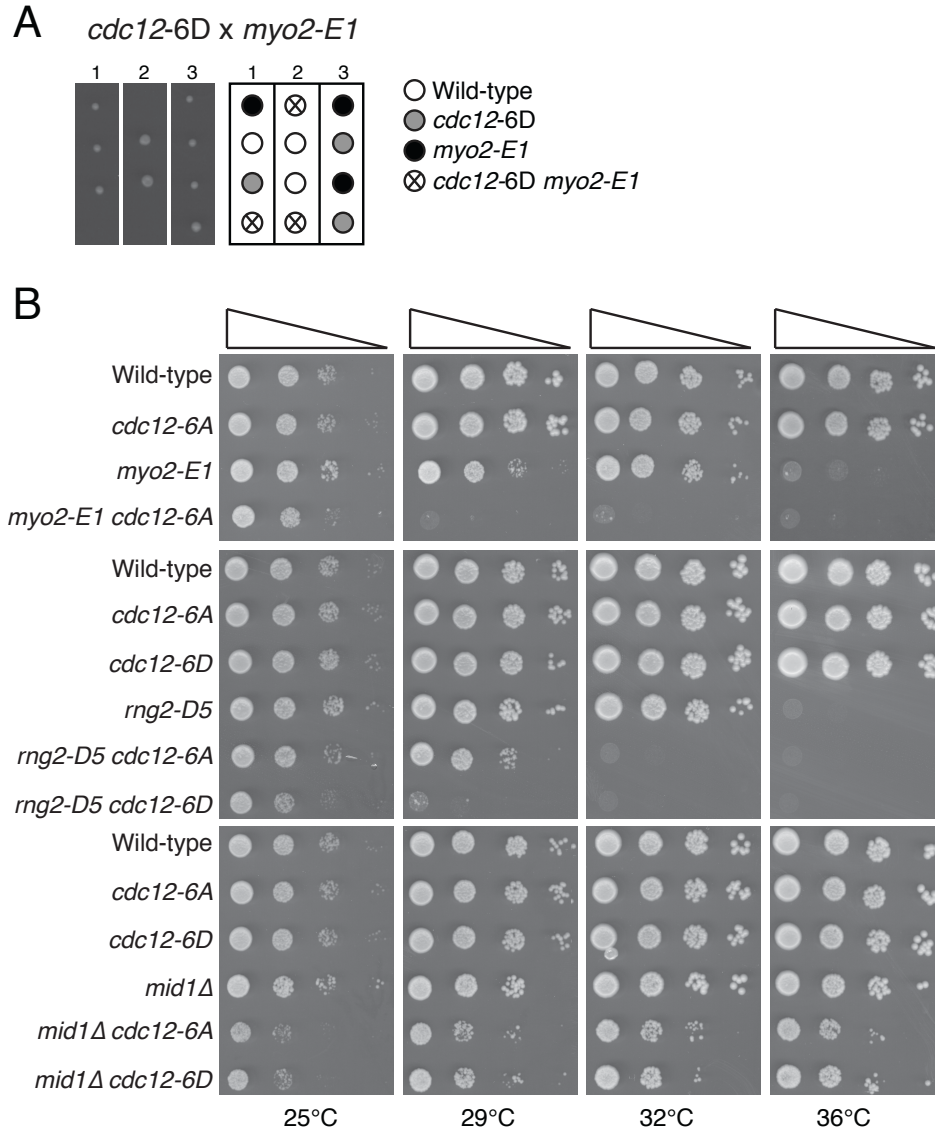


Figure 3-5

Genetic interactions of mutants *cdc12-6A* and *cdc12-6D*.

(A) Tetrads from *cdc12-6D* crossed to *myo2-E1* shown with a schematic of relevant genotypes. (B) Cells of the indicated genotypes were spotted on YE media in 10-fold serial dilutions, and plates were imaged after incubation for 3 days at the indicated temperatures.

mutated to phospho-mimetic aspartate (MBP-Cdc12N-6D) did not bind Cdc15 F-BAR *in vitro* (Fig. 3-3B). These results indicate that Cdk1 phosphorylates Cdc12 on six residues that, when phosphorylated, preclude Cdc12-Cdc15 binding.

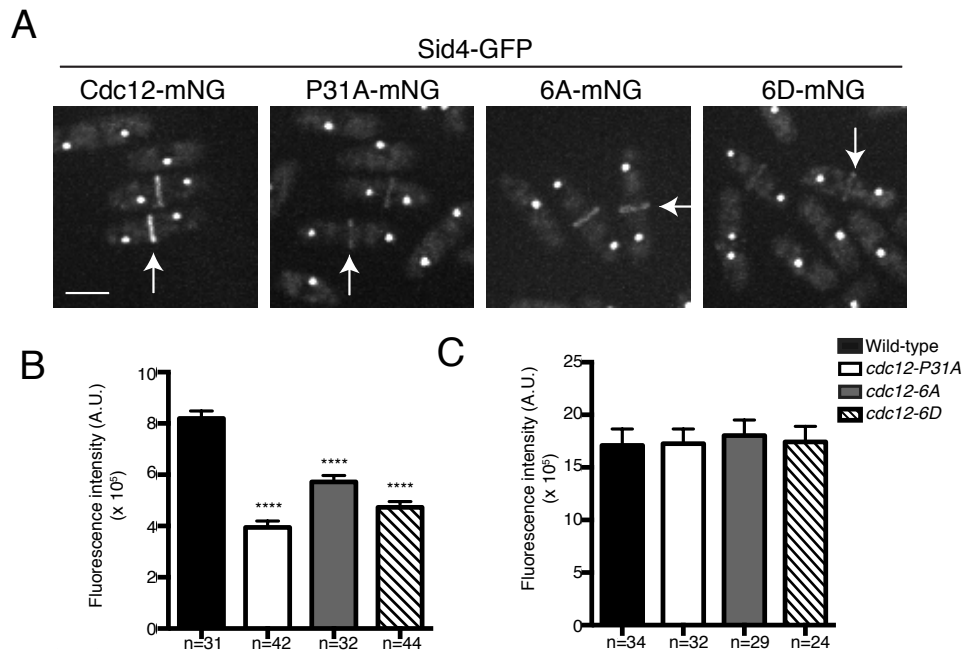


Figure 3-6

Cdc12 with constitutive Cdk1 phosphorylation accumulates less in the CR.

(A) Live-cell imaging of endogenously-tagged Cdc12-mNeonGreen (mNG), Cdc12-P31A-mNG, Cdc12-6A-mNG and Cdc12-6D-mNG with Sid4-GFP. Arrowheads indicate CR localization of Cdc12. (B) Quantification of fluorescence intensity of the CR from mNG images of cells of the indicated genotypes. (C) Quantification of whole cell fluorescence intensity from Cdc12-mNG images of cells with CRs of the indicated genotypes. These measurements were made with strains that do not contain Sid4-GFP. (Wildtype Cdc12 vs. Cdc12-P31A $p = 0.93$, wildtype Cdc12 vs. Cdc12-6A $p = 0.66$ and wildtype Cdc12 vs. Cdc12-6D $p = 0.88$) Measurements in the graphs from (B) and (C) represent three biological replicates. **** $p \leq 0.0001$. Error bars represent SEM.

Cell with constitutive inhibition of the Cdc12-Cdc15 interaction are prone to cytokinesis failure

To determine the functional consequence of abolishing or constitutively mimicking Cdc12 N-terminal phosphorylation by Cdk1 in cells, we examined *cdc12* alleles in which Cdc12's six Cdk1 phosphorylation sites were mutated to either all alanines (*cdc12-6A*) or aspartates (*cdc12-6D*). Based on the *in vitro* kinase and binding experiments, we expected that the *cdc12-6D* allele would exhibit similar phenotypes to the *cdc12-P31A* allele, which disrupts Cdc12's association with Cdc15 and was

synthetically lethal with *myo2-E1*, *rng2-D5* and *mid1Δ* (Willet et al., 2015a). As expected, *cdc12-6D* displayed a synthetic lethal genetic interaction with *myo2-E1* (Fig. 3-5A) and negative genetic interactions with *rng2-D5* and *mid1Δ* (Fig. 3-5B). Contrary to expectation, *cdc12-6A* also displayed slight negative genetic interactions with *myo2-E1*, *rng2-D5* and *mid1Δ* (Fig. 3-5B).

Cdk1-dependent regulation of the Cdc12-Cdc15 interaction is important for normal Cdc12 recruitment

Cdc12-Cdc15 binding is important to recruit Cdc12 to the cell division site (Laporte et al., 2011; Willet et al., 2015a). To test if Cdk1 phosphorylation of Cdc12 influences Cdc12 localization to the CR, we tagged wild-type and mutant *cdc12* alleles with a single copy of mNeonGreen (mNG) (Shaner et al., 2013). CRs had 31% less Cdc12-6A-mNG and 43% less Cdc12-6D-mNG than wild-type Cdc12-mNG (Fig. 3-6A and B). This finding is in accordance with a previous study where Cdc12-P31A-mNG, a mutant that lacks Cdc15 binding, had 52% less abundance at the CR (Willet et al., 2015a). However, there was no difference in total Cdc12 protein levels in mitotic cells amongst strains (Fig. 3-6C). Thus, Cdk1 phosphorylation of Cdc12 inhibits Cdc12 localization at the cell divisions site.

Cdc15 also influences Cdc12 localization in abnormal cell cycle situations (Carnahan and Gould, 2003; Roberts-Galbraith et al., 2010). For example, a *cdc15* phospho-mutant (*cdc15-S11A*) precociously localizes to the medial cortex when cells are arrested in G2; concomitantly, Cdc12 forms one or two medial cortical spots (Roberts-

Galbraith et al., 2010). It was previously found that the precocious recruitment of Cdc12 depends on the Cdc15 binding motif in Cdc12; Cdc12-P31A-mNG no longer localized as bright central dots. To test if this precocious Cdc12 recruitment also depends on Cdk1

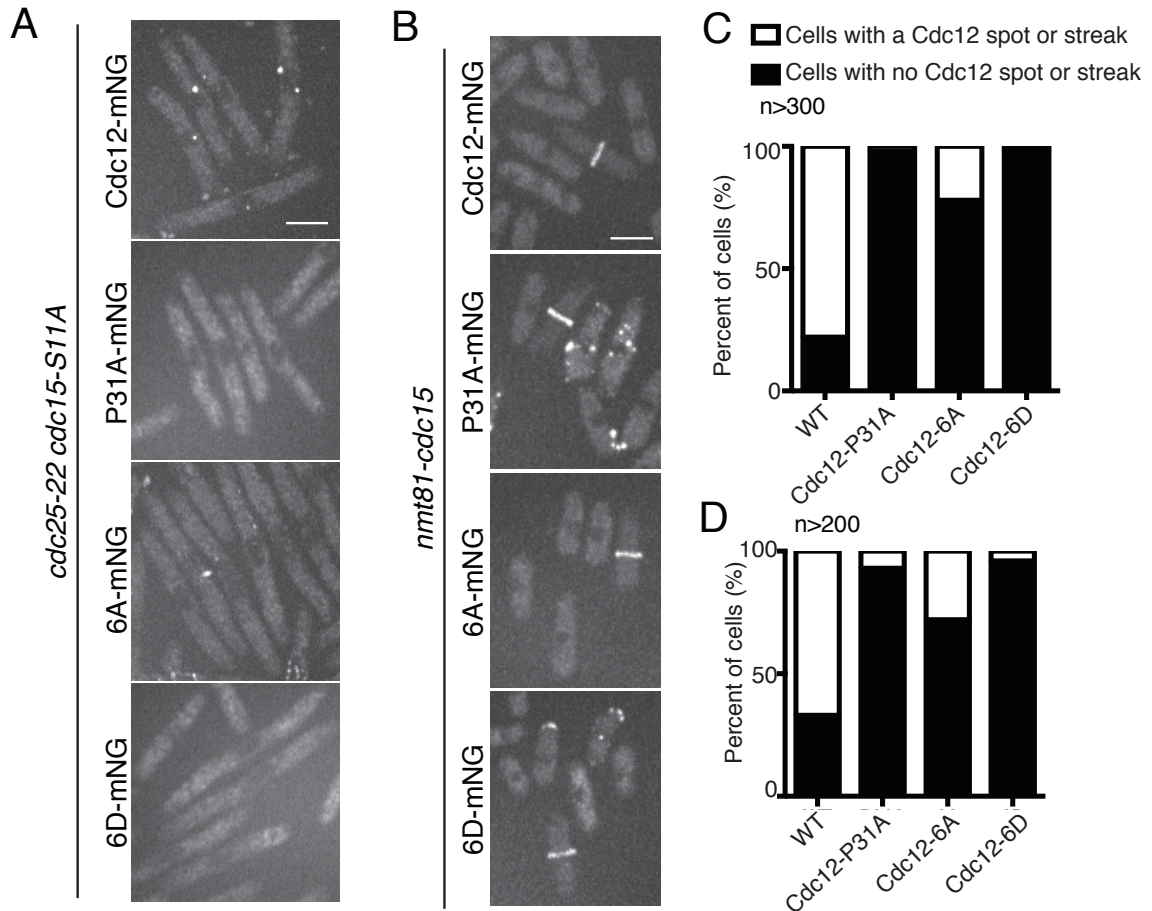


Figure 3-7

Cdc12 with constitutive Cdk1 phosphorylation cannot be recruited by Cdc15 in abnormal cell cycle conditions.

(A) Localization of Cdc12-mNG in cells overexpressing *cdc15* from the *nmt81* promoter for 20 hours at 32°C. (B) Cdc12-mNG localization in *cdc15-S11A cdc25-22* cells shifted to 36°C for 3.5 hours. (C) Quantification from (A). (D) Quantification from (B). Bars, 5 μm.

phosphorylation of Cdc12, we visualized *cdc25-22 cdc15-S11A* cells with Cdc12-mNG, Cdc12-P31A-mNG, Cdc12-6A-mNG or Cdc12-6D-mNG. As expected, Cdc12-mNG localized as bright central dots in 78% of cells and Cdc12-P31A-mNG only displayed this localization pattern 2% of the time (Fig. 3-7A and C). Cdc12-6A-mNG displayed an

intermediate phenotype with 22% of cells with medial dots. In contrast, Cdc12-6D-mNG was almost always diffuse in the cytoplasm with only 1% of cells with bright dots, revealing the importance of Cdk1 phosphorylation of Cdc12 for precocious Cdc12 medial recruitment. Over-expression of *cdc15* also results in the formation of large puncta of Cdc12 (Carnahan and Gould, 2003); as previously reported, this pattern was almost abolished by the P31A mutation in *cdc12* (7% of cells had puncta vs. 67% in wild-type) (Willet et al., 2015a). In addition cells expressing Cdc12-6A-mNG had large puncta 28% of the time, however Cdc12-6D-mNG displayed puncta in only 4% of cells under these conditions (Fig. 3-7B and D). All strains over-expressed Cdc15 to approximately the same levels as assayed by western blot analysis (Fig. 3-4B). Thus, in both normal and abnormal conditions, Cdk1-dependent phosphorylation of Cdc12 directs its localization via six residues that regulate Cdc12-Cdc15 binding.

Cdk1-dependent regulation of the Cdc12-Cdc15 interaction is important the initial formation of F-actin in the forming CR

Previous results showed that cells lacking the Cdc12-Cdc15 interaction have less Cdc12 at the division site and ultimately this leads to less F-actin during early mitosis, but not Anaphase B (Willet et al., 2015a). Thus, we analyzed the phospho-mutants by comparing the amount of F-actin in the CR between early mitotic and anaphase B cells. In early mitotic cells, there was 20% less F-actin, visualized with LifeAct-mCherry, in the CR of *cdc12*-P31A and 16% less for *cdc12*-6D compared to wild-type. There was no statistically significant difference for *cdc12*-6A ($p = 0.29$) compared to wild-type during

early mitosis (Fig. 3-8A and B). In addition, there was no statistically significant

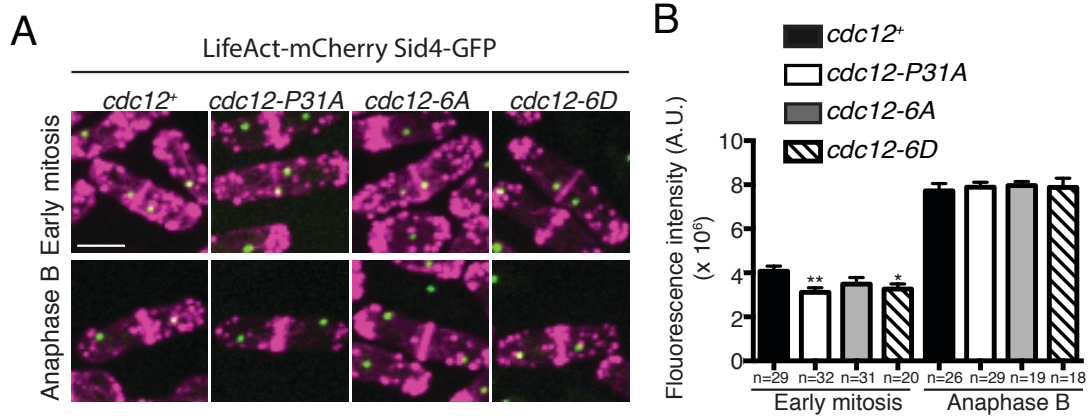


Figure 3-8

Cells with Cdc12 constitutive Cdk1 phosphorylation accumulate less F-actin in the CR.

(A) Live-cell imaging of *cdc12⁺*, *cdc12-P31A*, *cdc12-6A* or *cdc12-6D* cells expressing Life-Act-mCherry Sid4-GFP. (B) Quantification of fluorescence intensity of the CR in cells of the indicated genotypes and cell cycle stage. Wildtype early mitosis vs. *cdc12-6A* early mitosis $p = 0.29$, wildtype anaphase B vs. *cdc12-P31A* anaphase B $p = 0.67$, wildtype anaphase B vs. *cdc12-6A* anaphase B $p = 0.56$, wildtype anaphase B vs. *cdc12-6D* anaphase B $p = 0.76$. Measurements in the graphs from (B) represent three biological replicates. Bar, 5 μm . $**p \leq 0.01$ Error bars represent SEM.

difference in the amount of F-actin in the CR between all of the strains during anaphase B (Fig. 3-8A and B). Thus, the Cdc12-6D mutant protein, similar to the Cdc12-P31A, initially produces less F-actin in the forming CR but, with time there is the same amount of F-actin in the CR in anaphase B as wild-type.

Although there was less F-actin in the early mitotic CRs of *cdc12* mutants with disrupted Cdc12-Cdc15 binding, we expected that proteins targeted there independently of F-actin, such as Cdc15 (Wu et al., 2006) would not be affected in mutant cells (Willet et al., 2015a). Indeed, mCherry-Cdc15 did not have altered protein levels in CRs of mutants compared to wild-type in any mitotic stage (Fig. 3-9A and B). In contrast, we

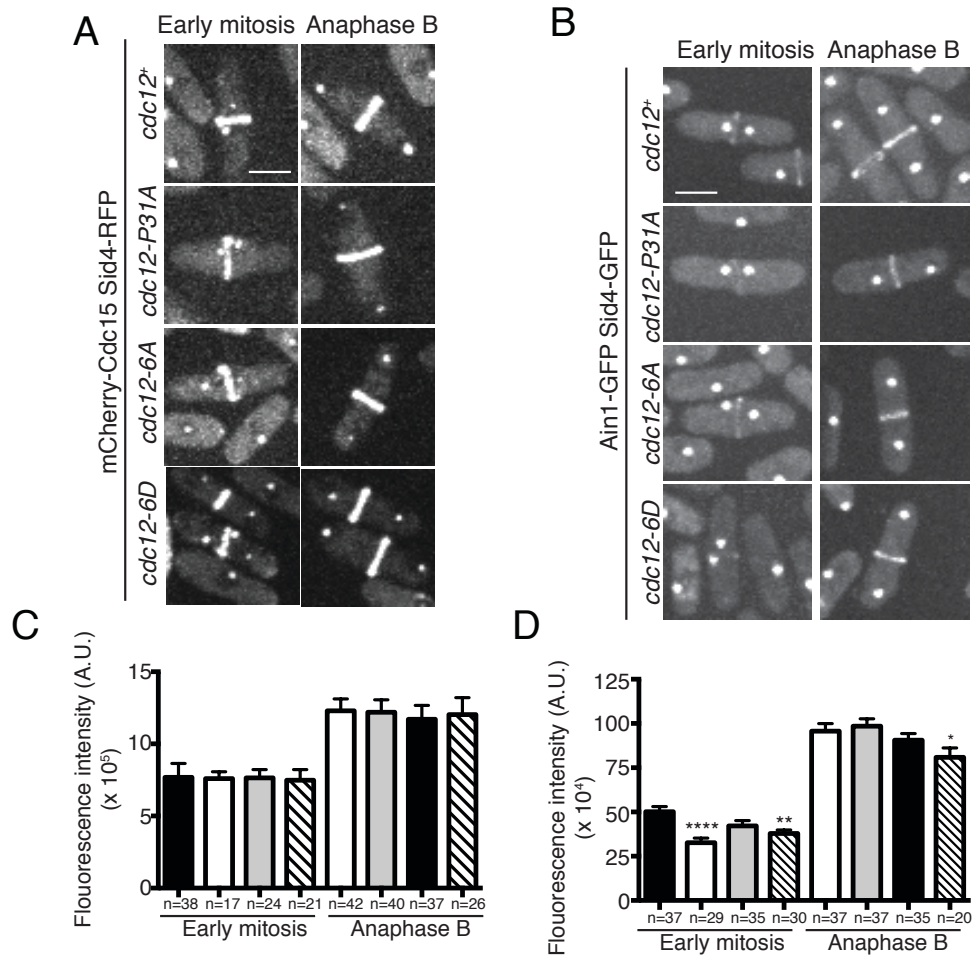


Figure 3-9

Cells with Cdc12 constitutive Cdk1 phosphorylation accumulate less Ain1 in the CR.

(A) Live-cell imaging of *cdc12*⁺, *cdc12-P31A*, *cdc12-6A* or *cdc12-6D* cells expressing mCherry-Cdc15 Sid4-RFP. (B) Live-cell imaging of *cdc12*⁺, *cdc12-P31A*, *cdc12-6A* or *cdc12-6D* cells expressing endogenously-tagged Ain-GFP Sid4-GFP. (C) Quantification of fluorescence intensity of CRs of the indicated genotypes and cell cycle stage from (A). Wildtype early mitosis vs. *cdc12-P31A* early mitosis $p = 0.95$, wildtype early mitosis vs. *cdc12-6A* early mitosis $p = 0.97$, wildtype early mitosis vs. *cdc12-6D* early mitosis $p = 0.88$, wildtype anaphase B vs. *cdc12-P31A* anaphase B $p = 0.92$, wildtype anaphase B vs. *cdc12-6A* anaphase B $p = 0.63$, wildtype anaphase B vs. *cdc12-6D* anaphase B $p = 0.84$. (D) Quantification of fluorescence intensity of CRs of the indicated genotypes and cell cycle stage from (B). Wild-type anaphase B vs. *cdc12-P31A* anaphase B $p = 0.63$, wild-type anaphase B vs. *cdc12-6A* anaphase B $p = 0.37$. Measurements in the graphs from (C-D) represent three biological replicates. Bars, 5 μm . * $p \leq 0.05$ ** $p \leq 0.01$ **** $p \leq 0.0001$. Error bars represent SEM.

anticipated that proteins localizing to the CR in an F-actin-dependent manner would exhibit decreased abundance in the CR of *cdc12* mutants (Willet et al., 2015a). Indeed, there was a 30% decrease in Ain1-GFP (an alpha-actinin protein) (Wu et al., 2001)

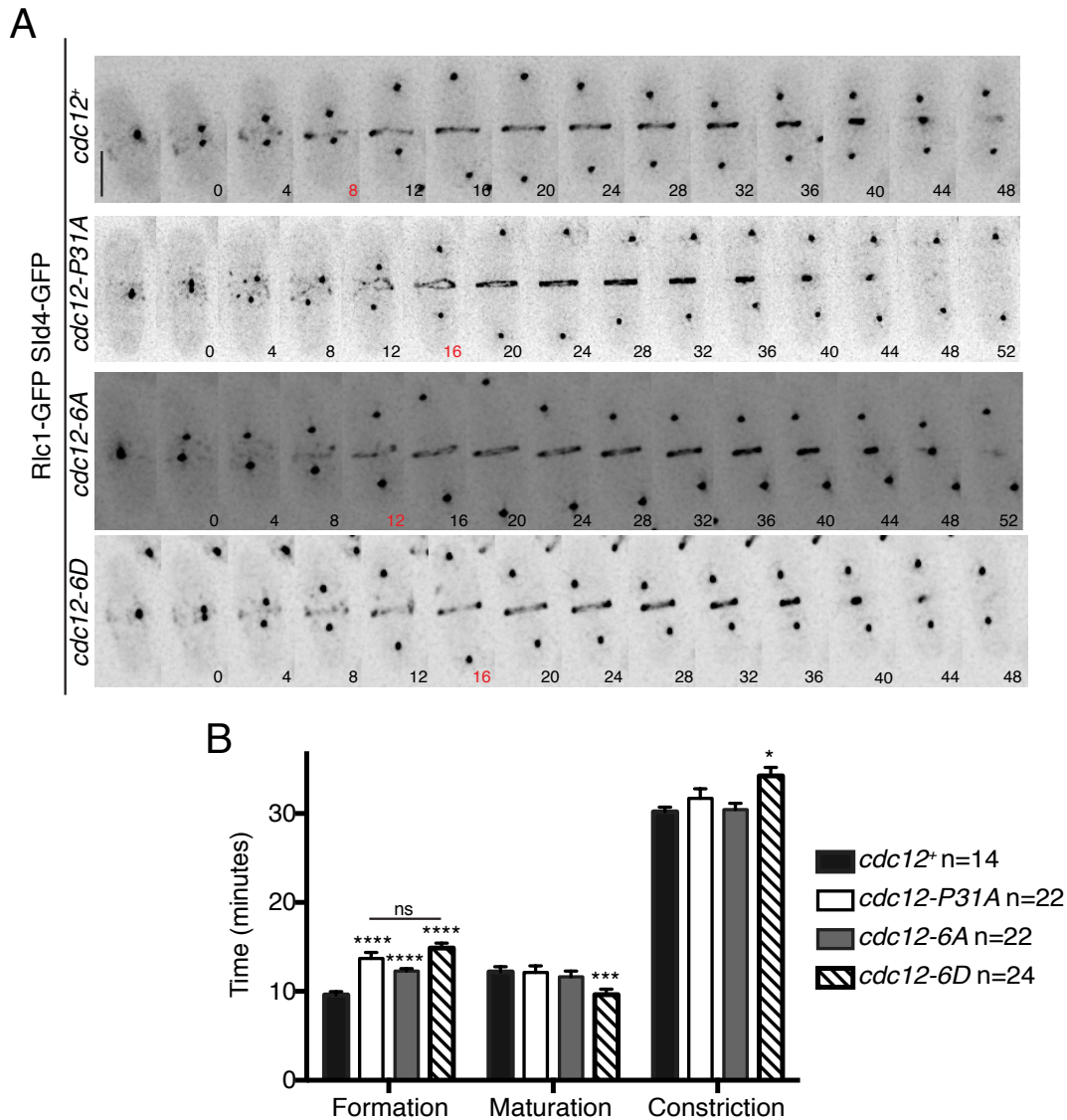


Figure 3-10

Cells with Cdc12 Cdk1 constitutive phosphorylation exhibit slower CR formation.

(A) Live-cell imaging of *cdc12+*, *cdc12-P31A*, *cdc12-6A* or *cdc12-6D* expressing Rlc1-GFP Sid4-GFP during cell division. Images were acquired every 2 minutes and representative time points are shown. Bar, 5 μm. (B) Quantification of cytokinesis event timing for each mutant from (A). Measurements from the graph are from at least three biological replicates. * $p \leq 0.05$ *** $p \leq 0.001$ **** $p \leq 0.0001$. Error bars represent SEM.

abundance in the CR in the *cdc12-P31A* and 24% decrease in *cdc12-6D* mutants

compared to wild-type during early mitosis (Fig. 3-9C and D). Like F-actin, Ain1-GFP

recovered to wild-type levels during anaphase B for every strain except *cdc12-6D* where

the levels were slightly reduced (Fig. 3-9C and D).

Cdk1-dependent phosphorylation of Cdc12 is important during CR formation

Because the above results indicated that phospho-regulation of the Cdc15-Cdc12 interaction adversely affects CR assembly (Figs. 3-5, 3-6 and 3-8), we used time-lapse microscopy to examine cytokinetic progression. Using Rlc1-GFP and Sid4-GFP as markers for the CR and mitotic progression, respectively. As we found previously, CR formation in *cdc12-P31A* mutants was delayed by about 4 minutes (29% increase compared to wild-type). A similar delay in CR formation was seen for *cdc12-6D* (35% slower), in remarkable agreement with the reduction in F-actin. *cdc12-6D* also displayed a faster maturation period and slightly delayed CR constriction (Fig. 3-10A and B). The *cdc12-6A* allele also had a slight delay in CR formation by about 21%.

Overall this study confirms that the formin Cdc12 is a Cdk1 substrate during cytokinesis. *In vitro*, Cdk1 phosphorylation of Cdc12 on 6 sites inhibits its ability to interact with F-BAR Cdc15. Cells with alleles of *cdc12* with phospho-mimicking mutations (*cdc12-6D*) showed similar phenotypes to cells with an allele of *cdc12* that cannot bind Cdc15 (*cdc12-P31A*); both have reduced Cdc12 CR localization, delayed F-actin accumulation in the CR that lead to a delay in the formation of the CR.

Unfortunately, we recently found that strains producing Cdc12 variants tagged at the C-terminus with sequence encoding *mNG:kan^R* versus *mNG:kan^R,hyg^R* had different Cdc12 levels. Cdc12 abundance when expressed from the *cdc12-mNG:kan^Rhyg^R* allele is about 50% of that expressed from the *cdc12-mNG:kan^R* allele (data not shown). We therefore conclude that *cdc12-mNG:kan^R,hyg^R* is a dampened allele due to abundant changes in the 3' non-coding region of the gene that may destabilize the mRNA. The

wildtype *cdc12* control in Figure 3-6 is tagged with *mNG:kan^R* while the mutant alleles are tagged with *mNG:kan^R,hyg^R*. This calls into question the accuracy of the comparisons we have made between wildtype Cdc12 and various mutant alleles. To address this issue, I am currently re-making all *cdc12* alleles using only *mNG:kan^R* sequences in order to more accurately measure the Cdc12 CR localization. We do still expect that there will be a reduction in Cdc12-6D-mNG at the CR relative to wildtype and we expect that Cdc12-6A-mNG levels will actually be very similar to wildtype Cdc12-mNG.

CHAPTER 4

PHOSPHOINOSITIDE-MEDIATED RING ANCHORING RESISTS PERPENDICULAR FORCES TO PROMOTE MEDIAL CYTOKINESIS

Snider CE^{*}, Willet AH^{*}, Chen JS, Arpağ G, Zanic M and Gould KL

The Journal of Cell Biology (in press)

4.1 Introduction

To divide, many eukaryotes assemble and constrict an actin- and myosin-based cytokinetic ring (CR) (Cheffings et al., 2016) that is anchored to the plasma membrane (PM) (Gould, 2016). Despite decades of work on how the division plane is selected and the CR assembles (Bohnert and Gould, 2012; Goyal et al., 2011; Lee et al., 2012; Pollard and Wu, 2010; Rincon and Paoletti, 2016), mechanisms of CR-PM anchoring remain incompletely understood.

One factor implicated in CR-PM attachment is PM lipid composition. Phosphatidylinositol-4,5-bisphosphate (PI(4,5)P₂) and PI5-kinases are enriched at the cleavage furrow of mammalian cells and when PI(4,5)P₂ is depleted, cortical actin separates from the PM (Emoto et al., 2005; Field et al., 2005). CR components such as RhoA, anillin and MgcRacGAP bind PI(4,5)P₂ (Cauvin and Echard, 2015); therefore they may mislocalize when PI(4,5)P₂ levels are reduced. A decrease in cortically-bound anillin may be particularly detrimental to CR-PM attachment because anillin binds components of the CR and PI(4,5)P₂ (D'Avino, 2009; Piekny and Glotzer, 2008; Sun et al., 2015). In

human and *Drosophila* cells, anillin loss causes cleavage furrow oscillations (Kechad et al., 2012). However, the exact combination of molecules involved in CR detachment when PI(4,5)P₂ is depleted remains to be determined.

S. pombe build a medial CR early in mitosis (Kitayama et al., 1997). How the CR remains anchored until constriction is not yet clear although several players have been implicated. One is the F-BAR protein Cdc15: when *cdc15* expression is repressed or Cdc15 oligomerization disrupted, the CR can slide along the PM and disassemble (Arasada and Pollard, 2014; McDonald et al., 2016). Paxillin Pxl1 also plays a role in CR anchoring and integrity evidenced by CR sliding and splitting during anaphase in *pxl1Δ* (Cortes et al., 2015; Ge and Balasubramanian, 2008). Another factor is the cell wall: loss of β(1,3)glucan (Munoz et al., 2013) or loss of the integral membrane protein Sbg1 (Davidson et al., 2016; Sethi et al., 2016) result in CR sliding and instability, suggesting that cell wall-PM linkage is important for CR maintenance. Finally, the microtubule post-anaphase array ensures a medial CR during a cytokinesis arrest (Pardo and Nurse, 2003). In each of these situations, CR sliding is observed in only a fraction of cells (Arasada and Pollard, 2014; Cortes et al., 2015; McDonald et al., 2016; Pardo and Nurse, 2003), indicating that multiple mechanisms contribute to CR anchoring. Consistent with this, combined repression of *pxl1* with a hypomorphic *cdc15* allele results in exacerbated CR sliding (Cortes et al., 2015).

Here we define a distinct mechanism which anchors CRs during anaphase, explaining why cells lacking *S. pombe efr3* divide asymmetrically (Chen et al., 2014). In *Saccharomyces cerevisiae*, Efr3 and its partner Ypp1 form a platform at the PM for Stt4,

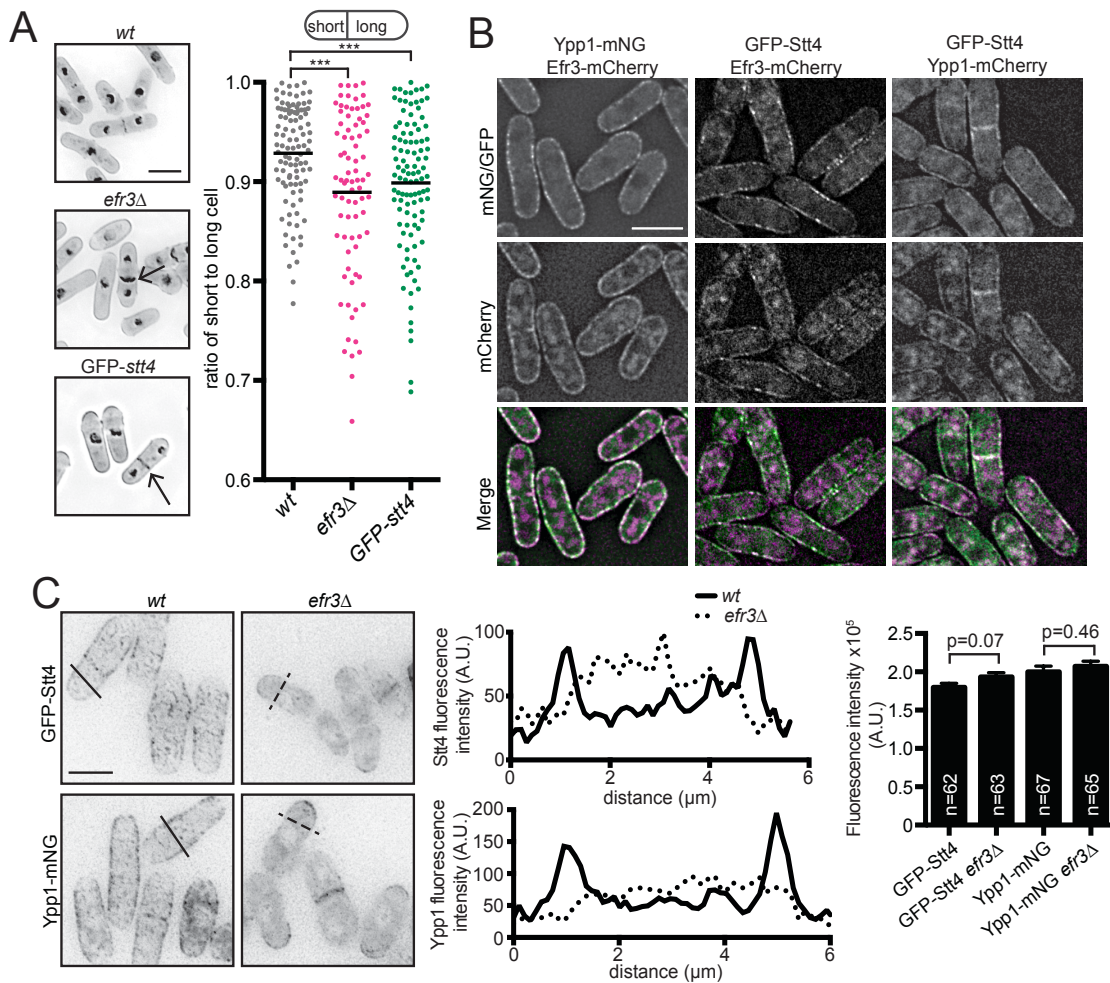


Figure 4-1

***efr3Δ* display off-center septa.**

(A, left) Representative images of indicated strains grown at 32°C, fixed and stained for cell wall and nuclei.

Arrows indicate off-center septa. (A, right) Schematic of the classification of centered and off-centered septa and quantification. Individual points represent the ratio of the length of the short to long daughter cell at septation and black bars denote mean. (B) Efr3-mCherry, Ypp1-mNeonGreen (mNG), Ypp1-mCherry and GFP-Stt4. Images are of a single medial Z-slice. (C, left) GFP-Stt4 or Ypp1-mNG in either wild-type (wt) or *efr3Δ*. Images are Z-projections and images are not scaled the same. (C, middle) Line scans of the fluorescence intensity of the solid (wt) and dotted (*efr3Δ*) black lines shown in left panels. (C, right) Whole-cell fluorescence intensity of the indicated strains.

a PI4-kinase, which regulates PIP composition and supports endocytosis (Baird et al., 2008). Similarly, human homologues of Efr3 and Ypp1 (EFR3A/B and TTC7) scaffold a PI4-kinase type-III α at the PM (Nakatsu et al., 2012).

We find that *S. pombe* lacking properly positioned Stt4 have altered PM PIPs. These cells form CRs in the cell middle that can then slide towards one end in a directed

manner. CR sliding in *efr3Δ* requires the type V myosin Myo51, indicating for the first time that the CR is subject to perpendicular forces in addition to being under constrictive tension (Proctor et al., 2012), and that these forces can dislodge the CR from the cell center. Thus, PM PIP composition contributes to CR anchoring, promoting proper septum positioning and ensuring accurate genome segregation.

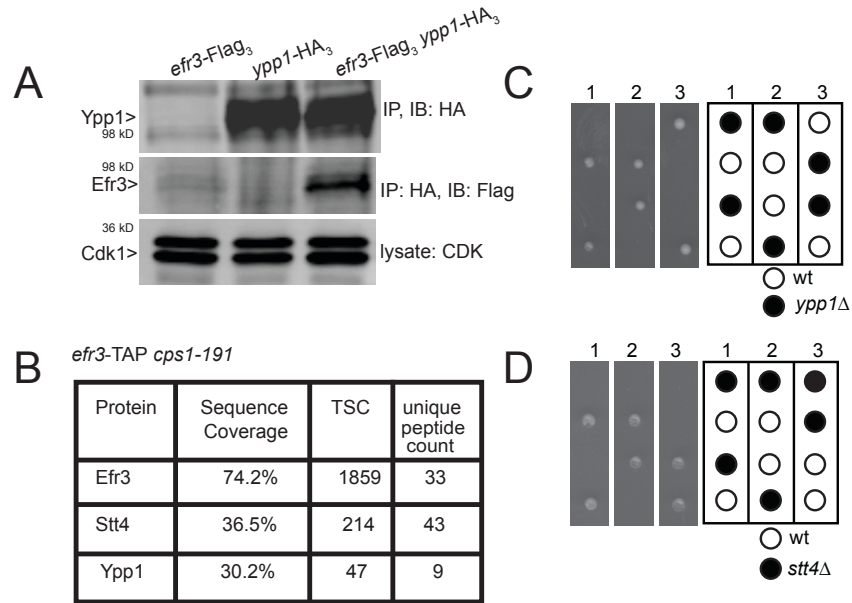


Figure 4-2

***stt4* and *ypp1* are essential in *S. pombe*.**

(A) anti-HA immunoblot (top), anti-Flag immunoblot (middle) of anti-HA and anti-Flag immunoprecipitations from the indicated strains. Anti-CDK was used as a loading control (bottom). (B) Proteins affinity purified with *efr3-TAP cps1-191* detected by mass spectrometry. TSC= total spectral count. (C,D) Diploids heterozygous for *ypp1::ura⁺* (C) or *stt4::ura⁺* (D) were sporulated on glutamate plates and tetrads were picked and allowed to germinate on YE at 29°C. Pictures of plates were taken after 5 days of growth at 29°C. All viable colonies were susceptible to growth media without uracil.

4.2 Results and discussion

The Stt4 complex is important for medial cell division in *S. pombe*

We previously observed that a high percentage of *efr3Δ* divide asymmetrically (Fig. 4-1A), sometimes resulting in a “cut” phenotype (Chen et al., 2014). To determine

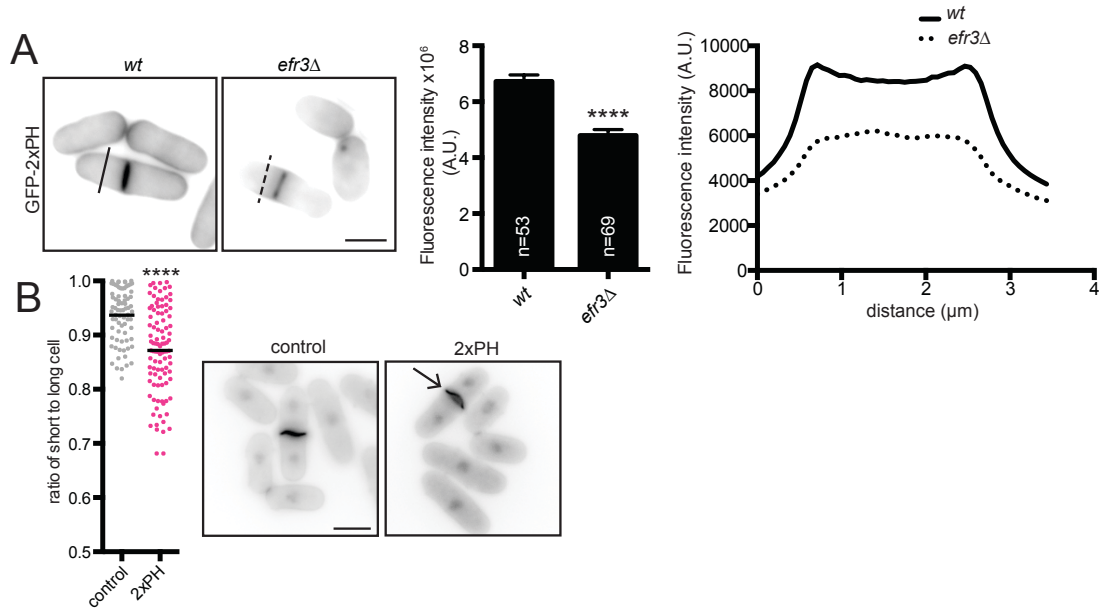


Figure 4-3

***efr3Δ* display abnormal PIP composition.**

(A, left) Representative images of GFP-2xPH(PLC δ) localization in either *wt* or *efr3Δ*. (A, middle) Quantification of the fluorescence intensity at the division septum. (A, right) Line scans of the fluorescence intensity of the solid (*wt*) and dotted (*efr3Δ*) black lines. Data in graphs are from three biological replicates. (B) Over-expression of GFP-2xPH(PLC δ) from an *nmt81* promoter induced for 24 hours. **** $p \leq 0.0001$; (D) Student's t-test. Error bars represent SEM. Scale bars = 5 μ m.

if this is due to altered PM PIP composition, we first determined if Efr3 co-localizes with Stt4 and Ypp1 in *S. pombe* by analyzing the localization of three distinct pairs of these proteins tagged with mCherry and mNeonGreen (mNG) or GFP. Each pair co-localized on the PM in a punctate pattern (Fig. 4-1B), resembling the PI kinase patch localization of the *S. cerevisiae* Stt4 complex (Baird et al., 2008). The PM enrichment of *S. pombe* Stt4 and Ypp1, but not their levels, depended on Efr3 (Fig. 4-1C). Efr3 co-immunoprecipitated with Ypp1 (Fig. 4-2A) and both Ypp1 and Stt4 were identified in an Efr3-TAP by LC-MS/MS analysis (Fig. 4-2B) indicating that these proteins associate in *S. pombe*. To further study the influence of Stt4 on septa positioning, we attempted to construct *stt4Δ* and *ypp1Δ*, but found that these genes are essential (Fig. 4-2C and D). However endogenous *GFP-stt4* displayed off-center septa indicating that although GFP-Stt4 localizes correctly to the PM, it is likely to be a hypomorphic allele (Fig. 4-1A and

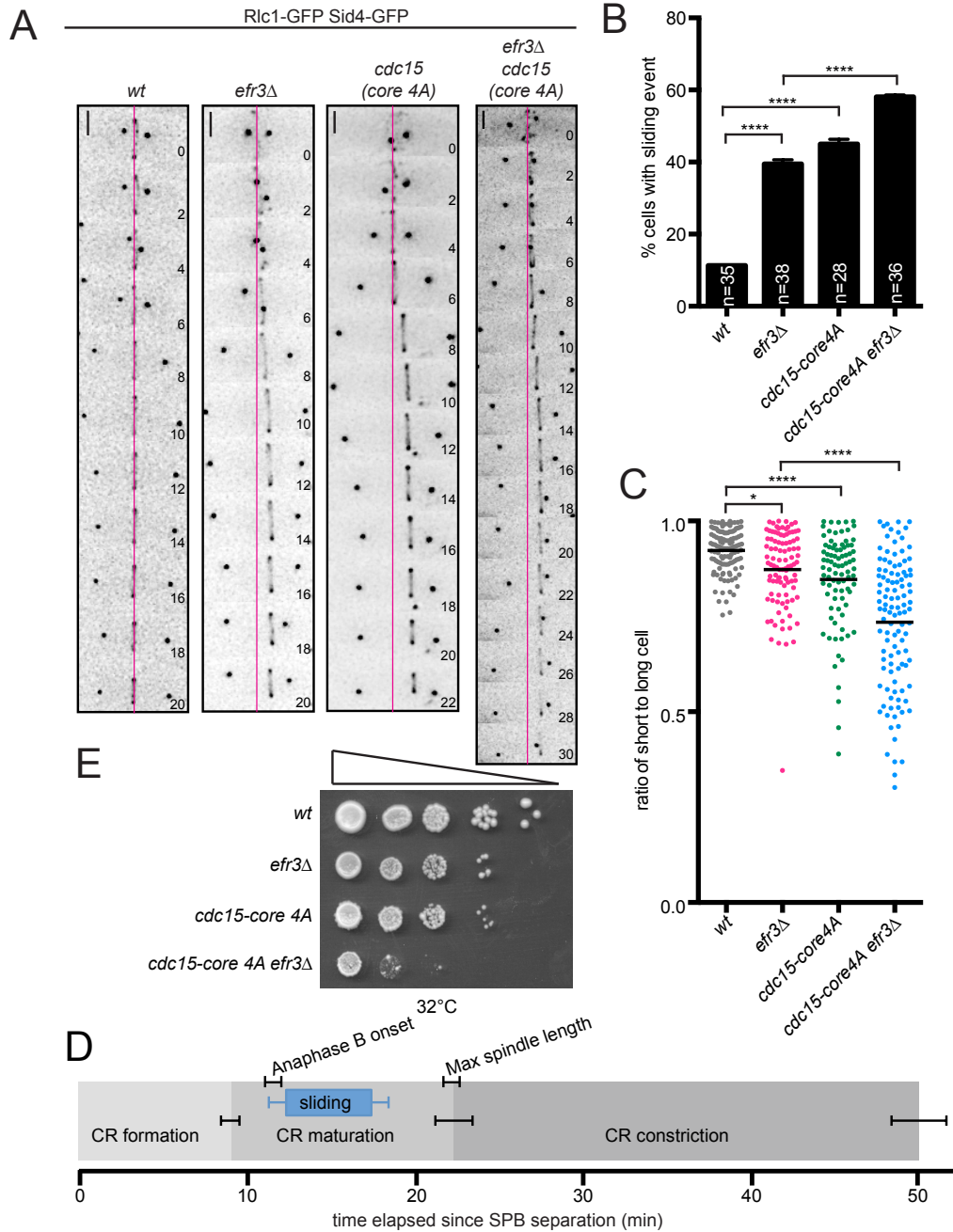


Figure 4-4

CRs slide from the cell middle in *efr3Δ*.

(A) Live-cell imaging of indicated strains expressing Rlc1-GFP and Sid4-GFP. Magenta lines represent the center of the cell. Scale bars = 2 μ m. (B) Quantification of the frequency of CR sliding events from (A). (C) Quantification of off-center septa. Individual points represent the ratio of the length of the short to long daughter cell at septation and black bars denote mean. (D) Average timing of CR events in *efr3Δ* determined from (A). (E) Growth assay of serial 10-fold dilutions of the indicated strains at 32°C on YE media. Error bars represent SEM. * $p \leq 0.05$ **** $p \leq 0.0001$, one-way ANOVA.

B). These data establish that proteins of the Stt4 complex are important for medial

division.

Stt4 phosphorylates PM PI to produce PI4P, which can be further modified to PI(4,5)P₂. Therefore, disruption of PI4-kinases results in a reduction of both PI4P and PI(4,5)P₂ (Audhya and Emr, 2002; Baird et al., 2008; Nakatsu et al., 2012). The PI(4,5)P₂ sensor GFP-2xPH(PLC δ) (Stefan et al., 2002a) was reduced at the cell cortex and at division site in *efr3 Δ* compared to wild-type (Fig. 4-3A), indicating that PIP PM abundance is reduced in *efr3 Δ* . In accord, overexpression of GFP-2xPH(PLC δ), expected to sequester PI(4,5)P₂, resulted in off-center septa (Fig. 4-3B).

efr3 Δ have off-center septa due to CR sliding

We next addressed how off-center septa arise in *efr3 Δ* . Because septum position is dictated by CR position (Marks et al., 1986), we reasoned that either the CR forms off-center or it slides from its original medial position. To distinguish between these possibilities, we imaged wild-type and *efr3 Δ* expressing CR (Rlc1-GFP) and spindle pole body (Sid4-GFP) markers. In wild-type the CR formed in the cell center and maintained this position during cytokinesis (Fig. 4-4A). In *efr3 Δ* , the CR formed in the cell center, but slid from its original position while remaining perpendicular to the cell's long axis (Fig. 4-4A and C). Temporal progression through cytokinesis was unchanged in *efr3 Δ* compared to wild-type (Fig. 4-5A and B). CR sliding occurred during anaphase B, after the CR formed in early mitosis, but stopped before or coincidentally with CR constriction (Fig. 4-4A and D). This indicates that the CR cannot slide in *efr3 Δ* once septation begins,

likely because septum formation locks the CR in position (Munoz et al., 2013; Willet et al., 2015b).

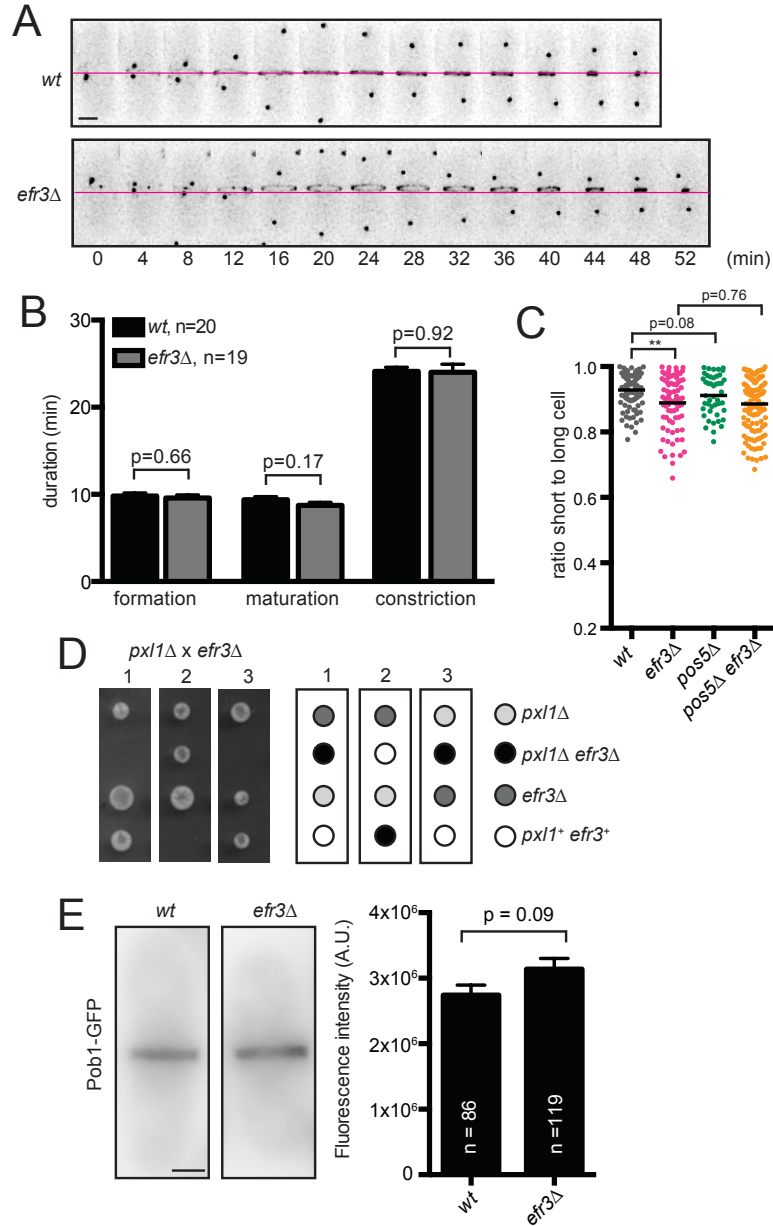


Figure 4-5

Cytokinesis timing is unperturbed in *efr3Δ*.

(A) Timing of cytokinesis events was monitored by Rlc1-GFP and Sid4-GFP in live cells. Scale bar = 2 μ m. (B) Quantification of cytokinesis timing in wt and *efr3Δ* from (A). Error bars represent SEM. (C) Off-center septa were measured in indicated strains. Individual points represent the ratio of the length of the short to long cell at septation and black bars denote mean. (D) Tetrads resulting from cross of *pxl1Δ* and *efr3Δ*. (E, left) Representative images of live-cell Pob1-GFP in wt and *efr3Δ*. (E, right) quantification of (E, left). **p<0.01, one-way ANOVA.

Efr3-dependent and Cdc15-dependent CR sliding are independent mechanisms

CR sliding, indicative of a CR anchoring defect, was observed when oligomerization of Cdc15's F-BAR domain was prevented or when *cdc15* expression was repressed (Arasada and Pollard, 2014; McDonald et al., 2016). To determine if Cdc15-mediated CR anchoring involves Efr3, we compared CR sliding events in *efr3Δ* and *cdc15-core 4A*, a mutation that specifically impairs membrane binding (McDonald et al., 2016). Alone, *cdc15-core 4A* displayed CR sliding. When combined with *efr3Δ*, the frequency of CR sliding events was increased compared to each single mutant (Fig. 4-4A and B). Also, CRs slid farther in the double mutant, indicated by the lower average ratio of short to long cell at septation (Fig. 4-4C), ultimately leading to growth defects (Fig. 4-4E). Therefore Cdc15- and Efr3-mediated CR anchoring are independent mechanisms that maintain central CR positioning. Mutants of *pxl1* also display CR sliding (Cortes et al., 2015), however *pxl1Δ efr3Δ* was inviable (Fig. 4-5D), suggesting that Pxl1 contributes to CR anchoring independently of Efr3. Because *efr3Δ* does not change the kinetics of cytokinesis (Fig. 4-5A and B), as do defects in β -glucan enzymes Bgs1 and Bgs4 (Davidson et al., 2016; Munoz et al., 2013; Sethi et al., 2016), Efr3-dependent anchoring appears to be an independent mechanism from cell wall anchoring as well.

Because *efr3Δ* have reduced levels of PM PI(4,5)P₂, we hypothesized that the cortical enrichment of proteins with membrane-binding domains (F-BAR, PH, PX or C2) would be diminished in *efr3Δ* compared to wild-type. Consistent with Cdc15 acting independently of Efr3 and interacting with a wide range of anionic phospholipids

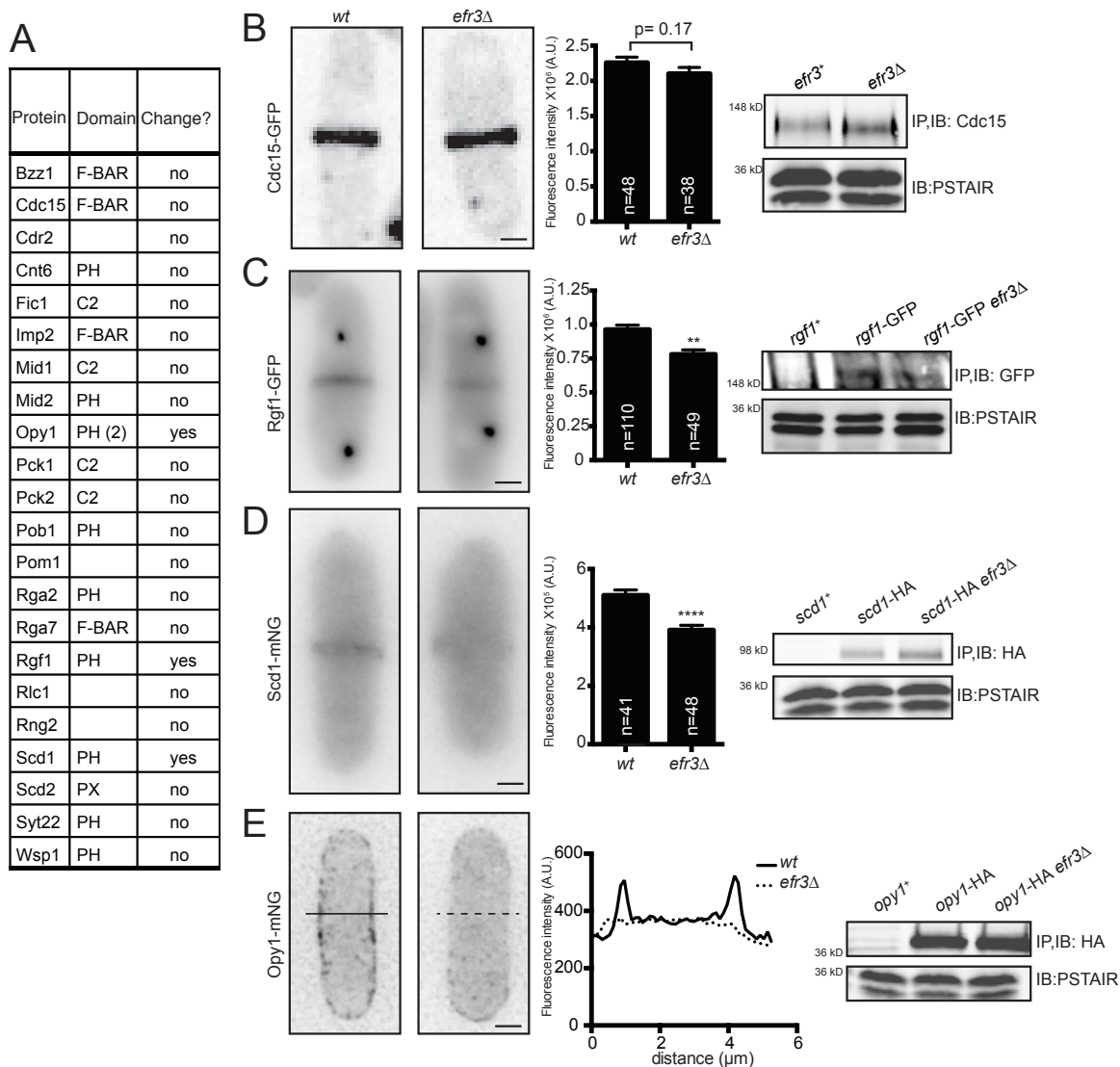


Figure 4-6

Localization of membrane-binding proteins in *efr3Δ*.

(A) List of all proteins endogenously tagged with GFP or mNG and screened for differences in protein localization in wt compared to *efr3Δ*. Fluorescence intensity at the division site was measured and statistically significant differences are noted. (B-E, Left) Live-cell imaging of Cdc15-GFP (B), Rgf1-GFP Sid4-GFP (C), Scd1-mNG (D), or Opy1-mNG (E) in either wt or *efr3Δ*. (B-D, Middle) Quantification of fluorescence intensity at the cell division site. (E, Middle) Line scan of fluorescence intensity. (A-E, Right) Western blots of protein levels in wt and *efr3Δ*. Measurements in (B-D) represent three biological replicates. ** $p \leq 0.01$ **** $p \leq 0.0001$, Student's t-test. Error bars represent SEM. Scale bar = 2 μm .

(McDonald et al., 2016), we found no difference in Cdc15 CR intensity (Fig. 4-6A and B). The localizations of many other membrane-binding proteins, such as Pob1 (Fig. 4-5E), were also unaltered in *efr3Δ* (Fig. 4-6A), suggesting that they do not rely upon PI4P or PI(4,5)P₂. However, we identified three PH domain-containing proteins with reduced

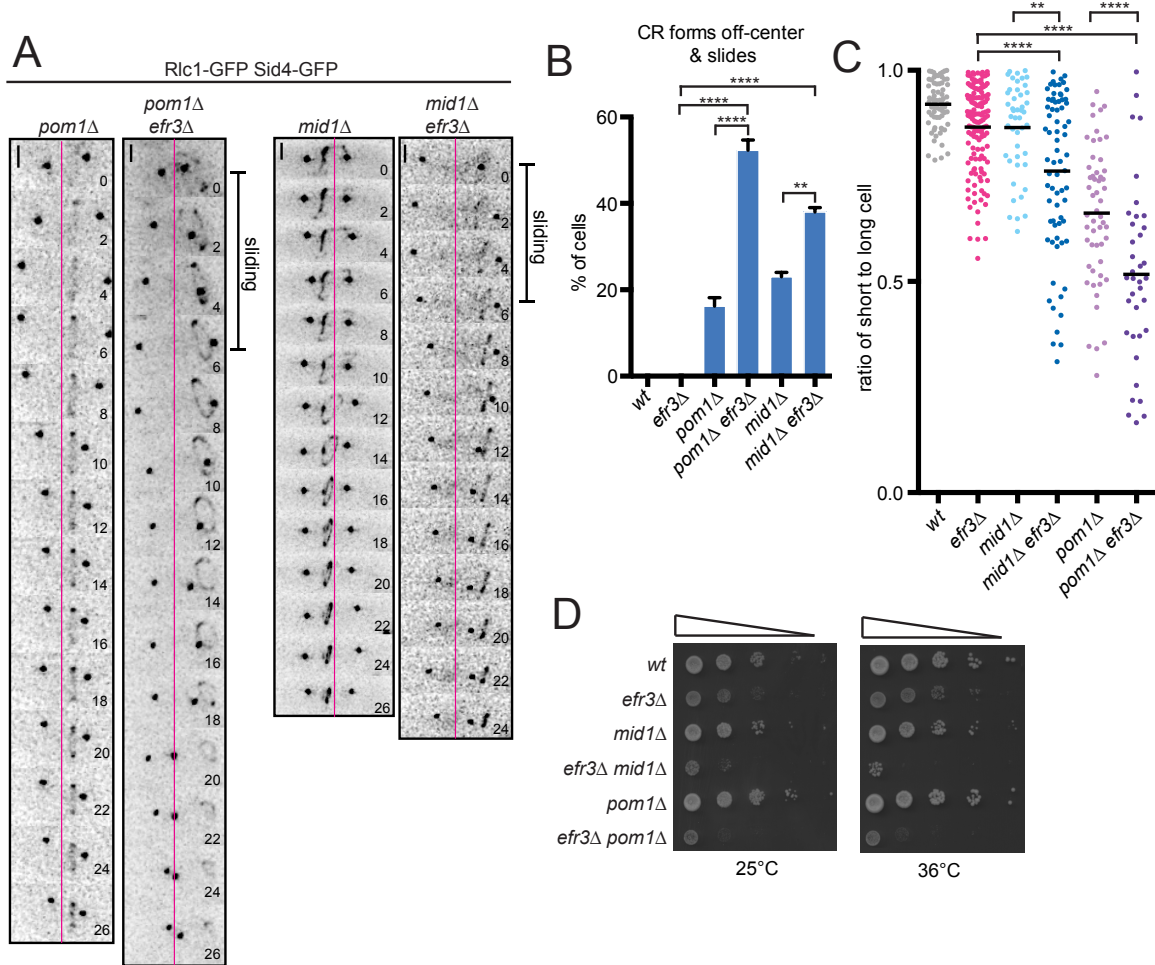


Figure 4-7

The Stt4-complex and CR positioning machinery cooperate in septum positioning.

(A) Live-cell imaging of indicated strains expressing Rlc1-GFP and Sid4-GFP. The magenta lines mark the center of the cell. Scale bars = 2 μ m. (B) Quantification of the frequency of events shown in (A) where the CR both forms off center and then slides. (C) Quantification of CR sliding. Individual points represent the ratio of the length of the short to long cell at septation and black bars denote mean. (D) Growth assay of serial 10-fold dilutions of the indicated strains at the indicated temperatures. ** $p \leq 0.01$ **** $p \leq 0.0001$, one-way ANOVA. Error bars represent SEM.

PM localization in *efr3Δ* compared to wild-type. The RhoGEF Rgf1 and Cdc42 GEF

Scd1 were reduced at the division site without any reduction in total protein levels (Fig.

4-6C and D). Opy1, encoded by the ORF SPCPB16A4.02c, is normally enriched at the

PM, but was diffusely localized in *efr3Δ* (Fig. 4-6E). Opy1 contains two PH domains and

the *S. cerevisiae* ortholog, Opy1, is implicated in sensing PI4P at the PM and inhibiting

the PI5-kinase Mss4 (Its3 in *S. pombe*) (Ling et al., 2012). Thus, it may be a collective reduction of several proteins at the cortex that compromises CR-PM attachment in *efr3Δ*.

efr3Δ combined with mutants that have misplaced CRs have exacerbated off-center septa defects

Off-center septa in *S. pombe* are observed when CRs slide and also when they assemble off-center. Mid1 and Pom1 dictate CR positioning (Rincon and Paoletti, 2016); cells lacking either divide asymmetrically due to misplaced CRs (Bahler and Pringle, 1998; Bahler et al., 1998; Sohrmann et al., 1996). In *mid1Δ*, CRs assemble at random positions and angles along the cortex but eventually coalesce into an orthogonal CR (Huang et al., 2008) although if CRs form within the curved cell pole of *mid1-18*, they can slide towards the tip, decreasing in diameter (Mishra et al., 2013). To test whether the Mid1 and Pom1 cues are influenced by PM composition, given that both proteins bind membrane PIPs (Celton-Morizur et al., 2004; Hachet et al., 2011), we combined *mid1Δ* or *pom1Δ* with *efr3Δ* and analyzed CR dynamics. We scored if CRs formed off-center and if fully formed CRs slid during anaphase. In our experiments, *mid1Δ* rarely formed CRs at the extreme cell tip that slid. As previously observed, *mid1Δ* and *pom1Δ* form off-center CRs but we did not detect a significant number of subsequent sliding events. Consistent with our finding that initial CR placement is not altered in *efr3Δ*, the localizations of PM-binding proteins Mid1 and Pom1 were not influenced by deletion of *efr3* (Fig. 4-7A). In combination with *efr3Δ*, CRs formed off-center *and* slid during anaphase, resulting in septa that were farther off-center than single mutants (Fig. 4-7A

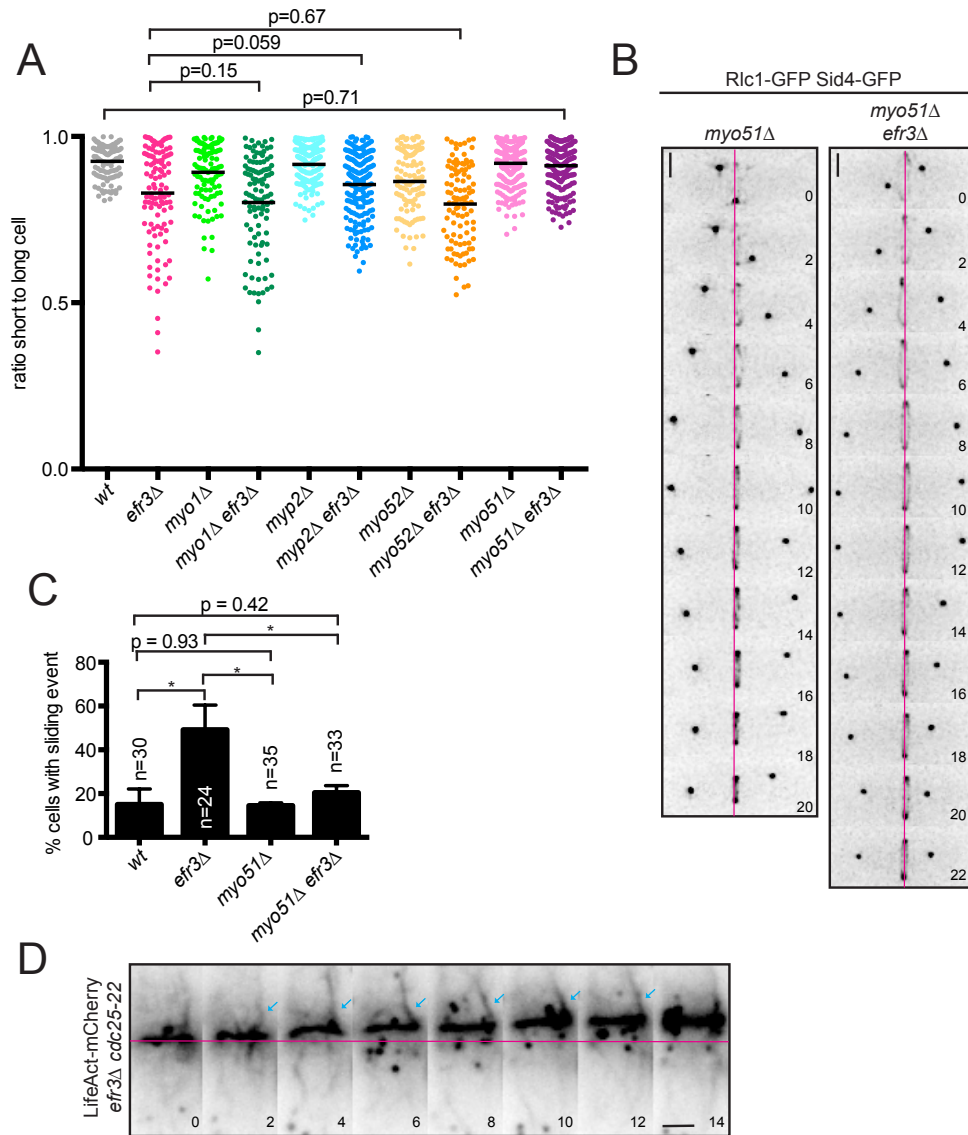


Figure 4-8

***efr3Δ* CR sliding events depend on Myo51.**

(A) Quantification of off-center septa. Individual points represent the ratio of the length of the short to long daughter cell at septation and black bars denote mean. (B) Live-cell imaging of indicated strains expressing Rlc1-GFP and Sid4-GFP. Magenta lines represent the center of the cell. (C) Quantification of the frequency of CR sliding events from (B). Error bars represent SEM. (D) Montage of time-lapse imaging of LifeAct-mCherry in *efr3Δ cdc25-22*. Cells were grown at 36°C for 4 hours prior to imaging at 25°C. Montage is of a single Z slice and arrows indicate an actin cable in close proximity to a sliding CR. Scale bars = 2 μm. *p ≤ 0.05, one-way ANOVA.

and C). These combinations also led to significant growth defects (Fig. 4-7D), most likely due to cutting of chromosomes by off-center septation.

We next considered whether CR sliding events in *efr3Δ* are enabled by diminishing cell circumference from the cell middle towards one end similar to CRs in spheroplasts that move along the cortex while constricting (Mishra et al., 2013). This seemed unlikely, however, because *efr3Δ* have normal morphology (Chen et al., 2014) and CRs slide only 1-2 μm (Fig. 4-4A), not approaching the region of curvature at the

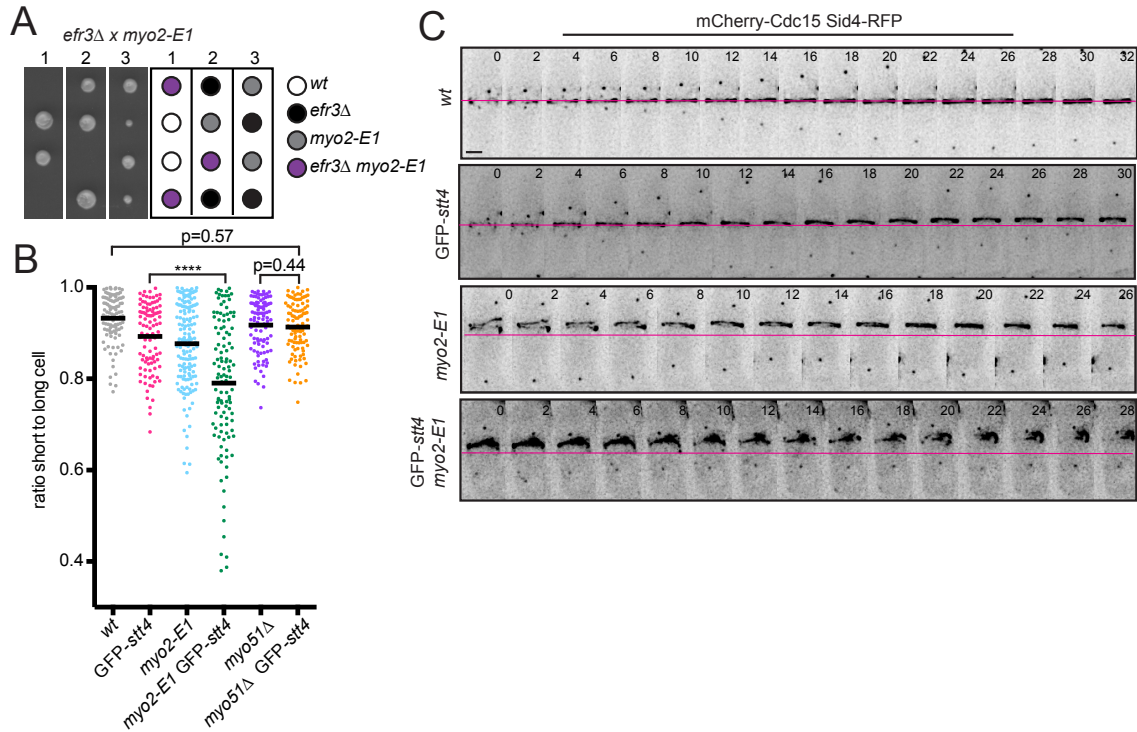


Figure 4-9

***efr3Δ* CR sliding does not depend on Myo2.**

(A) Analysis of resulting tetrads from cross of *efr3Δ* and *myo2-E1*. (B) Off-center septa were measured in the indicated strains. Individual points represent ratio of the length of the short to long cell at septation, black bars denote mean. (C) Live-cell imaging of indicated strains expressing mCherry-Cdc15 and Sid4-RFP. Magenta lines represent the center of the cell measured in a DIC image. **** $p \leq 0.0001$, one-way ANOVA.

hemispherical cell ends (Atilgan et al., 2015). Also *pos5Δ*, which is tapered at one cell end (Hayles et al., 2013), does not have off-center septa, indicating that a CR does not automatically slide toward a tapered end (Fig. 4-4C). The CR width, as a proxy of cell diameter, also does not decrease during a sliding event in *efr3Δ*, which would be expected if the circumference of the cell changed (Δ width = 0.045 μm +/- 0.039 μm

(SEM, n = 19)). Further, in *pos5Δ efr3Δ*, there is no worsening of the off-center septa phenotype compared to *efr3Δ* (Fig. 4-4C) and sliding CRs have no bias toward the tapered end of the cell (54% to tapered end vs 46% to non-tapered end) similar to *efr3Δ* where the CR is equally likely to slide to the old or new end of the cell (48% to old end vs 52% to new end). We conclude that CR sliding events in *efr3Δ* are not dictated by cell geometry.

Efr3-dependent CR sliding requires myosin V Myo51

Because CR sliding in spheroplasts and *cdc15* defective cells depends on type II myosins Myo2 and Myp2, respectively (Arasada and Pollard, 2014; Mishra et al., 2013), we tested if myosin-generated force is required for CR sliding in *efr3Δ*. Neither Myp2, the type I myosin Myo1, nor the type V myosin Myo52 were necessary for CR sliding in *efr3Δ* (Fig. 4-8A). To test if CR sliding depends on Myo2, we attempted to combine *efr3Δ* with the temperature sensitive *myo2-E1* allele (Balasubramanian et al., 1998) but these alleles were synthetically lethal (Fig. 4-9A). Instead, we used a *myo2-E1 GFP-stt4* combination. *GFP-stt4* (*GFP-stt4* is hypomorphic) and *myo2-E1* each had off-centered septa at 32°C, and the combination resulted in more cells with off-center septa that were even farther away from center (Fig. 4-9B). Live-cell imaging revealed that *GFP-stt4* CRs slid during anaphase while *myo2-E1* CRs formed off-center but did not slide (Fig. 4-9C). *GFP-stt4 myo2-E1* formed CRs off-center that then also slid along the cortex (Fig. 4-9C). Thus, CR sliding in *efr3Δ* does not depend on Myo2.

In contrast, deletion of the type V myosin Myo51 eliminated the *efr3Δ* off-center septa phenotype (Fig. 4-8A). CR sliding events no longer occurred in *myo51Δ efr3Δ* (Fig. 4-8B and C) and the average ratio of short to long cell was significantly higher than in *efr3Δ* (Fig. 4-8A). As expected given that Stt4 binds Efr3, the GFP-*stt4* off-center septa phenotype is also Myo51-dependent (Fig. 4-9B). Interestingly, none of the myosins were necessary for CR sliding in *cdc15-core 4A* or *pxl1Δ* mutants (Fig. 4-10A and B) consistent with the genetic evidence that Cdc15-, Pxl1-, and Efr3-dependent CR sliding events occur through independent mechanisms (Cortes et al., 2015). CR sliding in *cdc15* and *pxl1Δ* mutants, as well as in β -glucan synthase mutations, may occur due to structural instability of the CR rather than a directed movement of the CR along the cortex (Arai and Mabuchi, 2002; Arasada and Pollard, 2014; Balasubramanian et al., 1998; Davidson et al., 2016; Ge and Balasubramanian, 2008; Hachet and Simanis, 2008; Laporte et al., 2011; McDonald et al., 2016; Munoz et al., 2013; Roberts-Galbraith et al., 2009; Wachtler et al., 2006).

Myo51 contains an N-terminal motor head domain and a C-terminal tail domain necessary for CR localization (Wang et al., 2014). By testing Myo51 N- and C-terminal truncations in *efr3Δ*, we found that both the N-terminal head and C-terminal tail of Myo51 are necessary for CR sliding (Fig. 4-10C), suggesting that Myo51 tail binding to CR components and the ability to walk along actin filaments (Wang et al., 2014) are both required to move the CR.

The necessity of Myo51 force generation for CR movements in *efr3Δ* provides strong evidence for the existence of forces on the CR perpendicular to the cell axis. Such forces could be involved in the splitting of CRs observed in some mutants, e.g. *pxl1Δ* (Ge

and Balasubramanian, 2008) and *sbg1-3* (Sethi et al., 2016). We hypothesize that perpendicular forces are balanced in a wild-type cell and/or that CR-PM attachments are

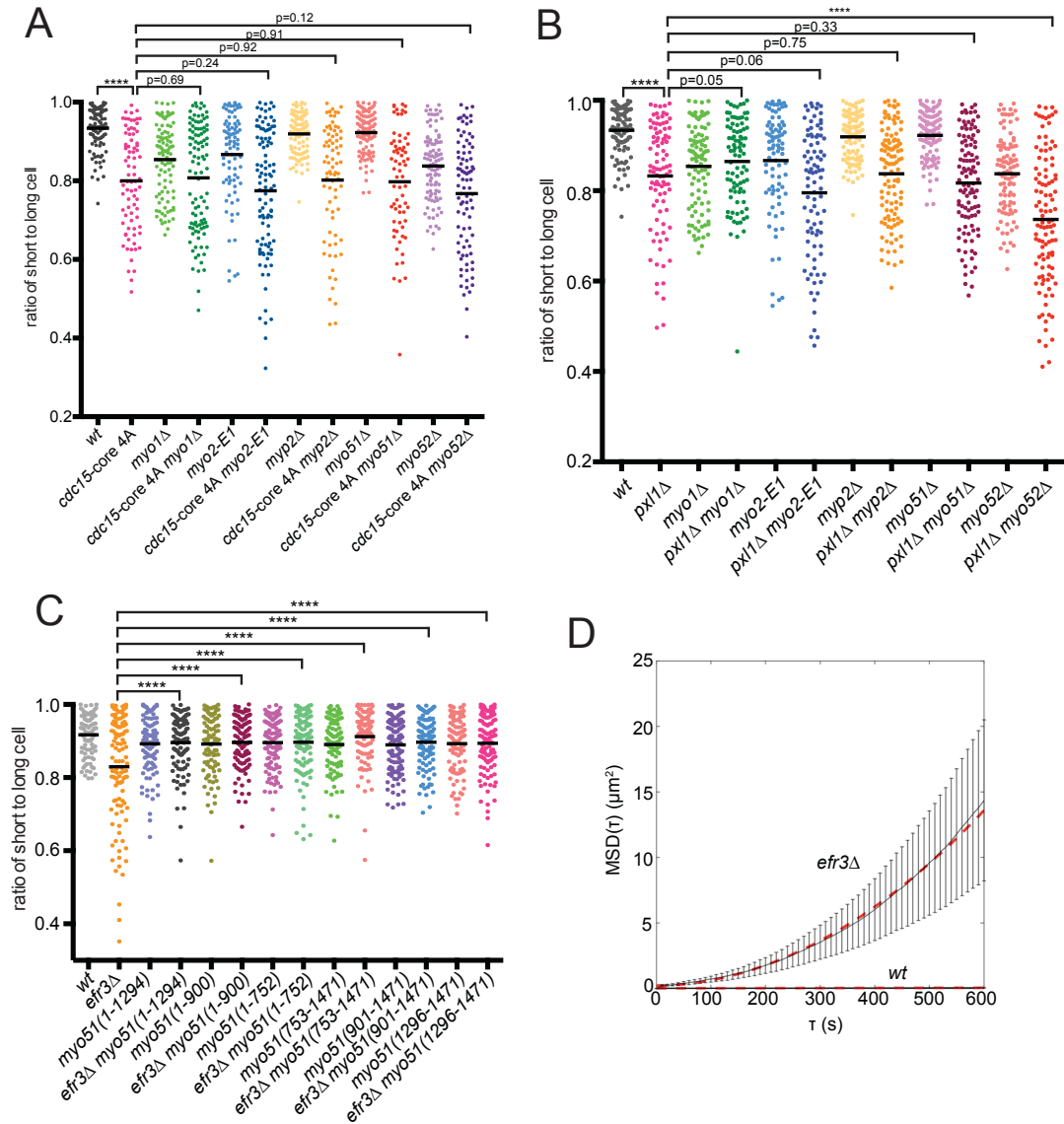


Figure 4-10

N- and C-termini of Myo51 are necessary for *efr3Δ* CR sliding.

(A-B) Off-center septa were measured in wt, *cdc15-core 4A* (A), *cdc15-core 4A* with myosin mutants (A), *pxl1Δ* (B), and *pxl1Δ* with myosin mutants (B). (A-C) Off-center septa were measured in the indicated strains. (D) Mean Squared Displacement (MSD) of cytokinetic ring position trajectories for wt (N=20 trajectories from 10 cells) and *efr3Δ* (N=34 trajectories from 17 cells). All trajectories are assumed to be independent realizations. Red-dashed lines are quadratic best fits to the MSD data, obtained over the first 600 seconds (see Methods). Error bars represent SEM. **** $p \leq 0.0001$, one-way ANOVA.

sufficient to resist these forces so that the CR remains in its central position. Further, in

efr3Δ force imbalances may arise that cannot be stabilized, resulting in Myo51-dependent CR sliding along the cell axis. In support of this hypothesis, mean squared displacement analysis of sliding *efr3Δ* CRs shows a statistically significant drift velocity term, suggesting directed transport of the CR (Fig. 4-10D, $v = 1.35$ nm/s, 95% confidence interval: 1.32-1.37 nm/s). No such transport term was measured for wild-type rings, which exhibit minimal changes in position over the imaging period ($D = 15.8$ nm²/s, 95% CI: 12.6-19 nm/s; $v = 0$ nm/s at 95% confidence level). A possible explanation for this behavior is that Myo51 in the CR associates with longitudinal actin cables as well as F-actin within the CR, pulling the CR along cables when PM anchoring is weakened. In support of this, Myo51 has been shown to play a role in the medial accumulation of actin cables during cytokinesis (Huang et al., 2012) and actin cables can be seen in proximity to sliding CRs in *efr3Δ* (Fig. 4-8D).

Altogether, our data reveal a novel CR anchoring mechanism that depends on a conserved PM-localized PI4-kinase complex (Fig. 4-11). An ensemble of proteins sensitive to correct PM PIP composition synergize with Cdc15-, Pxl1- and cell wall-dependent anchoring to promote stable CR placement and faithful segregation of the genetic material during cell division. Given the large number of lipid-binding proteins at the cell division site of many eukaryotes, and the importance of a PI4-kinase for cytokinesis (Brill et al., 2000a; Eggert et al., 2004a), it is likely to be a broadly relevant factor for CR-PM adhesion.

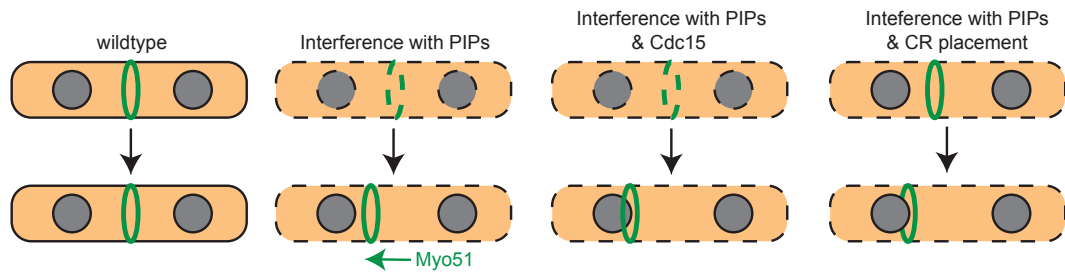


Figure 4-11

Model for CR anchoring during cytokinesis.

Proper PIP composition, dependent on Efr3, promotes CR ring anchoring. When PM lipid and CR protein composition is altered, CRs can slide. Cdc15 is an independent mechanism for CR anchoring as *cdc15* mutants combined with *efr3Δ* results in exacerbated CR sliding defects. Disruption of CR positioning machinery in combination with *efr3Δ* leads to exacerbation of off-center septa.

CHAPTER 5

CONCLUSIONS AND FUTURE DIRECTIONS

There are many remaining questions regarding how cytokinesis is regulated in order to for cells to faithfully divide. Some outstanding questions include: how is CR formation regulated, how are proteins (including F-actin) organized in the CR, how is the CR anchored and how is the final abscission step orchestrated? I focused my studies on understanding how the CR is formed and anchored using the model organism *S. pombe*. To better understand how the CR is formed, I was interested in how the essential proteins involved in forming the CR are regulated to ensure proper progression of cytokinesis. Some potential modes of regulation for key cytokinetic proteins are through direct protein interactions and post-translational modifications to control localization and activity. I explored both of these possibilities in chapters 2 and 3.

Both formin Cdc12 and F-BAR Cdc15 have essential roles in forming the CR during *S. pombe* cytokinesis (Chang et al., 1997; Fankhauser et al., 1995). It was previously reported that Cdc12's N-terminus and Cdc15's F-BAR domain directly interact (Carnahan and Gould, 2003); yet the function of this interaction was unknown. The work in the second chapter showed that Cdc12 interacts with Cdc15 F-BAR domain via a short N-terminal motif (residues 24-36) and that this interaction is important to recruit formin Cdc12 to the cell division site for timely formation of the CR during cytokinesis (Willet et al., 2015a). This interaction is of particular interest because the F-BAR domain of Cdc15 directly binds both the PM and formin, thereby directly linking

the PM to actin cytoskeletal rearrangements, a common feature of F-BARs (McDonald and Gould, 2016; Roberts-Galbraith and Gould, 2010). Not surprisingly, mutations that disrupt Cdc15's PM binding result in CR anchoring defects (McDonald et al., 2016). However, Cdc15 is not the only factor that recruits formin Cdc12 to the cell division site. Cdc12 can also localize to the CR via FH2 domain F-actin binding (Kovar et al., 2003; Yonetani et al., 2008). Additionally, in the absence of F-BAR binding and polymerized F-actin, Cdc12 can still localize to the medial cortex, indicating that there is at least one additional unidentified interaction that promotes Cdc12's CR localization (Willet et al., 2015a; Yonetani et al., 2008). Cdc12's N-terminal armadillo repeats (ARM) are possibly involved; Cdc12's N-terminus (including the ARM) is sufficient for CR localization (Yonetani et al., 2008) and the ARM in other formins has been shown to be important for proper localization (Petersen et al., 1998). Based on genetic evidence, some likely candidates for additional Cdc12 binding partners include the myosin II heavy chain Myo2, IQGAP Rng2 or the Anillin-like Mid1 (Laporte et al., 2011; Willet et al., 2015a), all of which localize early to the cell division site. Anillin homologs in other organisms have been shown to be important in cytokinetic formin localization and regulation (Watanabe et al., 2010), making Mid1 is an attractive candidate for a conserved formin binding partner and regulator. A comprehensive understanding of formin Cdc12 binding partners will give insight into how redundant mechanisms promote formin localization for proper function, which may be widely applicable.

An additional mode of cytokinetic regulation is through post-translational modifications of proteins. I played an instrumental role in helping discover that Cdc12 is

phosphorylated by the SIN kinase Sid2 (Bohnert et al., 2013), making Cdc12 the first essential protein target of this signaling network. The research in chapter 3

shows that Cdc12 is also phosphorylated by the master cell cycle regulator Cdk1, a finding that was recently confirmed *in vivo* (Swaffer et al., 2016). Cdk1 phosphorylation of Cdc12 inhibits the Cdc12-Cdc15 F-BAR interaction. As expected, an allele of *cdc12* with constitutive Cdk1 phosphorylation (*cdc12-6D*) shows similar phenotypes to an allele that cannot bind Cdc15 (*cdc12-P31A*); both alleles have reduced Cdc12 at the cell division site and delayed CR formation (Willet et al., 2015a). It was previously reported that Cdc12 and Cdc15 interact when Cdc15 is in a hypo-phosphorylated state during early mitosis (Roberts-Galbraith et al., 2010). These new findings indicate that Cdc12 must also be in a hypo-phosphorylated state for efficient recruitment via Cdc15 F-BAR binding. Even though this interaction occurs when Cdk1 activity is high (early mitosis), it is likely that counteracting phosphatases play an important role in regulating this interaction. One such phosphatase is Clp1; Cdc15 is a direct target of Clp1 (Chen et al., 2013b; Roberts-Galbraith et al., 2010) and Cdc12 is hyper-phosphorylated in *clp1Δ* cells, indicating that it may also be a target. In addition, Clp1 localizes to the CR in early mitosis, when Cdc12 and Cdc15 interact (Roberts-Galbraith et al., 2010; Trautmann et al., 2001). In future studies it will be interesting to determine how re-phosphorylation of both of these proteins at the end of cytokinesis contributes to the final abscission step and/or CR disassembly. It seems likely that other cell cycle regulators besides the Sid2 and Cdk1 participate in *S. pombe* Cdc12 regulation, because mutants lacking Sid2-targeted phosphosites or Cdk1-targeted phosphosites are still phosphorylated, but to a lesser degree than the wild-type protein (Bohnert et al.,

2013). Identification of the additional kinases responsible and analysis of their effects on Cdc12 activity, protein–protein interactions and targeting is important for assessing how various signaling pathways converge to control a formin molecule in cytokinesis. An interesting possibility is that Cdc12 is phosphorylated by a variety of kinases that cooperate in regulation of Cdc12 during cytokinesis. There is also the possibility that Cdc12 is targeted by post-translational modifications other than phosphorylation. Because *S. pombe* cells are highly sensitive to changes in Cdc12 protein levels (Chang et al., 1997; Kovar et al., 2003), it is possible that Cdc12, like mDia2 (DeWard and Alberts, 2009), is actively targeted for degradation by ubiquitination. If so, this modification could facilitate Cdc12 turnover within the CR during disassembly and aid in Cdc12 clearance from the division site. There is some evidence that Cdc12 is modified by additional post-translational modifications. Immunoprecipitation of Cdc12 from cells revealed a higher molecular weight band that is not collapsed by lambda phosphatase treatment, and this Cdc12 species is dependent on SIN signaling (Bohnert et al., 2013). It will be intriguing to identify the identity of this modified form of Cdc12, determine if it has a function in Cdc12 regulation and understand if there is crosstalk between different post-translational Cdc12 modifications. In summary, a more comprehensive understanding of the roles that post-translational modifications serve in cytokinetic formin regulation should enhance our understanding of the molecular cues guiding eukaryotic cell division.

My studies have shown that there are multiple domains that are potential modes of formin regulation. These domains include the newly identified C-terminal multimerization domain and the Cdc15-binding motif both of which contribute to Cdc12 function and regulation during cytokinesis (Bohnert et al., 2013; Willet et al., 2015a).

Separation of the Cdc12 multimerization domain, which permits F-actin bundling, from its FH1–FH2 core presents an opportunity for differential regulation of distinct facets of Cdc12-mediated actin assembly. In the future, it will be important to assess whether the Cdc12 C-terminus affects nucleation and elongation activities of the FH1–FH2 core in addition to directly conferring F-actin bundling capacity. We also hope to determine how proximity of a formin to membranes via F-BAR binding and phosphorylation may influence formin activities. Although the Cdc12 DAD motif appears to be unimportant (Yonetani et al., 2008), it remains possible that Cdc12 is autoinhibited in a non-canonical fashion, and further investigation of Cdc12 self-interactions could also be informative.

My studies also identified a previously unappreciated force perpendicular to the CR that helps maintain medial CR position. In cells where the Stt4 PI-4-kinase complex is disrupted, the PM lipid composition is altered and CRs slide from their original medial position in a myosin V-dependent movement. That this CR movement is dependent on myosin V Myo51 was surprising given that previously described CR sliding events in cells and spheroplasts were found to be dependent on type II myosins (Arasada and Pollard, 2014; Mishra et al., 2013). We also found that Efr3-dependent CR sliding is independent of other described CR sliding events that occur in *cdc15* or *pxl1* mutants (Cortes et al., 2015; McDonald et al., 2016), suggesting that the cells have multiple redundant mechanisms to maintain stable positioning of the CR. This is not surprising given that these asymmetric cell divisions can be detrimental to *S. pombe* cells, which sometimes “cut” their genomic material (Chen et al., 2014). It will be interesting to determine if other lipid species are important to anchor the CR and how these lipid kinases are regulated to ensure a proper concentration of lipids within the PM.

In conclusion, these studies have uncovered several new aspects of cytokinetic ring formation and anchoring, which provide insights into the process of cell division, and may inform our understanding of cell division in other contexts and in other organisms.

APPENDIX

A. Materials and Methods

Yeast methods

S. pombe strains were grown in yeast extract (YE). *cdc12*⁺, *cdc12-P31A*, *cdc12-6A*, *cdc12-6D*, *efr3*⁺, *ypp1*⁺, *opy1*⁺, *scd1*⁺, *pob1*⁺ and *rgf1*⁺ were tagged endogenously at the 3' end with TAP:kan^R, Flag₃:kan^R, HA₃:hyg^R, mCherry:kan^R, mNeonGreen:kan^R or mNeonGreen:hyg^R using pFA6 cassettes as previously described (Bahler et al., 1998; Wach et al., 1994). mNeonGreen, a recently reported green fluorescent protein derived from the lancelet *Branchiostoma lanceolatum*, was chosen for imaging experiments because of its superior brightness of ca. 93 (product of extinction coefficient and quantum yield), compared to ca. 34 for EGFP (Shaner et al., 2013) (Allele Biotechnology). mNeonGreen has an excitation maximum of 506 nm and emission maximum of 517 nm, and is currently the brightest known monomeric fluorescent protein in the green-yellow spectrum. A lithium acetate method (Keeney and Boeke, 1994) was used in *S. pombe* tagging transformations, and integration of tags was verified using whole-cell PCR and/or microscopy. Introduction of tagged loci into other genetic backgrounds was accomplished using standard *S. pombe* mating, sporulation, and tetrad dissection techniques. Fusion proteins were expressed from their native promoters at their normal chromosomal locus unless otherwise indicated.

To make the endogenous *cdc12-P31A*, *cdc12-6A* and *cdc12-6D* alleles, a pSK vector (pBluescript backbone) was constructed that contained in the following order: 5' *cdc12* flank including its promoter, full-length *cdc12*⁺, kan^R cassette, and 3' *cdc12* flank

(pKG 5431) (Bohnert et al., 2013). The *cdc12-P31A*, *cdc12-6A*, *cdc12-6D* mutations were created with mutagenesis of pKG 5431 by PCR and confirmed with sequencing. The mutant constructs were then released from the vector by digestion with Xba1 and Sac1, and transformed into wild-type *S. pombe* cells using a lithium acetate method (Keeney and Boeke, 1994). G418-resistant cells were selected and the *cdc12* locus was sequenced to identify transformants containing the desired and correct mutations.

Stt4 was N-terminally tagged with GFP at the endogenous locus using a Cre-loxP method as described (Werler et al., 2003). A cassette with the sequence that encodes GFP, the *sup3-5* selection marker and a temporary promoter (*nmt1*) is integrated at the N terminus of the *stt4* gene. Next the selection marker and temporary promoter are removed with Cre recombinase resulting in the sequences encoding GFP on the N-terminus of *stt4* under the normal promoter.

In order to express GFP-2xPH(PLC δ) in cells, the medium strength *cdc2* promoter (Carpy et al., 2014) was PCR amplified from *S. pombe* genomic DNA and GFP-2xPH(PLC δ) was PCR amplified from plasmid pRS426 (Stefan et al., 2002b). The two fragments were cloned into *S. pombe* integration vector pJK148 using Gibson Assembly. This construct was linearized and inserted into the *S. pombe leu1* locus by a lithium acetate method (Keeney and Boeke, 1994).

For growth assays, cells were grown to log phase at 25°C in YE, 10 million cells were resuspended in 1 mL of water and 10-fold serial dilutions were made. 2.5 μ l of each dilution was spotted on YE plates and the plates were incubated at the indicated temperatures.

Protein methods

Cdc12(aa1-764) was cloned into pMAL-2c for expression as an MBP fusion (Carnahan and Gould, 2003). Cdc15 F-BAR (aa19-312) was cloned into pET15b for expression as a 6xHis fusion. Proteins were induced in *Escherichia coli* Rosetta2(DE3)pLysS cells with 0.4mM IPTG overnight at 18°C. Protein was purified on amylose beads (New England Biolabs) or cComplete His-Tag resin (Roche) according to manufacturer's protocols. Cdc15(19-312)'s 6XHis tag was removed with thrombin protease and the protein was further purified on a HiTrap Q SP anion exchange column (GE Healthcare) and concentrated.

Cell pellets were snap-frozen in dry ice–ethanol baths. Lysates were prepared using a Fastprep cell homogenizer (MP Biomedicals). Immunoprecipitations were performed as previously described (Gould et al., 1991a) in NP40 buffer containing SDS for denatured lysates. Protein samples were resolved by SDS-PAGE and transferred to PVDF membrane (Immobilon P, EMD Millipore). Anti-HA (12CA5), anti-Cdc2 (Sigma) or anti-Cdc15 was used in immunoprecipitations and/or as primary antibodies in immunoblotting. Secondary antibodies were conjugated to IRDye800 or IRDye680 (LI-COR Biosciences). Blotted proteins were detected via an Odyssey machine (LI-COR Biosciences). For gel shifts, denatured lysates were treated with λ -phosphatase (New England Biolabs) in 25 mM HEPES-NaOH (pH 7.4), 150 mM NaCl, and 1 mM MnCl₂ and incubated for 30 min at 30°C with shaking. Where indicated, samples were

resolved by SDS-PAGE in the presence of 5 μ M PhosTag acrylamide per the manufacturer's protocol (Wako Chemical).

Kinase reactions were performed in protein kinase buffer (10 mM Tris, pH 7.4, 10 mM $MgCl_2$, and 1 mM DTT) with 10 μ M cold ATP, 3 μ Ci of [^{32}P]ATP, and 100 ng of kinase-active or kinase-dead insect cell-produced Cdc2-Cdc13 at 30°C for 30 min. Myelin basic protein (Sigma) was used as a control substrate for Cdc2-Cdc13. Reactions were quenched by the addition of SDS sample buffer. Proteins were separated by SDS-PAGE, transferred to polyvinylidene fluoride (PVDF) membrane, and phosphorylated proteins were visualized by autoradiography. For [$\gamma^{32}P$]ATP kinase assays, phosphoamino acid analysis, and tryptic peptide mapping were performed as described in (Feoktistova et al., 2012; Sparks et al., 1999) and references therein. In vitro phosphorylation of recombinant proteins used in in vitro binding assays was performed via identical kinase assays, except that radioactive [$\gamma^{32}P$]ATP was eliminated, and the final concentration of unlabeled ATP in reactions was increased to 2 mM.

In vitro binding

Recombinant proteins conjugated to amylose beads were incubated with recombinant Cdc15 F-BAR for 1 h at 4°C in binding buffer (50 mM Tris-HCl, pH 7.0, 250 mM NaCl, 2 mM EDTA, 0.1% NP-40). Following extensive washing in binding buffer, samples were resolved by SDS-PAGE for Coomassie blue staining.

Microscopy

Live-cell images of *S. pombe* cells were acquired using a personal DeltaVision microscope system (Applied Precision) that includes an Olympus IX71 microscope, 60× NA 1.42 PlanApo and 100× NA 1.40 UPlanSApo objectives, fixed- and live-cell filter wheels, a Photometrics CoolSnap HQ2 camera, and softWoRx imaging software. Images were acquired at 25-29°C and cells were imaged in YE media. Images in figures are maximum- intensity projections of z sections spaced at 0.2-0.5 μm. Images used for quantification were not deconvolved. Other images not used for fluorescence quantification were deconvolved with 10 iterations. Some time-lapse imaging was performed on cells in log phase on a YE agar pad at 32-36°C with the exception of LifeAct-mCherry *cdc25-22 efr3Δ*, where cells were shifted to 36°C for four hours and then imaged at 25°C. Other time-lapse imaging was performed on cells in log phase using an ONIX microfluidics perfusion system (CellASIC). Cells were loaded into Y04C plates for 5 sec at 8 psi, and YE liquid media flowed into the chamber at 5 psi throughout imaging.

Intensity measurements were made with ImageJ software (<http://rsweb.nih.gov/ij/>). For all intensity measurements, the background was subtracted by creating a region of interest (ROI) in the same image where there were no cells (Waters, 2009). The raw intensity of the background was divided by the area of the background, which was multiplied by the area of the ROI. This number was subtracted from the raw integrated intensity of that ROI (Waters, 2009). For CR intensity quantification, a ROI was drawn around the CR and measured for raw integrated density and for whole cell intensity quantification an ROI was drawn around the entire cell. In

order to compare populations of cells for all genotypes, cells were imaged on the same day with the same microscope parameters. The fluorescence intensity of the cell tips was quantified by using the exact same size circle, 3.5 μm in diameter, placed at the tip of each cell end and then subtracting background (Burke et al., 2014).

All cells were grown to log phase at 32°C before fixation. For nuclei and cell wall imaging, cells were fixed in 70% ethanol for 30 minutes before DAPI and methyl blue staining.

For quantification of CR dynamics, movies were acquired with either 1 or 2 minute intervals. Time zero was set to the first movie frame in which the SPBs were separated. CR formation was measured as time from SPB separation until the first frame in which there is a coherent ring. CR maturation was quantified as the time from CR formation until the first frame in which the CR begins to constrict. CR constriction was quantified as the time between the first and last frame during CR constriction.

For quantification of ring sliding, a line was drawn through the fully formed contractile ring marked by *rlc1*-GFP using ImageJ software. Any movement of the CR away from the original line placement during the entire length of imaging was scored as a ring sliding event. For ring sliding distances, fixed cells stained for nuclei and cell wall were imaged. The coordinates of the cell tips and septum were logged. Length of the shorter and longer cell were calculated from these coordinates and reported as a ratio.

Mean squared displacement analysis

Time-lapse images of a medial Z slice of a strain expressing a CR and spindle pole body marker were acquired every 10 seconds, registered for both DIC and fluorescent channels using ImageJ plugin Image Stabilizer (Li) and merged together to determine the position of the ring relative to the cell boundary. Cytokinetic ring positions were recorded for 17 wildtype and 18 *efr3Δ* mutant cells beginning when the CR was fully formed. Individual trajectories were obtained by reslicing the timelapse images to a 3-pixel wide line along the cell boundary and tracking the position of the ring with subpixel resolution using the ImageJ plugin TrackMate (Tinevez et al., 2017). Total absolute displacements for wild-type trajectories over a 300-second period were measured to be 83 ± 66 nm (SD, N=34 tracks from 17 cells), which is within the spatial resolution of the imaging (pixel size 106 nm). For *efr3Δ* mutant cells, 1-dimensional position over time data were used to perform Mean-squared displacement (MSD) analysis for the first 300s of the data using MATLAB[®] (R2016b, The MathWorks, Natick, MA) and @msdanalyzer tool as previously described (Tarantino et al., 2014). MSD data for *efr3Δ* mutant cells were fit by the 2nd degree polynomial function:

$$MSD(\tau) = 2D\tau + v^2\tau^2 + \sigma$$

where D is the diffusion coefficient, v is the drift velocity, and σ is the noise term. The fitting procedure yielded:

$$MSD(\tau) = \left(7.42 \times 10^{-5} \frac{\mu m^2}{s}\right) \tau + \left(1.82 \times 10^{-6} \frac{\mu m^2}{s^2}\right) \tau^2 + (1.24 \times 10^{-3} \mu m^2)$$

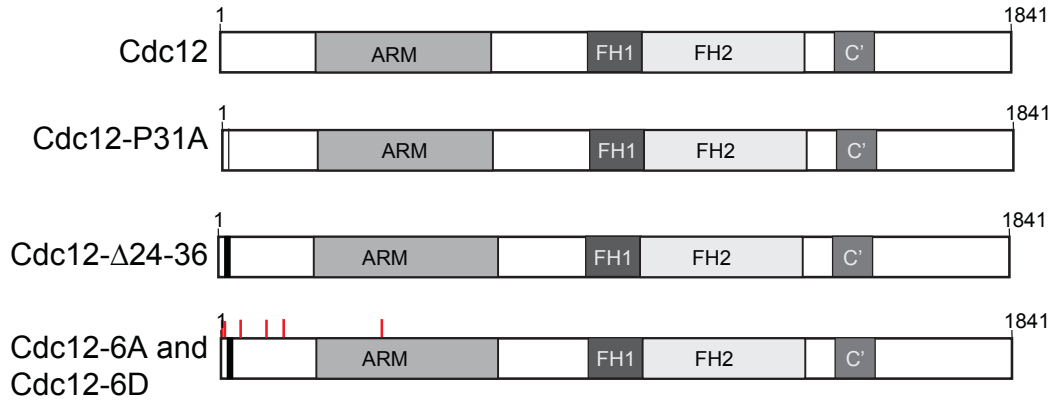
$$r^2=99.90\%$$

Mass Spectrometry

Purification of Efr3-TAP and subsequent identification of interacting proteins by mass spectrometry were performed as previously described (Chen et al., 2013a; Elmore et al., 2014; Gould et al., 2004) with the following changes: a newer version of Scaffold (Scaffold v4.4.1.1) was used and the minimum peptide identification probability was changed to 95.0%.

All ANOVA statistical analyses used Tukey's post-hoc analysis.

B. Cdc12 mutants used in Chapters 2 and 3



Appendix B

Cdc12 mutants used in Chapters 2 and 3.

A schematic of the domain layout of Cdc12 drawn to scale. The red lines on Cdc12 represent the residues that are phosphorylated by Cdk1 and mutated to either alanines or aspartates.

BIBLIOGRAPHY

- Akamatsu, M., J. Berro, K.M. Pu, I.R. Tebbs, and T.D. Pollard. 2014. Cytokinetic nodes in fission yeast arise from two distinct types of nodes that merge during interphase. *J Cell Biol.* 204:977-988.
- Arai, R., and I. Mabuchi. 2002. F-actin ring formation and the role of F-actin cables in the fission yeast *Schizosaccharomyces pombe*. *J Cell Sci.* 115:887-898.
- Arasada, R., and T.D. Pollard. 2014. Contractile Ring Stability in *S. pombe* Depends on F-BAR Protein Cdc15p and Bgs1p Transport from the Golgi Complex. *Cell Reports.*
- Atilgan, E., V. Magidson, A. Khodjakov, and F. Chang. 2015. Morphogenesis of the Fission Yeast Cell through Cell Wall Expansion. *Curr Biol.* 25:2150-2157.
- Audhya, A., and S.D. Emr. 2002. Stt4 PI 4-kinase localizes to the plasma membrane and functions in the Pkc1-mediated MAP kinase cascade. *Dev Cell.* 2:593-605.
- Bahler, J., and J.R. Pringle. 1998. Pom1p, a fission yeast protein kinase that provides positional information for both polarized growth and cytokinesis. *Genes Dev.* 12:1356-1370.
- Bahler, J., J.Q. Wu, M.S. Longtine, N.G. Shah, A. McKenzie, 3rd, A.B. Steever, A. Wach, P. Philippsen, and J.R. Pringle. 1998. Heterologous modules for efficient and versatile PCR-based gene targeting in *Schizosaccharomyces pombe*. *Yeast.* 14:943-951.

- Baird, D., C. Stefan, A. Audhya, S. Weys, and S.D. Emr. 2008. Assembly of the PtdIns 4-kinase Stt4 complex at the plasma membrane requires Ypp1 and Efr3. *J Cell Biol.* 183:1061-1074.
- Balasubramanian, M.K., D. McCollum, L. Chang, K.C. Wong, N.I. Naqvi, X. He, S. Sazer, and K.L. Gould. 1998. Isolation and characterization of new fission yeast cytokinesis mutants. *Genetics.* 149:1265-1275.
- Balasubramanian, M.K., R. Srinivasan, Y. Huang, and K.H. Ng. 2012. Comparing contractile apparatus-driven cytokinesis mechanisms across kingdoms. *Cytoskeleton (Hoboken).* 69:942-956.
- Bi, E., P. Maddox, D.J. Lew, E.D. Salmon, J.N. McMillan, E. Yeh, and J.R. Pringle. 1998. Involvement of an actomyosin contractile ring in *Saccharomyces cerevisiae* cytokinesis. *J Cell Biol.* 142:1301-1312.
- Bohnert, K.A., and K.L. Gould. 2012. Cytokinesis-based constraints on polarized cell growth in fission yeast. *PLoS Genet.* 8:e1003004.
- Bohnert, K.A., A.P. Grzegorzewska, A.H. Willet, C.W. Vander Kooi, D.R. Kovar, and K.L. Gould. 2013. SIN-dependent phosphoinhibition of formin multimerization controls fission yeast cytokinesis. *Genes Dev.* 27:2164-2177.
- Brandt, D.T., S. Marion, G. Griffiths, T. Watanabe, K. Kaibuchi, and R. Grosse. 2007. Dia1 and IQGAP1 interact in cell migration and phagocytic cup formation. *J Cell Biol.* 178:193-200.
- Brill, J.A., G.R. Hime, M. Scharer-Schuksz, and M.T. Fuller. 2000a. A phospholipid kinase regulates actin organization and intercellular bridge formation during germline cytokinesis. *Development.* 127:3855-3864.

- Brill, J.A., G.R. Hime, M. Scharer-Schuksz, and M.T. Fuller. 2000b. A phospholipid kinase regulates actin organization and intercellular bridge formation during germline cytokinesis. *Development*. 127:3855-3864.
- Burke, T.A., J.R. Christensen, E. Barone, C. Suarez, V. Sirotkin, and D.R. Kovar. 2014. Homeostatic actin cytoskeleton networks are regulated by assembly factor competition for monomers. *Curr Biol*. 24:579-585.
- Carnahan, R.H., and K.L. Gould. 2003. The PCH family protein, Cdc15p, recruits two F-actin nucleation pathways to coordinate cytokinetic actin ring formation in *Schizosaccharomyces pombe*. *J Cell Biol*. 162:851-862.
- Carpy, A., K. Krug, S. Graf, A. Koch, S. Popic, S. Hauf, and B. Macek. 2014. Absolute proteome and phosphoproteome dynamics during the cell cycle of fission yeast. *Molecular & Cellular Proteomics*:1925--1936.
- Castrillon, D.H., and S.A. Wasserman. 1994. Diaphanous is required for cytokinesis in *Drosophila* and shares domains of similarity with the products of the limb deformity gene. *Development*. 120:3367-3377.
- Cauvin, C., and A. Echard. 2015. Phosphoinositides: Lipids with informative heads and mastermind functions in cell division. *Biochim Biophys Acta*. 1851:832-843.
- Celton-Morizur, S., N. Bordes, V. Fraissier, P.T. Tran, and A. Paoletti. 2004. C-terminal anchoring of mid1p to membranes stabilizes cytokinetic ring position in early mitosis in fission yeast. *Mol Cell Biol*. 24:10621-10635.
- Chang, F., D. Drubin, and P. Nurse. 1997. cdc12p, a protein required for cytokinesis in fission yeast, is a component of the cell division ring and interacts with profilin. *J Cell Biol*. 137:169-182.

- Chang, F., A. Woollard, and P. Nurse. 1996. Isolation and characterization of fission yeast mutants defective in the assembly and placement of the contractile actin ring. *J Cell Sci.* 109 (Pt 1):131-142.
- Chang, L., J.L. Morrell, A. Feoktistova, and K.L. Gould. 2001. Study of cyclin proteolysis in anaphase-promoting complex (APC) mutant cells reveals the requirement for APC function in the final steps of the fission yeast septation initiation network. *Mol Cell Biol.* 21:6681-6694.
- Cheffings, T.H., N.J. Burroughs, and M.K. Balasubramanian. 2016. Actomyosin Ring Formation and Tension Generation in Eukaryotic Cytokinesis. *Curr Biol.* 26:R719-737.
- Chen, J.-S., M.R. Broadus, J.R. McLean, A. Feoktistova, L. Ren, and K.L. Gould. 2013a. Comprehensive proteomics analysis reveals new substrates and regulators of the fission yeast clp1/cdc14 phosphatase. *Molecular & Cellular Proteomics.* 12:1074-1086.
- Chen, J.S., J.R. Beckley, N.A. McDonald, L. Ren, M. Mangione, S.J. Jang, Z.C. Elmore, N. Rachfall, A. Feoktistova, C.M. Jones, A.H. Willet, R. Guillen, D.A. Bitton, J. Bahler, M.A. Jensen, N. Rhind, and K.L. Gould. 2014. Identification of new players in cell division, DNA damage response, and morphogenesis through construction of *Schizosaccharomyces pombe* deletion strains. *G3 (Bethesda).* 5:361-370.
- Chen, J.S., M.R. Broadus, J.R. McLean, A. Feoktistova, L. Ren, and K.L. Gould. 2013b. Comprehensive proteomics analysis reveals new substrates and regulators of the fission yeast clp1/cdc14 phosphatase. *Mol Cell Proteomics.* 12:1074-1086.

- Chesarone, M.A., A.G. DuPage, and B.L. Goode. 2010. Unleashing formins to remodel the actin and microtubule cytoskeletons. *Nat Rev Mol Cell Biol.* 11:62-74.
- Clifford, D.M., B.A. Wolfe, R.H. Roberts-Galbraith, W.H. McDonald, J.R. Yates, 3rd, and K.L. Gould. 2008. The Clp1/Cdc14 phosphatase contributes to the robustness of cytokinesis by association with anillin-related Mid1. *J Cell Biol.* 181:79-88.
- Coffman, V.C., A.H. Nile, I.J. Lee, H. Liu, and J.Q. Wu. 2009. Roles of formin nodes and myosin motor activity in Mid1p-dependent contractile-ring assembly during fission yeast cytokinesis. *Mol Biol Cell.* 20:5195-5210.
- Coffman, V.C., J.A. Sees, D.R. Kovar, and J.Q. Wu. 2013. The formins Cdc12 and For3 cooperate during contractile ring assembly in cytokinesis. *J Cell Biol.* 203:101-114.
- Copeland, S.J., B.J. Green, S. Burchat, G.A. Papalia, D. Banner, and J.W. Copeland. 2007. The diaphanous inhibitory domain/diaphanous autoregulatory domain interaction is able to mediate heterodimerization between mDia1 and mDia2. *J Biol Chem.* 282:30120-30130.
- Cortes, J.C., N. Pujol, M. Sato, M. Pinar, M. Ramos, B. Moreno, M. Osumi, J.C. Ribas, and P. Perez. 2015. Cooperation between Paxillin-like Protein Pxl1 and Glucan Synthase Bgs1 Is Essential for Actomyosin Ring Stability and Septum Formation in Fission Yeast. *PLoS Genet.* 11:e1005358.
- Cortes, J.C., M. Sato, J. Munoz, M.B. Moreno, J.A. Clemente-Ramos, M. Ramos, H. Okada, M. Osumi, A. Duran, and J.C. Ribas. 2012. Fission yeast Ags1 confers the essential septum strength needed for safe gradual cell abscission. *J Cell Biol.* 198:637-656.

- D'Avino, P.P. 2009. How to scaffold the contractile ring for a safe cytokinesis - lessons from Anillin-related proteins. *J Cell Sci.* 122:1071-1079.
- Davidson, R., J.A. Pontasch, and J.Q. Wu. 2016. Sbg1 Is a Novel Regulator for the Localization of the beta-Glucan Synthase Bgs1 in Fission Yeast. *PLoS One.* 11:e0167043.
- DeWard, A.D., and A.S. Alberts. 2009. Ubiquitin-mediated degradation of the formin mDia2 upon completion of cell division. *J Biol Chem.* 284:20061-20069.
- Dischinger, S., A. Krapp, L. Xie, J.R. Paulson, and V. Simanis. 2008. Chemical genetic analysis of the regulatory role of Cdc2p in the *S. pombe* septation initiation network. *J Cell Sci.* 121:843-853.
- Dong, Y., D. Pruyne, and A. Bretscher. 2003. Formin-dependent actin assembly is regulated by distinct modes of Rho signaling in yeast. *J Cell Biol.* 161:1081-1092.
- Eggert, U.S., A.A. Kiger, C. Richter, Z.E. Perlman, N. Perrimon, T.J. Mitchison, and C.M. Field. 2004a. Parallel chemical genetic and genome-wide RNAi screens identify cytokinesis inhibitors and targets. *PLoS Biology.* 2:e379.
- Eggert, U.S., A.A. Kiger, C. Richter, Z.E. Perlman, N. Perrimon, T.J. Mitchison, and C.M. Field. 2004b. Parallel chemical genetic and genome-wide RNAi screens identify cytokinesis inhibitors and targets. *PLoS Biol.* 2:e379.
- Elmore, Z.C., J.R. Beckley, Chen Jun-Song, and K.L. Gould. 2014. Histone H2B ubiquitination promotes the function of the anaphase-promoting complex/cyclosome in *Schizosaccharomyces pombe*. *G3: Genes|Genomes|Genetics.* 4:1529--1538.

- Emoto, K., H. Inadome, Y. Kanaho, S. Narumiya, and M. Umeda. 2005. Local change in phospholipid composition at the cleavage furrow is essential for completion of cytokinesis. *J Biol Chem.* 280:37901-37907.
- Fankhauser, C., A. Reymond, L. Cerutti, S. Utzig, K. Hofmann, and V. Simanis. 1995. The *S. pombe cdc15* gene is a key element in the reorganization of F-actin at mitosis. *Cell.* 82:435-444.
- Feierbach, B., and F. Chang. 2001. Roles of the fission yeast formin for3p in cell polarity, actin cable formation and symmetric cell division. *Curr Biol.* 11:1656-1665.
- Feoktistova, A., J. Morrell-Falvey, J.S. Chen, N.S. Singh, M.K. Balasubramanian, and K.L. Gould. 2012. The fission yeast septation initiation network (SIN) kinase, Sid2, is required for SIN asymmetry and regulates the SIN scaffold, Cdc11. *Mol Biol Cell.* 23:1636-1645.
- Field, S.J., N. Madson, M.L. Kerr, K.A. Galbraith, C.E. Kennedy, M. Tahiliani, A. Wilkins, and L.C. Cantley. 2005. PtdIns(4,5)P₂ functions at the cleavage furrow during cytokinesis. *Curr Biol.* 15:1407-1412.
- Fujiwara, T., M. Bandi, M. Nitta, E.V. Ivanova, R.T. Bronson, and D. Pellman. 2005. Cytokinesis failure generating tetraploids promotes tumorigenesis in p53-null cells. *Nature.* 437:1043-1047.
- Fujiwara, T., K. Tanaka, A. Mino, M. Kikyo, K. Takahashi, K. Shimizu, and Y. Takai. 1998. Rho1p-Bni1p-Spa2p interactions: implication in localization of Bni1p at the bud site and regulation of the actin cytoskeleton in *Saccharomyces cerevisiae*. *Mol Biol Cell.* 9:1221-1233.

- Ge, W., and M.K. Balasubramanian. 2008. Pxl1p, a paxillin-related protein, stabilizes the actomyosin ring during cytokinesis in fission yeast. *Mol Biol Cell*. 19:1680-1692.
- Gordon, D.J., B. Resio, and D. Pellman. 2012. Causes and consequences of aneuploidy in cancer. *Nat Rev Genet*. 13:189-203.
- Gould, G.W. 2016. Animal cell cytokinesis: The role of dynamic changes in the plasma membrane proteome and lipidome. *Semin Cell Dev Biol*. 53:64-73.
- Gould, K.L., S. Moreno, D.J. Owen, S. Sazer, and P. Nurse. 1991a. Phosphorylation at Thr167 is required for *Schizosaccharomyces pombe* p34cdc2 function. *EMBO J*. 10:3297-3309.
- Gould, K.L., S. Moreno, D.J. Owen, S. Sazer, and P. Nurse. 1991b. Phosphorylation at Thr167 is required for *Schizosaccharomyces pombe* p34cdc2 function. *EMBO J*. 10:3297-3309.
- Gould, K.L., L. Ren, A.S. Feoktistova, J.L. Jennings, and A.J. Link. 2004. Tandem affinity purification and identification of protein complex components. *Methods*. 33:239--244.
- Goyal, A., M. Takaine, V. Simanis, and K. Nakano. 2011. Dividing the spoils of growth and the cell cycle: The fission yeast as a model for the study of cytokinesis. *Cytoskeleton (Hoboken)*. 68:69-88.
- Graziano, B.R., A.G. DuPage, A. Michelot, D. Breitsprecher, J.B. Moseley, I. Sagot, L. Blanchoin, and B.L. Goode. 2011. Mechanism and cellular function of Bud6 as an actin nucleation-promoting factor. *Mol Biol Cell*. 22:4016-4028.
- Green, R.A., E. Paluch, and K. Oegema. 2012. Cytokinesis in animal cells. *Annu Rev Cell Dev Biol*. 28:29-58.

- Gu, Y., and S. Oliferenko. 2015. Comparative biology of cell division in the fission yeast clade. *Curr Opin Microbiol.* 28:18-25.
- Guertin, D.A., L. Chang, F. Irshad, K.L. Gould, and D. McCollum. 2000. The role of the sid1p kinase and cdc14p in regulating the onset of cytokinesis in fission yeast. *EMBO J.* 19:1803-1815.
- Hachet, O., M. Berthelot-Grosjean, K. Kokkoris, V. Vincenzetti, J. Moosbrugger, and S.G. Martin. 2011. A phosphorylation cycle shapes gradients of the DYRK family kinase Pom1 at the plasma membrane. *Cell.* 145:1116-1128.
- Hachet, O., and V. Simanis. 2008. Mid1p/anillin and the septation initiation network orchestrate contractile ring assembly for cytokinesis. *Genes Dev.* 22:3205-3216.
- Hagan, I.M. 1998. The fission yeast microtubule cytoskeleton. *J Cell Sci.* 111 (Pt 12):1603-1612.
- Harris, E.S., I. Rouiller, D. Hanein, and H.N. Higgs. 2006. Mechanistic differences in actin bundling activity of two mammalian formins, FRL1 and mDia2. *J Biol Chem.* 281:14383-14392.
- Hayles, J., V. Wood, L. Jeffery, K.L. Hoe, D.U. Kim, H.O. Park, S. Salas-Pino, C. Heichinger, and P. Nurse. 2013. A genome-wide resource of cell cycle and cell shape genes of fission yeast. *Open Biol.* 3:130053.
- He, X., T.E. Patterson, and S. Sazer. 1997. The *Schizosaccharomyces pombe* spindle checkpoint protein mad2p blocks anaphase and genetically interacts with the anaphase-promoting complex. *Proc Natl Acad Sci U S A.* 94:7965-7970.
- Higgs, H.N. 2005. Formin proteins: a domain-based approach. *Trends Biochem Sci.* 30:342-353.

- Huang, J., Y. Huang, H. Yu, D. Subramanian, A. Padmanabhan, R. Thadani, Y. Tao, X. Tang, R. Wedlich-Soldner, and M.K. Balasubramanian. 2012. Nonmedially assembled F-actin cables incorporate into the actomyosin ring in fission yeast. *J Cell Biol.* 199:831-847.
- Huang, Y., H. Yan, and M.K. Balasubramanian. 2008. Assembly of normal actomyosin rings in the absence of Mid1p and cortical nodes in fission yeast. *J Cell Biol.* 183:979-988.
- Humbel, B.M., M. Konomi, T. Takagi, N. Kamasawa, S.A. Ishijima, and M. Osumi. 2001. In situ localization of beta-glucans in the cell wall of *Schizosaccharomyces pombe*. *Yeast.* 18:433-444.
- Imamura, H., K. Tanaka, T. Hihara, M. Umikawa, T. Kamei, K. Takahashi, T. Sasaki, and Y. Takai. 1997. Bni1p and Bnr1p: downstream targets of the Rho family small G-proteins which interact with profilin and regulate actin cytoskeleton in *Saccharomyces cerevisiae*. *EMBO J.* 16:2745-2755.
- Johnson, M., D.A. East, and D.P. Mulvihill. 2014. Formins determine the functional properties of actin filaments in yeast. *Curr Biol.* 24:1525-1530.
- Kamei, T., K. Tanaka, T. Hihara, M. Umikawa, H. Imamura, M. Kikyo, K. Ozaki, and Y. Takai. 1998. Interaction of Bnr1p with a novel Src homology 3 domain-containing Hof1p. Implication in cytokinesis in *Saccharomyces cerevisiae*. *J Biol Chem.* 273:28341-28345.
- Kechad, A., S. Jananji, Y. Ruella, and G.R. Hickson. 2012. Anillin acts as a bifunctional linker coordinating midbody ring biogenesis during cytokinesis. *Curr Biol.* 22:197-203.

- Keeney, J.B., and J.D. Boeke. 1994. Efficient targeted integration at *leu1-32* and *ura4-294* in *Schizosaccharomyces pombe*. *Genetics*. 136:849-856.
- Kessels, M.M., J. Dong, W. Leibig, P. Westermann, and B. Qualmann. 2006. Complexes of syndapin II with dynamin II promote vesicle formation at the trans-Golgi network. *J Cell Sci*. 119:1504-1516.
- Kitayama, C., A. Sugimoto, and M. Yamamoto. 1997. Type II myosin heavy chain encoded by the *myo2* gene composes the contractile ring during cytokinesis in *Schizosaccharomyces pombe*. *J Cell Biol*. 137:1309-1319.
- Kostan, J., U. Salzer, A. Orlova, I. Toro, V. Hodnik, Y. Senju, J. Zou, C. Schreiner, J. Steiner, J. Merilainen, M. Nikki, I. Virtanen, O. Carugo, J. Rappsilber, P. Lappalainen, V.P. Lehto, G. Anderluh, E.H. Egelman, and K. Djinovic-Carugo. 2014. Direct interaction of actin filaments with F-BAR protein pacsin2. *EMBO Rep*.
- Kovar, D.R., E.S. Harris, R. Mahaffy, H.N. Higgs, and T.D. Pollard. 2006. Control of the assembly of ATP- and ADP-actin by formins and profilin. *Cell*. 124:423-435.
- Kovar, D.R., J.R. Kuhn, A.L. Tichy, and T.D. Pollard. 2003. The fission yeast cytokinesis formin Cdc12p is a barbed end actin filament capping protein gated by profilin. *J Cell Biol*. 161:875-887.
- Kovar, D.R., and T.D. Pollard. 2004. Progressing actin: Formin as a processive elongation machine. *Nat Cell Biol*. 6:1158-1159.
- Laporte, D., V.C. Coffman, I.J. Lee, and J.Q. Wu. 2011. Assembly and architecture of precursor nodes during fission yeast cytokinesis. *J Cell Biol*. 192:1005-1021.

- Lee, I.J., V.C. Coffman, and J.Q. Wu. 2012. Contractile-ring assembly in fission yeast cytokinesis: Recent advances and new perspectives. *Cytoskeleton (Hoboken)*. 69:751-763.
- Li, K. The image stabilizer plugin for ImageJ., http://www.cs.cmu.edu/~kangli/code/Image_Stabilizer.html.
- Ling, Y., C.J. Stefan, J.A. Macgurn, A. Audhya, and S.D. Emr. 2012. The dual PH domain protein Opy1 functions as a sensor and modulator of PtdIns(4,5)P(2) synthesis. *EMBO J.* 31:2882-2894.
- Liu, J., H. Wang, and M.K. Balasubramanian. 2000. A checkpoint that monitors cytokinesis in *Schizosaccharomyces pombe*. *J Cell Sci.* 113 (Pt 7):1223-1230.
- Liu, J., H. Wang, D. McCollum, and M.K. Balasubramanian. 1999. Drc1p/Cps1p, a 1,3-beta-glucan synthase subunit, is essential for division septum assembly in *Schizosaccharomyces pombe*. *Genetics.* 153:1193-1203.
- Liu, W., F.H. Santiago-Tirado, and A. Bretscher. 2012. Yeast formin Bni1p has multiple localization regions that function in polarized growth and spindle orientation. *Mol Biol Cell.* 23:412-422.
- Marks, J., I.M. Hagan, and J.S. Hyams. 1986. Growth polarity and cytokinesis in fission yeast: the role of the cytoskeleton. *J Cell Sci Suppl.* 5:229-241.
- McDonald, N.A., and K.L. Gould. 2016. Linking up at the BAR: Oligomerization and F-BAR protein function. *Cell Cycle.* 15:1977-1985.
- McDonald, N.A., Y. Takizawa, A. Feoktistova, P. Xu, M.D. Ohi, C.W. Vander Kooi, and K.L. Gould. 2016. The Tubulation Activity of a Fission Yeast F-BAR Protein Is Dispensable for Its Function in Cytokinesis. *Cell Rep.* 14:534-546.

- Mishra, M., J. Kashiwazaki, T. Takagi, R. Srinivasan, Y. Huang, M.K. Balasubramanian, and I. Mabuchi. 2013. In vitro contraction of cytokinetic ring depends on myosin II but not on actin dynamics. *Nat Cell Biol.* 15:853-859.
- Mitchison, J.M., and P. Nurse. 1985. Growth in cell length in the fission yeast *Schizosaccharomyces pombe*. *J Cell Sci.* 75:357-376.
- Mizuguchi, S., T. Uyama, H. Kitagawa, K.H. Nomura, K. Dejima, K. Gengyo-Ando, S. Mitani, K. Sugahara, and K. Nomura. 2003. Chondroitin proteoglycans are involved in cell division of *Caenorhabditis elegans*. *Nature.* 423:443-448.
- Mocciaro, A., and E. Schiebel. 2010. Cdc14: a highly conserved family of phosphatases with non-conserved functions? *J Cell Sci.* 123:2867-2876.
- Mogilner, A., and G. Oster. 2003. Force generation by actin polymerization II: the elastic ratchet and tethered filaments. *Biophys J.* 84:1591-1605.
- Moseley, J.B., and B.L. Goode. 2005. Differential activities and regulation of *Saccharomyces cerevisiae* formin proteins Bni1 and Bnr1 by Bud6. *J Biol Chem.* 280:28023-28033.
- Munoz, J., J.C. Cortes, M. Sipiczki, M. Ramos, J.A. Clemente-Ramos, M.B. Moreno, I.M. Martins, P. Perez, and J.C. Ribas. 2013. Extracellular cell wall beta(1,3)glucan is required to couple septation to actomyosin ring contraction. *J Cell Biol.* 203:265-282.
- Nabeshima, K., T. Nakagawa, A.F. Straight, A. Murray, Y. Chikashige, Y.M. Yamashita, Y. Hiraoka, and M. Yanagida. 1998. Dynamics of centromeres during metaphase-anaphase transition in fission yeast: Dis1 is implicated in force balance in metaphase bipolar spindle. *Mol Biol Cell.* 9:3211-3225.

- Nakano, K., K. Satoh, A. Morimatsu, M. Ohnuma, and I. Mabuchi. 2001. Interactions among a fimbrin, a capping protein, and an actin-depolymerizing factor in organization of the fission yeast actin cytoskeleton. *Mol Biol Cell*. 12:3515-3526.
- Nakatsu, F., J.M. Baskin, J. Chung, L.B. Tanner, G. Shui, S.Y. Lee, M. Pirruccello, M. Hao, N.T. Ingolia, M.R. Wenk, and P. De Camilli. 2012. PtdIns4P synthesis by PI4KIIIalpha at the plasma membrane and its impact on plasma membrane identity. *J Cell Biol*. 199:1003-1016.
- Naqvi, N.I., K. Eng, K.L. Gould, and M.K. Balasubramanian. 1999. Evidence for F-actin-dependent and -independent mechanisms involved in assembly and stability of the medial actomyosin ring in fission yeast. *EMBO J*. 18:854-862.
- Nurse, P., P. Thuriaux, and K. Nasmyth. 1976. Genetic control of the cell division cycle in the fission yeast *Schizosaccharomyces pombe*. *Mol Gen Genet*. 146:167-178.
- Otomo, T., D.R. Tomchick, C. Otomo, S.C. Panchal, M. Machius, and M.K. Rosen. 2005. Structural basis of actin filament nucleation and processive capping by a formin homology 2 domain. *Nature*. 433:488-494.
- Padmanabhan, A., K. Bakka, M. Sevugan, N.I. Naqvi, V. D'Souza, X. Tang, M. Mishra, and M.K. Balasubramanian. 2011. IQGAP-related Rng2p organizes cortical nodes and ensures position of cell division in fission yeast. *Curr Biol*. 21:467-472.
- Paoletti, A., and F. Chang. 2000. Analysis of mid1p, a protein required for placement of the cell division site, reveals a link between the nucleus and the cell surface in fission yeast. *Mol Biol Cell*. 11:2757-2773.
- Pardo, M., and P. Nurse. 2003. Equatorial retention of the contractile actin ring by microtubules during cytokinesis. *Science*. 300:1569-1574.

- Pelham, R.J., and F. Chang. 2002. Actin dynamics in the contractile ring during cytokinesis in fission yeast. *Nature*. 419:82-86.
- Petersen, J., O. Nielsen, R. Egel, and I.M. Hagan. 1998. FH3, a domain found in formins, targets the fission yeast formin Fus1 to the projection tip during conjugation. *J Cell Biol*. 141:1217-1228.
- Piekny, A.J., and M. Glotzer. 2008. Anillin is a scaffold protein that links RhoA, actin, and myosin during cytokinesis. *Curr Biol*. 18:30-36.
- Pollard, T.D., and J.Q. Wu. 2010. Understanding cytokinesis: lessons from fission yeast. *Nat Rev Mol Cell Biol*. 11:149-155.
- Proctor, S.A., N. Minc, A. Boudaoud, and F. Chang. 2012. Contributions of turgor pressure, the contractile ring, and septum assembly to forces in cytokinesis in fission yeast. *Curr Biol*. 22:1601-1608.
- Pruyne, D., M. Evangelista, C. Yang, E. Bi, S. Zigmond, A. Bretscher, and C. Boone. 2002. Role of formins in actin assembly: nucleation and barbed-end association. *Science*. 297:612-615.
- Qualmann, B., J. Roos, P.J. DiGregorio, and R.B. Kelly. 1999. Syndapin I, a synaptic dynamin-binding protein that associates with the neural Wiskott-Aldrich syndrome protein. *Mol Biol Cell*. 10:501-513.
- Ren, L., A.H. Willet, R.H. Roberts-Galbraith, N.A. McDonald, A. Feoktistova, J.S. Chen, H. Huang, R. Guillen, C. Boone, S.S. Sidhu, J.R. Beckley, and K.L. Gould. 2015. The Cdc15 and Imp2 SH3 domains cooperatively scaffold a network of proteins that redundantly ensure efficient cell division in fission yeast. *Mol Biol Cell*. 26:256-269.

- Rincon, S.A., and A. Paoletti. 2016. Molecular control of fission yeast cytokinesis. *Semin Cell Dev Biol.* 53:28-38.
- Roberts-Galbraith, R.H., J.S. Chen, J. Wang, and K.L. Gould. 2009. The SH3 domains of two PCH family members cooperate in assembly of the Schizosaccharomyces pombe contractile ring. *J Cell Biol.* 184:113-127.
- Roberts-Galbraith, R.H., and K.L. Gould. 2010. Setting the F-BAR: functions and regulation of the F-BAR protein family. *Cell Cycle.* 9:4091-4097.
- Roberts-Galbraith, R.H., M.D. Ohi, B.A. Ballif, J.S. Chen, I. McLeod, W.H. McDonald, S.P. Gygi, J.R. Yates, 3rd, and K.L. Gould. 2010. Dephosphorylation of F-BAR protein Cdc15 modulates its conformation and stimulates its scaffolding activity at the cell division site. *Mol Cell.* 39:86-99.
- Romero, S., C. Le Clainche, D. Didry, C. Egile, D. Pantaloni, and M.F. Carlier. 2004. Formin is a processive motor that requires profilin to accelerate actin assembly and associated ATP hydrolysis. *Cell.* 119:419-429.
- Roncero, C., and Y. Sanchez. 2010. Cell separation and the maintenance of cell integrity during cytokinesis in yeast: the assembly of a septum. *Yeast.* 27:521-530.
- Rouso, T., A.M. Shewan, K.E. Mostov, E.D. Schejter, and B.Z. Shilo. 2013. Apical targeting of the formin Diaphanous in Drosophila tubular epithelia. *Elife (Cambridge).* 2:e00666.
- Sagot, I., A.A. Rodal, J. Moseley, B.L. Goode, and D. Pellman. 2002. An actin nucleation mechanism mediated by Bni1 and profilin. *Nat Cell Biol.* 4:626-631.
- Saha, S., and T.D. Pollard. 2012. Anillin-related protein Mid1p coordinates the assembly of the cytokinetic contractile ring in fission yeast. *Mol Biol Cell.* 23:3982-3992.

- Schmidt, M., B. Bowers, A. Varma, D.H. Roh, and E. Cabib. 2002. In budding yeast, contraction of the actomyosin ring and formation of the primary septum at cytokinesis depend on each other. *J Cell Sci.* 115:293-302.
- Seth, A., C. Otomo, and M.K. Rosen. 2006. Autoinhibition regulates cellular localization and actin assembly activity of the diaphanous-related formins FRLalpha and mDia1. *J Cell Biol.* 174:701-713.
- Sethi, K., S. Palani, J.C. Cortes, M. Sato, M. Sevugan, M. Ramos, S. Vijaykumar, M. Osumi, N.I. Naqvi, J.C. Ribas, and M. Balasubramanian. 2016. A New Membrane Protein Sbg1 Links the Contractile Ring Apparatus and Septum Synthesis Machinery in Fission Yeast. *PLoS Genet.* 12:e1006383.
- Severson, A.F., D.L. Baillie, and B. Bowerman. 2002. A Formin Homology protein and a profilin are required for cytokinesis and Arp2/3-independent assembly of cortical microfilaments in *C. elegans*. *Curr Biol.* 12:2066-2075.
- Shaner, N.C., G.G. Lambert, A. Chammas, Y. Ni, P.J. Cranfill, M.A. Baird, B.R. Sell, J.R. Allen, R.N. Day, M. Israelsson, M.W. Davidson, and J. Wang. 2013. A bright monomeric green fluorescent protein derived from *Branchiostoma lanceolatum*. *Nat Methods.* 10:407-409.
- Simanis, V. 2015. Pombe's thirteen - control of fission yeast cell division by the septation initiation network. *J Cell Sci.* 128:1465-1474.
- Skau, C.T., E.M. Neidt, and D.R. Kovar. 2009. Role of tropomyosin in formin-mediated contractile ring assembly in fission yeast. *Mol Biol Cell.* 20:2160-2173.

- Skoumpla, K., A.T. Coulton, W. Lehman, M.A. Geeves, and D.P. Mulvihill. 2007. Acetylation regulates tropomyosin function in the fission yeast *Schizosaccharomyces pombe*. *J Cell Sci.* 120:1635-1645.
- Sohrmann, M., C. Fankhauser, C. Brodbeck, and V. Simanis. 1996. The *dmf1/mid1* gene is essential for correct positioning of the division septum in fission yeast. *Genes Dev.* 10:2707-2719.
- Sparks, C.A., M. Mophew, and D. McCollum. 1999. Sid2p, a spindle pole body kinase that regulates the onset of cytokinesis. *J Cell Biol.* 146:777-790.
- Stachowiak, M.R., C. Laplante, H.F. Chin, B. Guirao, E. Karatekin, T.D. Pollard, and B. O'Shaughnessy. 2014. Mechanism of cytokinetic contractile ring constriction in fission yeast. *Dev Cell.* 29:547-561.
- Stark, B.C., T.E. Sladewski, L.W. Pollard, and M. Lord. 2010. Tropomyosin and myosin-II cellular levels promote actomyosin ring assembly in fission yeast. *Mol Biol Cell.* 21:989-1000.
- Stefan, C.J., A. Audhya, and S.D. Emr. 2002a. The yeast synaptojanin-like proteins control the cellular distribution of phosphatidylinositol (4,5)-bisphosphate. *Mol Biol Cell.* 13:542-557.
- Stefan, C.J., A. Audhya, and S.D. Emr. 2002b. The yeast synaptojanin-like proteins control the cellular distribution of phosphatidylinositol (4,5)-bisphosphate. *Molecular Biology of the Cell.* 13:542--557.
- Stegmeier, F., and A. Amon. 2004. Closing mitosis: the functions of the Cdc14 phosphatase and its regulation. *Annu Rev Genet.* 38:203-232.

- Suarez, C., R.T. Carroll, T.A. Burke, J.R. Christensen, A.J. Bestul, J.A. Sees, M.L. James, V. Sirotkin, and D.R. Kovar. 2015. Profilin regulates F-actin network homeostasis by favoring formin over Arp2/3 complex. *Dev Cell*. 32:43-53.
- Sun, L., R. Guan, I.J. Lee, Y. Liu, M. Chen, J. Wang, J.Q. Wu, and Z. Chen. 2015. Mechanistic insights into the anchorage of the contractile ring by anillin and Mid1. *Dev Cell*. 33:413-426.
- Swaffer, M.P., A.W. Jones, H.R. Flynn, A.P. Snijders, and P. Nurse. 2016. CDK Substrate Phosphorylation and Ordering the Cell Cycle. *Cell*. 167:1750-1761 e1716.
- Takeya, R., K. Taniguchi, S. Narumiya, and H. Sumimoto. 2008. The mammalian formin FHOD1 is activated through phosphorylation by ROCK and mediates thrombin-induced stress fibre formation in endothelial cells. *EMBO J*. 27:618-628.
- Tao, E.Y., M. Calvert, and M.K. Balasubramanian. 2014. Rewiring Mid1p-Independent Medial Division in Fission Yeast. *Curr Biol*.
- Tarantino, N., J.Y. Tinevez, E.F. Crowell, B. Boisson, R. Henriques, M. Mhlanga, F. Agou, A. Isral, and E. Laplantine. 2014. TNF and IL-1 exhibit distinct ubiquitin requirements for inducing NEMO-IKK supramolecular structures. *Journal of Cell Biology*. 204:231--245.
- Tebbs, I.R., and T.D. Pollard. 2013. Separate roles of IQGAP Rng2p in forming and constricting the *Schizosaccharomyces pombe* cytokinetic contractile ring. *Mol Biol Cell*. 24:1904-1917.

- Tinevez, J.-Y., N. Perry, J. Schindelin, G.M. Hoopes, G.D. Reynolds, E. Laplantine, S.Y. Bednarek, S.L. Shorte, and K.W. Eliceiri. 2017. TrackMate: An open and extensible platform for single-particle tracking. *Methods*. 115:80-90.
- Tolliday, N., M. Pitcher, and R. Li. 2003. Direct evidence for a critical role of myosin II in budding yeast cytokinesis and the evolvability of new cytokinetic mechanisms in the absence of myosin II. *Mol Biol Cell*. 14:798-809.
- Tolliday, N., L. VerPlank, and R. Li. 2002. Rho1 directs formin-mediated actin ring assembly during budding yeast cytokinesis. *Curr Biol*. 12:1864-1870.
- Trautmann, S., B.A. Wolfe, P. Jorgensen, M. Tyers, K.L. Gould, and D. McCollum. 2001. Fission yeast Clp1p phosphatase regulates G2/M transition and coordination of cytokinesis with cell cycle progression. *Curr Biol*. 11:931-940.
- Tsujita, K., S. Suetsugu, N. Sasaki, M. Furutani, T. Oikawa, and T. Takenawa. 2006. Coordination between the actin cytoskeleton and membrane deformation by a novel membrane tubulation domain of PCH proteins is involved in endocytosis. *J Cell Biol*. 172:269-279.
- Vavylonis, D., D.R. Kovar, B. O'Shaughnessy, and T.D. Pollard. 2006. Model of formin-associated actin filament elongation. *Mol Cell*. 21:455-466.
- Vavylonis, D., J.Q. Wu, S. Hao, B. O'Shaughnessy, and T.D. Pollard. 2008. Assembly mechanism of the contractile ring for cytokinesis by fission yeast. *Science*. 319:97-100.
- Vinciguerra, P., S.A. Godinho, K. Parmar, D. Pellman, and A.D. D'Andrea. 2010. Cytokinesis failure occurs in Fanconi anemia pathway-deficient murine and human bone marrow hematopoietic cells. *J Clin Invest*. 120:3834-3842.

- Vjestica, A., X.Z. Tang, and S. Oliferenko. 2008. The actomyosin ring recruits early secretory compartments to the division site in fission yeast. *Mol Biol Cell*. 19:1125-1138.
- Wach, A., A. Brachat, R. Pohlmann, and P. Philippsen. 1994. New heterologous modules for classical or PCR-based gene disruptions in *Saccharomyces cerevisiae*. *Yeast*. 10:1793-1808.
- Wachtler, V., Y. Huang, J. Karagiannis, and M.K. Balasubramanian. 2006. Cell cycle-dependent roles for the FCH-domain protein Cdc15p in formation of the actomyosin ring in *Schizosaccharomyces pombe*. *Mol Biol Cell*. 17:3254-3266.
- Wang, J., S.P. Neo, and M. Cai. 2009. Regulation of the yeast formin Bni1p by the actin-regulating kinase Prk1p. *Traffic*. 10:528-535.
- Wang, N., L. Lo Presti, Y.H. Zhu, M. Kang, Z. Wu, S.G. Martin, and J.Q. Wu. 2014. The novel proteins Rng8 and Rng9 regulate the myosin-V Myo51 during fission yeast cytokinesis. *J Cell Biol*. 205:357-375.
- Watanabe, S., Y. Ando, S. Yasuda, H. Hosoya, N. Watanabe, T. Ishizaki, and S. Narumiya. 2008. mDia2 induces the actin scaffold for the contractile ring and stabilizes its position during cytokinesis in NIH 3T3 cells. *Mol Biol Cell*. 19:2328-2338.
- Watanabe, S., K. Okawa, T. Miki, S. Sakamoto, T. Morinaga, K. Segawa, T. Arakawa, M. Kinoshita, T. Ishizaki, and S. Narumiya. 2010. Rho and anillin-dependent control of mDia2 localization and function in cytokinesis. *Mol Biol Cell*. 21:3193-3204.

- Waters, J.C. 2009. Accuracy and precision in quantitative fluorescence microscopy. *J Cell Biol.* 185:1135-1148.
- Werler, P.J., E. Hartsuiker, and A.M. Carr. 2003. A simple Cre-loxP method for chromosomal N-terminal tagging of essential and non-essential *Schizosaccharomyces pombe* genes. *Gene.* 304:133-141.
- Willet, A.H., N.A. McDonald, K.A. Bohnert, M.A. Baird, J.R. Allen, M.W. Davidson, and K.L. Gould. 2015a. The F-BAR Cdc15 promotes contractile ring formation through the direct recruitment of the formin Cdc12. *J Cell Biol.* 208:391-399.
- Willet, A.H., N.A. McDonald, and K.L. Gould. 2015b. Regulation of contractile ring formation and septation in *Schizosaccharomyces pombe*. *Curr Opin Microbiol.* 28:46-52.
- Wolf, F., R. Sigl, and S. Geley. 2007. '... The end of the beginning': cdk1 thresholds and exit from mitosis. *Cell Cycle.* 6:1408-1411.
- Wu, J.Q., J. Bahler, and J.R. Pringle. 2001. Roles of a fimbrin and an alpha-actinin-like protein in fission yeast cell polarization and cytokinesis. *Mol Biol Cell.* 12:1061-1077.
- Wu, J.Q., J.R. Kuhn, D.R. Kovar, and T.D. Pollard. 2003. Spatial and temporal pathway for assembly and constriction of the contractile ring in fission yeast cytokinesis. *Dev Cell.* 5:723-734.
- Wu, J.Q., and T.D. Pollard. 2005. Counting cytokinesis proteins globally and locally in fission yeast. *Science.* 310:310-314.

- Wu, J.Q., V. Sirotkin, D.R. Kovar, M. Lord, C.C. Beltzner, J.R. Kuhn, and T.D. Pollard. 2006. Assembly of the cytokinetic contractile ring from a broad band of nodes in fission yeast. *J Cell Biol.* 174:391-402.
- Xu, X., and B.E. Vogel. 2011. A secreted protein promotes cleavage furrow maturation during cytokinesis. *Curr Biol.* 21:114-119.
- Xu, Y., J.B. Moseley, I. Sagot, F. Poy, D. Pellman, B.L. Goode, and M.J. Eck. 2004. Crystal structures of a Formin Homology-2 domain reveal a tethered dimer architecture. *Cell.* 116:711-723.
- Yonetani, A., R.J. Lustig, J.B. Moseley, T. Takeda, B.L. Goode, and F. Chang. 2008. Regulation and targeting of the fission yeast formin cdc12p in cytokinesis. *Mol Biol Cell.* 19:2208-2219.
- Zhou, Z., E.L. Munteanu, J. He, T. Ursell, M. Bathe, K.C. Huang, and F. Chang. 2015. The contractile ring coordinates curvature-dependent septum assembly during fission yeast cytokinesis. *Mol Biol Cell.* 26:78-90.